STRESS AND STABILITY ANALYSIS OF STEEL PIPING SYSTEMS IN THE PETROLEUM INDUSTRY

by

Justin Pillay

21139232

Submitted in fulfilment of the academic requirements for the degree of
Master of Engineering: Mechanical Engineering
in the Faculty of Engineering and the Built Environment

Durban University of Technology
Durban
2020

Abstract

This study aims to reach a level of proficiency on the available technical theories to assess steel pressure piping systems and the identification of potential risks of failure. The research focuses mainly on piping systems in the petroleum industry. The importance of this study is based on the risk reduction of petroleum plant downtime and the harming of life as a result of piping failures.

The apparent need for piping systems stress analysis was a result of the many failures that occurred at Indy Oil's petroleum plant. The recent acquisition of the petroleum plant under the GUD Holdings group brought along minimum engineering experience with regards to piping systems. GUD's inhouse engineering teams executed the many plant expansion and upgrade projects. A common industry perception is that piping systems are basic and do not require much attention. These misconceptions are a result of many piping failures in the industry. The failures that occurred called for a thorough investigation of all equipment setups and piping installations at Indy Oil. Specific failure identifications at the petroleum plant were done. The research and analysis of piping systems stress analysis were performed to aid in understanding the cause of these failures.

Fluid dynamics, as a major contributor to stress and strain state in pipes, is the object of much attention. The dimensional specification and layout optimization of a piping system is highly dependent on the internal piping pressure. Studies, developments, and prediction analysis on the impact of sustained and thermal loads are reviewed to understand the numerical and analytical techniques available which enables the analysis of various piping systems. A risk-informed approach is applied that incorporates various design criteria, as well as, failure contributors in piping systems. At first, each component and failure mode is determined separately. Thereafter, the instances of simultaneous loading and increased risk of failure in piping systems have been determined.

The available literature is used to source necessary data, as well as, compare the obtained results with those available in the literature. Government statutory requirements are used as a basis in the design process. Material specifications and engineering quality is controlled by these governing standards.

The application of this study is done by the design and analysis of a piping system for Indy Oil's Tank Farm. Piping systems failures as a result of improper design raised importance for a thorough stress analysis at the Petrochemical site. The calculations of stress-strain contributions are done using theoretical methods, as well as, computer software programs. The piping system is analysed on various conditions according to the process requirements of the Plant. Various load cases were developed to account for simultaneous loadings. The expected result of the system is for stress contributions to not exceed the maximum allowable stresses.

CAESAR II software is selected as the most suitable for the analysis. The simulation is done on each pipe element and demonstrates a three-dimensional analysis. The results of the study were used to determine the failure modes of previously installed piping systems and to create a design guide for all future piping systems projects.

Declaration

The Registrar (Academic)
Durban University of Technology

1. **Declaration by student**

I hereby declare that this submission is my work and to the best of my knowledge it neither contains material previously published or written by another person, nor material which to a major extent has been accepted for the award of any other degrees at Durban University of Technology (DUT) or any other educational institution. I also declare that the intellectual content of this dissertation is the product of my work. Any contribution made to the research by others has been explicitly acknowledged in the dissertation.

---------- 18 January 2021

(Signature) (Date)

2. **Declaration by supervisor**

I, Prof Pavel Tabakov, as the student supervisor, have proposed for this thesis to be submitted for examination.

18 January 2021

(Signature) (Date)

Acknowledgements

I would like to acknowledge the Durban University of Technology, for the facilities and resources provided which enabled me to fulfil the requirements to complete this dissertation.

I acknowledge the company that I work at for allowing me to perform this study at their petroleum plant.

I would like to thank my supervisor Prof Pavel Tabakov for all of his support. Behind an excelling student is a dedicated supervisor.

I would like to thank my family for their constant motivation, encouragement, and support.

Nomenclature

E	Weld quality factor
S	Allowable stress range
t	Pipe thickness
W	Weld joint reduction

Abbreviations

ASME	American Society of Mechanical Engineers
ASTM	American Society of Testing and Materials
FEA	Finite Element Analysis
OSH ACT	Operational Safety and Health Act
SANS	South African National Standards
SIF	Stress Intensification Factors
UDL	Uniformly Distributed Load

List of Figures

List of Tables

Table of Contents

CHAPTER 1

1.0 Introduction

1.1 Description of Study

The thesis focuses on the analysis of piping systems in the petroleum industry. Petroleum plant processes or handles petroleum and products that are derived directly from it. Typical plants are gasoline recovery plants, treating plants, gas or lubricant processing plants. Many inconsistencies that have existed in the field of piping design increase the risk of potential failures. Maximum assurance of safety would require a thorough understanding of the effects of primary and secondary loads experienced and the effects of combinational loads. Failures become difficult to predict using general engineering analytical methods when a system is complex. A system fails when the stresses and strains experienced from severe different loads reach a critical value. Static loading forms only one part of the influence of stresses on piping systems. The manner of application, occurrence, duration, and frequency of loadings is just as important. More often failures occur over many years from the repetitive applications of temperature and pressure variation which results in fatigue on piping. Rapid dynamic loading is another call for concern which effects can lead to the possibility of direct shock failure and brittle fractures.

The study specifically focuses on the analysis of piping systems at Indy Oil's petroleum plant. Improper design of a piping system can also cause failure to connected process equipment. The plant experienced pump failures, cracks on process equipment connections, piping joints failures, weld failures, and piping support failures. All failures can lead to production downtime or the harming of life. Both of these circumstances result in a negative impact financially on the business.

The interpretation of the mechanical nature of piping materials will ensure the accuracy of predictions. The most cost-effective, commonly used, and versatile material available in the petroleum industry is steel. The mechanical properties of steel allow it to be put to a wide variety of different uses. Although there is a vast amount of data available on the material science for steel, analysing challenges are faced when a system is complex and the material experiences simultaneous loading.

Piping is a combination of a mechanical structure and a pressure vessel. Therefore the studies, techniques, and experience available in these fields are used to improve the analysis of piping systems.

The field of applied mechanics related to piping systems is treated in great detail. Techniques to calculate the stresses and strains from independently applied loads must be adopted. The effects of various independently applied loads are first analysed thereafter the effects of simultaneous loading are studied. This will result in a more rigorous analysis which will increase the accuracy of results.

Design principles and formulas in both national and international statutory design codes for pressure piping in the petroleum industry are applied as a basis for the study. The purpose of the pressure piping design code is to ensure the uniform application of engineering principles throughout the petroleum industry. The design and selection guide is applied as a minimum thereafter a more rigorous analysis is done. Piping elements and components are specified according to the American Society of Mechanical Engineers (ASME) codes listed standards. References were made to ASME code listed standards that detail material specifications, dimensional requirements, and pressure-temperature ratings.

1.2 Problem Statement/ Aim

The aim of the study, through research and interpretation of theorical analyses, is to aid in the design and stress analysis of piping systems for the petroleum industry. The use of this study will reduce the number of revisions required during piping systems conceptual and detailed design. The application of the data and conclusions of this study on small to medium scale projects will remove the need for detailed stress analyses.

The following must be addressed:

- Stresses-strain contributions from dead load and applied loads.
- The fluid dynamics of piping systems resulting in internal pressure gains.
- The critical combinations of loads causing a component or system failure.
- Application of applied mechanics, plasticity & rheology.
- The effects of structural changes in piping components due to creep.
- The effects of thermal expansion of both material and fluid. Predictions of thermal load straining simulated through fatigue failure by mechanical loading.
- Interpretation of results to identify the cause of failures on previously installed piping systems.

1.3 Research Methodology

- The review and understanding of historical literature until presently used data. Understanding the development of analytical approaches and the tests that were done to determine various equations.
- Existing systems failure identification, to understand the cause of failure on various systems and the factors that were under-compensated for or neglected.
- Develop and apply analytical and numerical equations for stress evaluations from sustained and thermal loading.
- Develop and apply analytical and numerical flexibility analysis on piping systems.
- Computer FEA analysis of complex piping systems

1.4 Literature Review

Iron pipe was first used for petroleum products just after 1859 when the first commercial oil well was drilled by Colonel Edwin Drake in Pennsylvania. A pipe is defined as a pressure-tight cylinder used to convey a fluid or for the transmitting of fluid pressure. The first pipes used for the petroleum industry were short and basic. Pipes were used for transferring oil from drill holes to nearby tanks and refineries. The increased need for product led to the growth of refineries and the need for more piping, for transfers between process equipment (Materials, 2017). The piping engineer had very little information for guidance in the evaluation of piping which made it difficult to guarantee a safe and reliable system. Most piping failures occurred after many years of service which resulted from deterioration with time and fatigue. The increased need for pressure piping analysis became apparent after the many failures of pressure equipment like boilers and steam engines (J.E Meyer, 2014).

Studies and tests on petroleum piping analysis were conducted dating back to the 1800s. This information was used to determine stresses and strains experienced and what could cause failure. These component behavioural predictions prevented many failures but some of these predictions were incorrect which led to many more failures. Another reason for failure was the oversight of some stress contributors. Failures called for more investigation and tests throughout the years which improved the information available to engineers for guidance in predictions of overstress and failure. (J.E Meyer, 2014)

A piping system is an irregular space frame that experiences stress and strain from initial fabrication, site erection, and various circumstances during operation**.** All piping analysis is based on the principles of strength of materials. The variation in publications on piping analysis is the manner of application of strength of materials and the approach to analyse the space frame. A piping system is exposed to multi-axial stresses. The analysis of piping systems requires the application of Mohr's circle, failure theories, stress intensity (Tresca stress), von Mises stress, and beam formulas. To obtain a practical result the principles of the finite element method were adopted by piping designers. The system was broken down into two elements, straight pipe, and curved pipe. Each element has a node at the beginning and one at the end, with each node having six degrees of freedom, three in translation, and three in rotation. Therefore each node is associated with three displacements, three rotations, three forces, and three moments. Before a piping system is analysed all elements on the system have to be identified. Each node's stiffness matrix forms part of the overall matrix for analysis. The more complex a system is the more complicated and tedious the finite element calculation is. The analysis of piping systems is broken up into 1.Primary loads - sustained loads; 2.secondary loads - thermal expansion (flexibility) and 3.localized stresses. (Peng L.-C. (., 2009) (Nayyar, 2000) (Don Mckeehan, Design of Piping Systems, 1941) (Botermans, 2008)

Theory developments:

In 1926 Hovgaard developed a theory for calculating principle stresses from sustained loads in piping which resulted in transverse stresses being higher than longitudinal stresses. He later

established a different conclusion that states that the transverse stress chances of failure are very low and can be ignored. He explained that transverse stresses only produce local yielding.

A.M. Wahl initially concluded after an investigation that bending stresses are negligible but later in another publication stated that bending stresses must be considered.

Van den Broek published that reduced stiffness in one plane would increase rigidity in the transverse plane. Hovgaard challenged this theory and stated that this occurred from the redistribution of stresses. (Don Mckeehan, Design of Piping Systems, 1941) (Markl, 1955)

Before computers were invented it was very difficult or impossible to calculate the exact stresses from sustained loads for complicated piping systems. Therefore, a simplified analytical approach was required. Wahl and Hovgaard developed an analysis for single-plane bends which was later modified by Shipman to be applied to any single-plane problem to determine principle stresses, moments, and forces in piping. This method helped designers who did not have much knowledge of mechanics but the results produced were of low accuracy. Improvements were done by Tingey who further modified the approach to include the virtual centre of gravity and the introduction of conjugate axes. Karelitz and Merchant extended the approach to space lines. After further investigation, Hovgaard restated his formulae to be applied to multi-plane bends which include secondary effects. The MW Kellogg recognized the advantages of the method to analyse multi-plane bends and further developed it to be used on all other components and restraints. (Don Mckeehan, Design of Piping Systems, 1941) (Don Mckeehan, Design of Piping Systems, 1956)

In the early 1900s, the first analysis of the flexibility of piping from thermal expansion was observed and reported by Dr A Bantlin. The results proved higher stress increases than primary loading. Bantlin also stated that the corrugations or wrinkles in the pipe wall formed during manufacturing were the reason for added flexibility obtained. Three other experts in the field of engineering in the 1900s namely Dr Th. v Karman, M. Marbec, and Prof. Lorenz all performed tests and studies independently and resulted in similar conclusions but not in line with Dr Bantlins statement. The others concluded that the bending couple forced the concave and convex side towards the neutral axis with a concurrent increase in the angular deflection. (Don Mckeehan, Design of Piping Systems, 1941) (Kannappan, 1986) In 1955, ARC Markl published work on the flexibility analysis of piping which is regarded as the major breakthrough in this field. His paper focused only on the importance of providing flexibility in piping and the problems experienced in the industry. He intended to find the balance between the scientific truth and the simplicity of analysis which can be used on a wide range of problems. Standard practice at the time was the use of expansion joints but over time it was preferable to utilize the flexibility of the pipe run to act as a spring in tension and torsion to compensate for the thermal expansion. A completely separate analysis from primary loading was generated to calculate forces, moments, and stresses from the influence of thermal expansion on piping. Flexibility analysis focused more on piping components rather than straight pipe because of the increased flexibility in components. A simplified step by step approach to determine stresses and strains from thermal expansion for any piping material and process fluid was developed. The analysis was based on data from tests on straight pipes stress, bending moment, flexibility, and fatigue limits. Fatigue tests were performed on two straight

lengths of pipe, butt welded together that were cyclic stressed until failure. All other piping components were based on a factor of the flexibility and stress intensity of straight pipe. It is the ratio of rotation per unit length of the component produced by a moment, to the rotation per unit length of straight pipe of the same nominal size, material, and thickness. Piping bends produced the highest flexibility in a system therefore these were used to create expansion loops along long lengths of pipes. (Markl, 1955) Woods and Rodabaugh verified the stress intensification factors by lab test simulations. (Woods, WFI/PVRC Moment fatigue tests on 4x3 ANSI B16.9 Tees, 1989) (Rodabaugh, 1994) The progressive effects of fatigue from thermal expansion can be divided into the following three stages: Crack initiation, crack propagation, and unstable rupture. In piping, this fatigue is considered high cycle fatigue which is stress-governed because it involves almost no plastic action. The cumulative method is used to determine the cycle life of piping. (Nayyar, 2000) (Peng L.-C. (., 2009)

Historical piping failures highlighting the consequential damage:

The Flixborough plant in England processes caprolactam and cyclohexane (petroleum products) to produce nylon. The heat variation on the piping to the reactors during plant operation and shut down caused fatigue. Inadequate supports also resulted in overstressing of the piping and bellows. The pipe and bellows cracked and released flammable vapour which ignited and caused an explosion. This killed twenty-eight people. (A.Crowl, 2011)

A major fire occurred at a Louisiana Refinery on the 2nd of August 1993, costing the company 65 million dollars in damage. A 45-degree elbow along a pipeline to a coker unit exploded. The cause being the overstress from primary loads. The materials allowable stress was too low for the application. (Sanders, 2005) (Fullwood, 1989)

In October 1992, a six-inch elbow made of carbon steel ruptured due to cyclic loading during processing, releasing a hydrocarbon mixture. This failure happened in Los Angeles. The vapour mixture ignited causing an explosion that damaged equipment and the buildings nearby costing the refinery 78.3 million dollars in damage. (Sanders, 2005)

An eight-inch pipeline failed due to overstress while operating at sub-freezing weather conditions in December 1989. The designer did not determine the effects of combinational loads in the design. A factor of safety would have prevented failure during normal operating conditions but the decrease in allowable stress values at extreme temperatures failed. (Sanders, 2005)

An LPG pipeline in Mexico City ruptured and released the Liquefied Petroleum Gas into the atmosphere. The gas ignited causing an explosion that spread to six spheres and 48 bullet tanks. A total of 500 people died from this failure. The cause was the rupture of a pipeline during service and led to a leak of LPG. (Sanders, 2005) (Fullwood, 1989)

MW Kellogg published a book in 1956 on the Design of Piping systems which was developed from analysing and improving all existing data on piping designs, tests, and failures. Another publication that changed the approach of piping analysis worldwide. The publication included analytical methods for the forces, moments and stresses in piping systems, as well as

improvements on the Flexibility analysis method developed by Markl. Peng and Botermans published much more user-friendly books using the same principles as Kellogg on the analysis of piping. One statement highlighted in all of these books is these approaches should be the minimum analysis to ensure a safe reliable system. (Botermans, 2008) (Peng L.-C. (., 2009) (Fullwood, 1989)

Engineering committees in the USA recognised and approved of Markls and MW Kelloggs work. They were asked to be a part of the committee in developing the standard code for pressure piping. The functions of standards and rules achieve minimum requirements for safe construction and omissions of which increases operational hazards. All latest publications on the design of pressure piping are based on the Piping-Flexibility Analysis by A.R.C Markl and Design of Piping Systems by The M.W Kellogg Company. (Peng L.-C. (., 2009) (J.E Meyer, 2014)

Failures are not specific throughout the industry. It can be caused by vibration, thermal bowing, flexibility, environmental loading, thermal fatigue, and so forth. The reason being neglecting one loading factor could cause the failure of an entire system. The analysis of specific stresses and strains have advanced throughout the years with greater emphasis by computer programs on the effects of combinational loading. Even though catastrophic failures of piping systems are a rare event if one does occur the damage could be tremendous. A breakdown could result in millions of losses in production or even worse the loss of lives. (Sanders, 2005)

Development of governing design, fabrication, and operating codes:

To regulate and ensure that pressure equipment is manufactured to withstand maximum operating conditions government organisations have developed statutory design codes and standards. The recognition of the need to develop codes and standards was first realised after the invention of the steam engine. Thomas Savery from England successfully manufactured the first steam engine in 1698, which he patented. The Savery engine followed by several improved steam engines gave birth to the beginning of the first industrial revolution. The steam engine provided an economical source of energy that powered machines in factories and aided new forms of transportation to be developed. The construction of the boilers for the steam engines was of simple construction similar to a tea kettle. To generate steam the walls of the boiler were directly heated. These simple boilers were the introduction of pressure containment systems. The first designers and manufacturers of boilers relied solely on their acquired knowledge during development and manufacturer of the boilers. There were no previous studies and governing design codes and standards available to ensure the manufacture of a safe operating steam boiler. The apparent need arose after the many boiler explosions that occurred. From the year 1895 to 1905 there were a total of 3 612 boiler explosions recorded, approximately 1 explosion per day. The loss of life totalled an amount of 7 600 people.

The reliability of steam boilers was clearly defined as a problem and an engineering solution to govern the safety of boilers had to be developed. The first set of rules for the design and manufacturer of pressure equipment was set out by the State of Massachusetts in the USA. Other states in the USA followed by setting up their governing design and manufacturer rules.

No two states had the same rules which caused great difficulties in the validation of steam boilers manufactured for out of state use. There were instances of materials and welding procedures that were deemed safe in one state that was prohibited in another state.

The American Society of Mechanical Engineers (ASME) was founded in the 1880s to highlight concerns of the rise of industrialization and mechanization. Their significance was realised when ASME was requested by various American states and other engineering committees to create a uniform standard specification for the design, construction, and operating of pressure equipment including steam boilers. The first ASME boiler code was submitted for approval on the 5th of February 1915. In the next eleven years, other ASME codes followed relating to the different types of boilers. ASME created multiple committees with expertise in the design, fabrication, and operation of boilers. The committee's duty was to develop governing codes detailing formulated safety rules. ASME later created a code for Pressure vessels which was later understood to be less conservative than the Boiler codes. A code that superseded both the Boiler code and Pressure vessel code was later introduced – ASME Boiler and Pressure Code.

Similar to the introduction of the Pressure vessel code, the code for Pressure piping was introduced. To fulfil the need for a pressure piping code, Project B31 was created in March 1926 with a key representative from the American Standards Association. The wide field in the development of the Piping Pressure code required involvement from about 40 different engineering societies, industries, trade associations, and government bureaus. The first code was published in 1935 as the American tentative standard code of pressure piping. Over the next couple of years, multiple revisions were released due to new developments. The first piping code directly related to Petroleum Refinery piping was published in 1959 with revisions in 1962, 1966, and 1973. Separate codes were published for Chemical Plant piping and Cryogenic piping. The ASME committee realised that the Petroleum Refinery piping, Chemical Plant piping, and Cryogenic piping were all developed using similar principles and theories therefore a single code was released covering all three, named Process Piping.

The units of measurement in the ASME Process piping code is metric as primary and US customary units as secondary.

The regulations set out in South Africa for the safety and health of persons at work in connection with the use of plant and machinery is in the Operational Health and Safety Act (OSH Act). The OSH Act refers to the South African National Standards (SANS) 347 for the hazardous classification and inspection requirements of pressure equipment. The SANS 347 standard is based on the European Directive with changes made for the specific requirements of pressure regulations. Reference is made in the SANS 347 standard to ASME B31.3 for the design, fabrication, installation, and operation of pressure piping in South Africa.

CHAPTER 2

2.0 Piping Systems Stress Analysis

Introduction to Piping Systems

The purpose of piping is to deliver fluid from one point to the desired location in the safest, most reliable, and economic way. A piping system includes all fittings and equipment required for the transfer of fluid in industrial processes. The system includes the interconnection of pipes, pipe fittings, pumps, valves, etc. Piping systems serve as a major component of Petrochemical plant processes. A piping failure could result in downtime of the plant, leading to revenue loss for the company. To optimize fluid processing, process equipment is installed as close as possible, confining the area available for piping.

Piping connections are commonly done by screwed connections, flanged connections, or welded joints. There are advantages and disadvantages to each method of connection.

I. Screwed connections are made by cutting a thread onto the end of a pipe. A pipe fitting manufactured with a threaded end is screwed onto the end of the threaded pipe. This connection is generally used for small diameter pipes working at moderate to low pressures. The advantage of this connection is the ease of assembling and disassembling. However, the disadvantage is screwed connections are prone to leakage.
II. Flanged connections use flanges at the end of pipes that are connected using bolts. It also has the advantage of assembling and disassembling but can within higher pressures than screwed connections. A gasket is installed between the flanges to aid with sealing. Any misalignment of the flange faces could lead to fluid leaking out of the piping.
III. Welded connections are done by welding one end of a pipe to the end of another pipe or a pipe end to pipe fittings. Although the installation of welded piping is more challenging, there are many advantages of this connection. The possibility of a leaking connection is eliminated. Maintenance over time is greatly reduced compared to screwed and flanged connections. Welded joints are more flexible therefore simplify the design.

A piping system is a tubular frame structure that is supported in a manner that prevents its weight from being transferred to the equipment being serviced. Supports prevent sagging of the piping but also allow free movement of the piping as a result of expansion or contraction. The supporting structure must cater to the weight of the fluid, the weight of the piping, and dynamic loadings during operation. The most effective method of determining forces and moments at pipe joints is by modelling the piping system as a frame and applying the classical beam theories principles.

Piping Stress Analysis

There have been many piping failures in the petroleum industry. From careful observation of a failed system, one will notice possibly a failed weld, pipe section that failed, or a joint that separated. The first reaction to this is usually that the material is not fit for purpose. While improper material selection or material impurities is sometimes the cause, more than often an improper design is the cause of over-stressing piping material. A piping system where pipe stress has not been carefully considered can face detrimental problems when putting into operation.

Stress analysis of a piping system is an integral step in the design process. The main objective of piping stress analysis is the prevention of premature failure of the piping system by ensuring the stresses experienced are kept within the allowable limits. A proper analysis can optimize the design which can reduce the installation and operating costs. A stress analysis also maintains the reliability and safety of the system. Many designers use their experiential knowledge and rule of thumb to design piping systems. These methods may result in a working system but are more than likely to increase installation and operational costs.

The analysing of stresses caused by a piping system is a design function that considers the piping layout, pipe supports, and the hydraulic profile of the system. Each stress contributor affects the other therefore the effects should be greatly understood. One of the biggest challenges faced by a piping designer is the balance between systems stress reduction and layout optimization. Frequent situation piping designers face is the impractical routing of piping to reduce stress on the system.

The design should account for occasional primary loading, as well as, infrequent occasional loads such as fluid transients, civil settling, natural disasters, etc., which overstress piping if not accounted for. The loads experienced by a piping system are classified as either Primary (Sustained) Loads or Secondary (Expansion) Loads. Primary loads are forces and stresses experienced during normal operation from dead weight and pressure. Secondary stresses are due to the displacements of the piping system from thermal expansion.

A petroleum piping system should follow the following design procedure:

I. Process parameters are set or calculated i.e. flow rates, design temperature, design pressure. The piping system is designed according to the process parameters which are not determined by the piping designer. These parameters are usually determined by a Process Engineer.
II. A piping layout is modelled including all process equipment. The layout is done with a sufficient understanding of stress and strain contributors, pipe thermal expansion, and pipe support positioning.
III. Piping dimensions are determined based on the relationship between the pipes' internal pressure to the velocity of the fluid. A pressure analysis is done using Fluid Dynamics theories and principles.

IV. Stress and strain due to internal pressure are calculated using the Failure Theories namely Tresca criteria and von Mises failure theories.
V. Tubular frame analysis is performed on the piping system using the classical beam theories to determine the forces, moments, stresses, and strains experienced due to dead weight.
VI. The effects of secondary stresses are calculated due to the temperature cycle of the system using Fracture mechanics theories and principles.
VII. The piping material is then selected based on the compatibility of the fluid carried in the pipe. The combinational stresses and strains experienced by the piping system shall be less than the materials allowable stress range. Material thickness is critical to the allowable stress range of the material.

Analysing the steps taken for a piping system one can neglect a stress contributor. A piping system can be implemented without considering one of the stress contributors to the system which could lead to failure.

Piping Failures Experienced

The object of much attention is the specific failures that occurred at Indy Oils petroleum plant. This study aims at determining the failure modes for these types of failures thereafter create design guides to prevent designers and fabricators from repeating these mistakes. The following failures were experienced:

I. Cracks on piping welds
II. Failure of piping supports
III. Failure of piping joints
IV. Cracks on process connections
V. Pump cracks

During every stress contributor study, the failure limiting factors shall be understood. Thereafter the failure mode relations to the above failures will be determined.

Material Selection

To ensure the safety and reliability of pressure equipment, all pressure equipment is governed by safety standards and codes that are developed by various engineering bodies. The equations developed for allowable temperatures, stresses, pressures, and forces in a specific code relates to a specific type of material or materials. The selection of materials is based on the following criteria:

Pressure – The pressure experienced by piping can range from below atmospheric pressure to high above atmospheric pressure. On the lower end of the pressure scale, a pipe could experience pressures slightly below atmospheric pressure to full vacuum. The effects of negative pressure on a system can collapse a pipe or piping system. Higher pressures can cause a pipe or piping system to explode like a bomb. Fractures could also occur on the pipe wall

resulting in the release of fluid into the atmosphere. In instances of piping carrying dangerous fluids that are flammable or toxic, this could result in the harming of life.

Temperature – The properties of material change with the change of temperature of the material. At higher temperatures the stiffness and strength of the material reduce. At lower temperatures, ductile materials behave like brittle materials and vice versa at higher temperatures. The growth and shrinkage of material are also affected by the change of temperature. Most materials tend to creep over time when exposed to elevated temperatures.

Commodity – At a minimum, the compatibility of the piping material to the fluid it carries needs to be determined. Incompatibility between the piping material and fluid can lead to material breakdown and corrosion. The corrosion rate of the material effects the life of the piping system and the product preservation of the fluid in the pipe.

The equations developed in the ASME B31.3 code are based on the listed materials specified in the code. All listed materials have been rigorously tested by the American Society of Testing and Materials (ASTM) to determine the materials allowable temperature range, Tensile Strength, and Yield Strength. Figure 1.4-1 below is extracted from the ASME B31.3 code which lists the acceptable materials and their properties.

Dissimilar materials - All materials expand or contract at different rates. The rate of expansion is expressed as the thermal expansion coefficient. When two different piping materials are welded together, thus having different expansion coefficients, differential radial thermal expansion will occur. This radial thermal expansion will result in secondary stress at the weld. In the instance of flanged connections of a different material or varying piping and piping support materials, the same phenomenon will be experienced. The thermal expansion data is detailed in Appendix G.

(14)

Table A-1M Basic Allowable Stresses in Tension for Metals (Metric)

Numbers in Parentheses Refer to Notes for Appendix A Tables; Specifications Are ASTM Unless Otherwise Indicated

Line No.	Nominal Composition	Product Form	Spec. No.	Type/ Grade	UNS No.	Class/ Condition/ Temper	Notes	Min. Temp., °C (6)	Min. Tensile Strgth., MPa	Min. Yield Strgth., MPa	Max. Use Temp., °C
1	Fe	Castings	A48	20	F11401	...	(2)(8e)(48)	−30	138	...	204
2	Fe	Castings	A278	20	F11401	...	(2)(8e)(48)	−30	138	...	204
3	Fe	Castings	A126	A	F11501	...	(2)(8e)(9)(48)	−30	145	...	204
4	Fe	Castings	A48	25	F11701	...	(2)(8e)(48)	−30	172	...	204
5	Fe	Castings	A278	25	F11701	...	(2)(8e)(48)	−30	172	...	204
6	Fe	Castings	A48	30	F12101	...	(2)(8e)(48)	−30	207	...	204
7	Fe	Castings	A278	30	F12101	...	(2)(8e)(48)	−30	207	...	204
8	Fe	Castings	A126	B	F12102	...	(2)(8e)(9)(48)	−30	214	...	204
9	Fe	Castings	A48	35	F12401	...	(2)(8e)(48)	−30	241	...	204
10	Fe	Castings	A278	35	F12401	...	(2)(8e)(48)	−30	241	...	204
11	Fe	Castings	A48	40	F12801	...	(2)(8e)(9)(48)	−30	276	...	204
12	Fe	Castings	A126	C	F12802	...	(2)(8e)(9)(48)	−30	283	...	204
13	Fe	Castings	A278	40	F12803	...	(2)(8e)(9)(53)	−30	276	...	343
14	Fe	Castings	A48	45	F13101	...	(2)(8e)(48)	−30	310	...	204
15	Fe	Castings	A48	50	F13501	...	(2)(8e)(48)	−30	345	...	204
16	Fe	Castings	A278	50	F13502	...	(2)(8e)(53)	−30	345	...	343
17	Fe	Castings	A48	55	F13801	...	(2)(8e)(48)	−30	379	...	204
18	Fe	Castings	A48	60	F14101	...	(2)(8e)(48)	−30	414	...	204
19	Fe	Castings	A278	60	F14102	...	(2)(8e)(53)	−30	414	...	343
20	Fe	Castings	A197	...	F22000	...	(2)(8e)(9)	−30	276	207	343
21	Fe	Castings	A47	32510	F22200	...	(2)(8e)(9)	−30	345	224	343
22	Fe	Castings	A395	60-40-18	F32800	...	(2)(8d)(9)	−30	414	276	343
23	Fe	Castings	A571	D-2M	F43010	1	(2)(8d)	−30	448	207	40

Figure 1.4-1: *Material properties table (ASME, 2017)*

Chapter Summary

A piping system experiences multiple loading throughout its serviceable life. The following sections detail the loadings experienced by a piping system and the importance that each section has on the design and life of a piping system. This chapter is organized into four sections based on the design procedure detailed above:

2.1. Fluid Dynamics in Piping Systems
2.2. Primary Stresses due to Internal Pressure
2.3. Primary Stresses due to Dead Weight and Dynamic Loading
2.4. Secondary Stresses on Piping systems - Flexibility analysis

2.1 Fluid Dynamics in Piping Systems

Piping components used in the Petroleum industry are manufactured out of various steel grades. A wide range of pipe diameters is manufactured for each material grade. Pipe diameters are further broken down into various thicknesses. Depending on the application of the system, the pipes wall thickness shall be suitability specified to withstand overstress, damage, collapsing and buckling of the pipe wall. Pipe thicknesses are specified according to their pressure rating. In other words, the maximum allowable pressure that the pipe can experience.

The minimum allowable thickness of piping components under internal pressure is calculated using the following equations:

Straight Pipe:

$$t = \frac{PD}{2\,(SEW+PY)} \qquad (2.1\text{—}1)$$

Where:

P - Internal pressure (Pa)
D - Pipe outside diameter (m)
S - Allowable stress (Pa) - Defined in figure 2.1-1
W - Weld joint reduction factor - See Appendix A
E - Weld quality factor - See Appendix B
Y - Coefficient See Appendix C

Pipe bends:

$$t = \frac{PD}{2\,(SEW/I+PY)} \qquad (2.1\text{—}2)$$

Where:

I at intrados (inside bend radius) $= \dfrac{4\left(\frac{R_1}{D}\right)-1}{4\left(\frac{R_1}{D}\right)-2}$

I at extrados (outside bend radius) $= \dfrac{4\left(\frac{R_1}{D}\right)+1}{4\left(\frac{R_1}{D}\right)+2}$

R_1 = Bend radius of the pipe bend

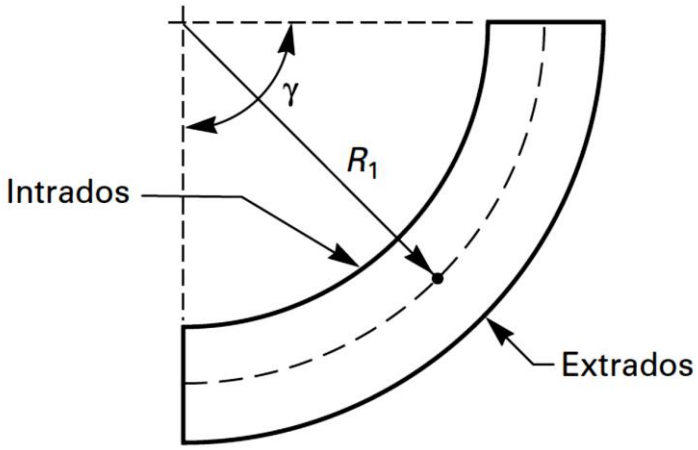

Figure 2.1-1: *Pipe bend (Engineers, 2014)*

Quality factors are determined from experimental tests to compensate for the reduction in strength of a joint or material due to welding or casting. The strength of welded joints reduces compared to that of parent metal when temperature cycles are experienced. The weld joint strength reduction factor is the ratio of a weld joint failure stress to that of parent material failure stress over the same duration. The same rules apply to the different types of castings.

One of the key calculations that a piping designer needs to perform is to determine the internal pressure experienced by a piping system. The design pressure of all components in a piping system shall not be less than the most severe case of pressure experienced. This shall be used as a basis to specify the dimensional properties of the system. The internal pressure experienced in a pipe is calculated using Fluid Dynamics principles and theories. The magnitude of pressure is related to fluid viscosity, the velocity of the fluid, and pipe internal diameter. The theories and equations in the following subsection shall be applied to determine internal pressure experienced in a piping system.

There are two types of fluid flow within conduits namely closed conduit and open conduit. Both types are similar barring closed conduit does not have a free surface exposed to the atmosphere. The pipe flow is a closed conduit system, but the system is only classified as pipe flow when it operates at full capacity. Fluid flowing through the conduit only exerts hydraulic pressure and not atmospheric pressure. The energy in pipe flow is expressed as a pressure head which will be explained further in this chapter.

One of the main causes of stress in piping is from the frictional effects of fluid flow in piping. The behavioural properties of fluid flow in piping are governed by the effects of fluid viscosity and the gravitational forces relative to the inertial forces of the flow. The categorisation of liquids is done by their behavioural properties when undergoing shear. The viscosity of a fluid is the measure of liquids shear rates. Liquids that maintain a constant shear rate with a change of velocity are classified as Newtonian. Liquids that experience a change in shear rates with varying velocity are classified as Non-Newtonian.

The theory of fluid flow is greatly understood although theoretical solutions are mainly true to fully developed laminar flow. No two systems are exactly alike therefore to fully determine the exact properties of a system: empirical relations or experimental lab tests must be conducted. An error factor or factory of safety should always be added to the theoretical results obtained.

The primary stress in piping is caused by internal pressure which is directly related to frictional forces. Pressure drop in piping is the primary consequence of friction in fluid flow. The friction between the fluid particles also causes a slight increase in the temperature of the fluid due to sensible thermal energy created during the conversion of mechanical energy. But for most systems, this frictional heating is too small to alter the results, therefore, is disregarded. For applications with very high viscosity fluids, fluid friction can result in high-temperature spikes.

To calculate the internal pressure of piping systems the theory of flow patterns, pipe velocity profiles and the Reynolds number needs to be understood. These theories are used to develop the equations for pressure drop in piping due to frictional forces, change in kinetic energy, and gravitational forces.

2.1.1. Flow Patterns

Fluid flow in piping can be categorized into two forms namely Laminar flow and Turbulent flow. This phenomenon was first discovered by a British scientist Osborne Reynolds. Reynolds set up an experiment using pipe, dye, and water to distinguish the difference between the two classifications. The dye streak along the flow path showed distinct patterns at different flow rates.

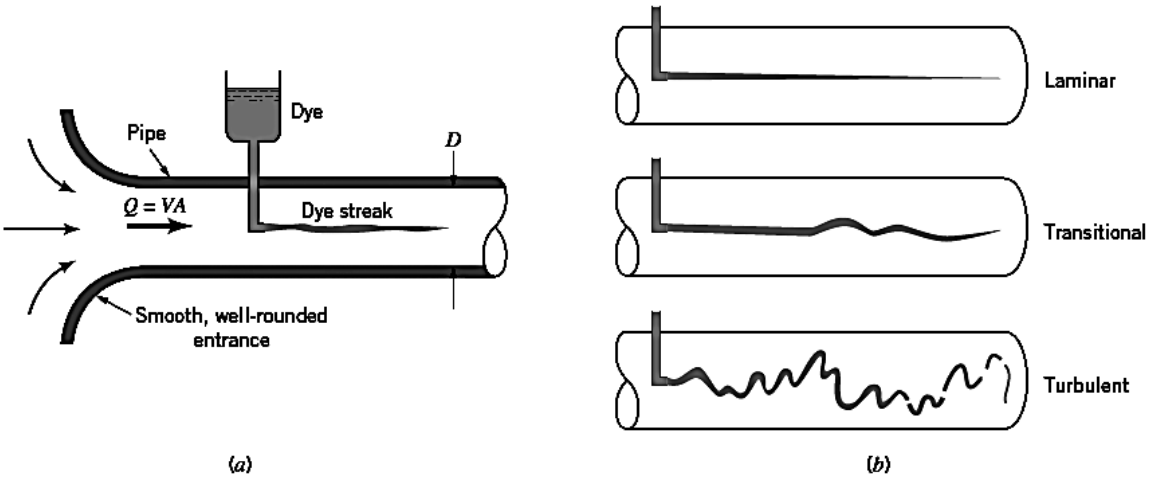

Figure 2.1-2: *Flow pattern experiments (Churchill, 1987)*

It was noticed by injecting neutrally buoyant dye into water that flowed through a pipe of diameter D at an average velocity V. At low flow rates, the introduced dye would form a well-defined line along the flow direction, with slight ripples caused by molecular diffusion between the dye and water. At higher intermediate flow rates the dye streaks fluctuated along the flow

direction. For large flow rates, the dye almost instantly scatters all over the pipe in a nonuniform manner.

Laminar flow is characterized by smooth streamlines of highly ordered motion with no cross-currents perpendicular to the flow layers. The fluid flows as parallel layers with no interruption or swirls of fluid between the layers. The layers slide over each other without adjacent mixing. This flow regime is characterized by great momentum diffusion and slight momentum convection. To help describe the difference between laminar and turbulent flow in non-scientific terms, laminar flow can be classified as smooth while turbulent flow as rough.

Turbulent flow has high-velocity fluctuations and highly disordered motion. The turbulent flow regime is characterized by low momentum diffusion and high momentum convection. Along the flow path, many vortices form and interact with each other. The chaotic properties of the fluid flow increases drag through boundary layer skin friction. The irregular fluctuations and mixing of the fluid in turbulent flow results in high momentum transfers between fluid particles which increase the frictional force on the surface of the piping. This affecting the internal pressure on the piping which causes higher stresses on the piping.

The flow remains laminar in a pipe at low velocities and moves towards turbulent as the velocity increases. The transitions from laminar flow to turbulent flow do not occur suddenly. This transition happens over a region at which the flow fluctuates between laminar and turbulent until becoming fully turbulent flow. The transition depends on several factors including geometry, flow velocity, viscosity, surface roughness, temperature, etc.

2.1.2. Velocity Profile

A boundary layer appears in a fluid flowing when it comes into contact with a stationary surface. The fluid layer in contact with the pipe surface comes to a complete stop due to the no-slip condition. The molecules in direct contact with the surface of the pipe are brought to a complete stop due to the microscopic roughness of the pipe wall surface. This layer has a ripple effect causing adjacent layers to gradually slow down by viscous action. Due to viscosity, shear is experienced between the fluid layers which are expressed by $\tau = \mu \frac{dv}{dy}$. This results in a layer of fluid near the surface of the pipe wall where the velocity changes from zero at the pipe wall to the free stream velocity of the fluid. The term used for this phenomenon is the *boundary layer*. To make up for this velocity reduction, the midsection of the pipe which experiences the least amount of resistance increases in velocity. This results in a velocity gradient developing along the pipe.

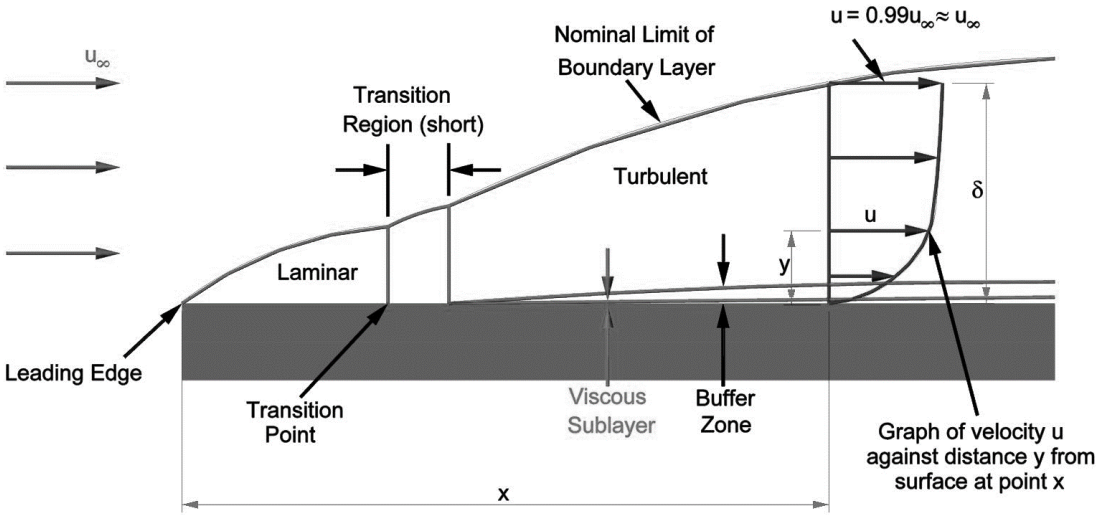

Figure 2.1-3: *Boundary conditions (Cimbala, 2004)*

The average velocity in a pipe can be determined from the requirement of the conservation of mass principle

$$\dot{m} = \rho V_{avg} A_C = \int_{A_C} \rho u(r) dA_C \qquad (2.1—3)$$

Where:

$\dot{m}$	- mass flow rate
ρ	- density (kg/m^3)
A_c	- cross sectional area (m^2)
$u(r)$	- velocity profile (m/s)

The above formula can be manipulated to determine the average velocity for incompressible flow in a pipe of radius R.

$$V_{avg} = \frac{\int_{A_C} \rho u(r) dA_C}{\rho A_C} = \frac{\int_0^R \rho u(r) 2\pi\, r\, dr}{\rho \pi R^2} = \frac{2}{R^2} \int_0^R u(r) r\, dr \qquad (2.1—4)$$

2.1.3. Reynolds Number

The Reynolds number is a dimensionless number used to determine flow patterns. Using the Reynolds number, referred to as Re, flow can be categorised as either laminar or turbulent. The flow regime is dependent mainly on the ratio of inertial forces to viscous forces in the fluid as discovered by Osborne Reynolds in the 1880s. This ratio is called the Reynolds number. When the inertial forces are dominant which resist a change in velocity and are the object of fluid movement, the flow is classified as Turbulent. Otherwise, when viscous forces are dominant which resists fluid flow, the flow is classified as laminar.

$$R_e = \frac{Inertial\ forces}{Viscous\ forces} = \frac{V_{avg}D}{v} = \frac{\rho V_{avg}D}{\mu} \quad (2.1—5)$$

Where:

V_{avg} - average flow velocity (m/s)
D - diameter (m)
v - kinematic viscosity (m^2)

Reynolds conducted experiments using various tube diameters at various temperatures. It was observed that a flow initially laminar, changes to turbulent when the ratio of inertial forces to viscous forces in a fluid reaches a certain value. This value is expressed as the critical Reynolds number Re_{cr}. The experiments also showed that any change of the variants did not affect the laminar state as long as the value for Re was below the critical Reynolds number. Above this value, the flow would customarily be turbulent. Looking at the Reynolds number equation it is evident that high viscosity fluids in the same diameter pipe achieve laminar flow. In the case of large inertial forces relative to viscous forces, random and rapid fluctuations of the fluid cannot be prevented therefore the flow is turbulent. It is ideal to have precise values of Reynolds number but the degree of disturbances during operation continuously alters the results.

The following assumptions and conclusions can be made based on the understanding of the Moody diagram and the boundary layer phenomena:

I. The pipe flow is laminar for Re ≤ 2300 and is independent of the roughness of the pipe wall.
II. 2300 ≤ Re ≤ 4000 – A Reynolds number between this region is referred to as the critical zone or transitional region. The flow can be either laminar or turbulent.
III. Beyond Re = 4000 the flow is turbulent. At this point, the Reynolds number is dependent on surface roughness.
IV. Considering that the laminar sublayer is very thin, if the surface roughness is large, it will protrude past the laminar sublayer and cause obstruction. In this situation, the flow is classified as fully turbulent. In this region, frictional forces are independent of the Reynolds number.
V. When the surface roughness is fully covered, this situation is referred to as hydraulically smooth. Frictional forces are calculated using formulas and curves for smooth pipes.
VI. The Moody diagram is valid for all Newtonian fluids. For which: $\tau = \mu dv/dy$.

2.1.4. Pressure Drop

The main focal point on Fluid Dynamics for this thesis is the analysis of pressure drop in piping generated from frictional forces between the fluid and pipe wall. The pressure drop in a piping system is used to determine the primary stresses experienced by a system. As fluid flows through a pipe pressure drops occur as a result of the resistance to flow. Pressure loss is

dependent on the geometry of the pipe fittings that the fluid flows through. One of the most effective methods to optimize the pressure in a piping system is by adjusting the pipe diameter.

Many competing forces influence the drop/gain in pressure:

- Friction between the pipe surface and fluid
- Friction between the adjacent layers of the fluid flowing through the pipe
- Friction loss at pipe fittings, bends, valves, expansions joints.
- Pressure loss due to elevation difference along the run of the pipe
- Pressure gain from the piping systems pump

In summary from the points listed above the change in pressure is the sum of the following three factors:

I. Pressure change due to gravitational forces – Change in elevation
II. Pressure change due to change in kinetic energy
III. Pressure change due to frictional effects

The first two factors can be classified as reversible changes. Meaning that the loss/gain can be reversed by reversing the process. The third factor (friction) is an irreversible process always resulting in a loss in pressure in the direction of the flow, where mechanical energy is converted into heat during the process.

The derived equation from basic thermodynamics for change in pressure for fluid flowing is represented as:

$$dP = -(\rho g dz + \alpha \rho V dV + \frac{1}{2}\rho V^2 df) \qquad (2.1—6)$$

Where:

z - elevation of pipe above datum (m)
α - kinetic energy factor
V - fluid velocity (m/s)
f - friction coefficient

Equation 2.1.4-1 is derived from the three main factors that influence pressure change namely Gravitational forces on the fluid, Kinetic energy of the fluid, and lastly frictional forces.

The kinetic energy factor (α) accounts for the variance in velocity as described previously. The factor changes according to the flow regime through the pipe.

Pressure Loss due to Frictional Forces

Many equations to calculate Pressure loss have been formulated. Each equation has limitations to its range of applications for the parameters used during development. The most suitable equation for industrial piping is the Darcy-Weisbach equation. The Darcy-Weisbach equation

is named after Henry Darcy and Julius Weisbach, the two researchers who have made the greatest contribution in the development of the formula.

The derivation of the Darcy-Weisbach equation is shown below:

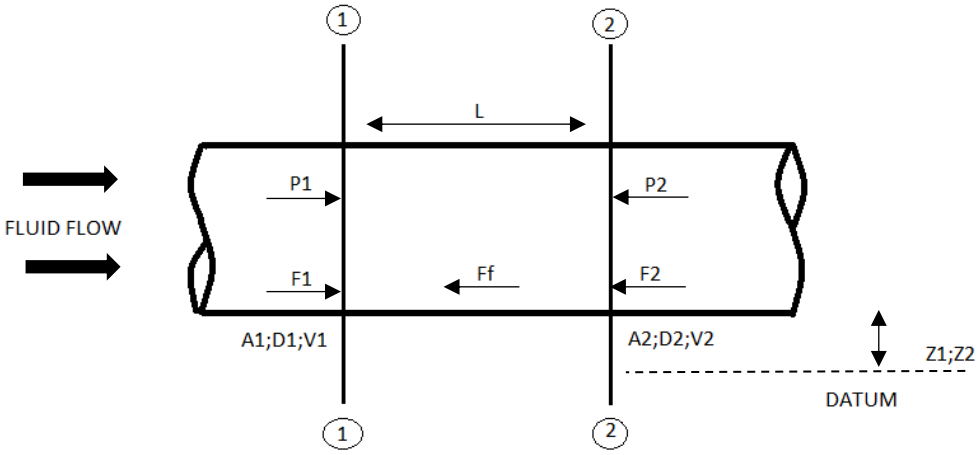

Figure 2.1-4: *Pipe flow analysis*

Apply Bernoulli's equation from Point 1 to Point 2 in Figure 5 above:

$$\frac{P_1}{\rho g} + \frac{{V_1}^2}{2g} + Z_1 = \frac{P_2}{\rho g} + \frac{{V_2}^2}{2g} + Z_2 + hf \qquad (2.1—7)$$

Where:

P	- pressure (Pa)
ρ	- density (kg/m^3)
v	- fluid velocity (m/s)
z	- elevation (m)
h_f	- head loss due to friction (m)

Since:

- Elevation at point 1 and 2 is equal ∴ Z1 = Z2

- Uniform pipe diameter ∴ velocity is equal through the pipe.

$$\frac{P_1}{\rho g} = \frac{P_2}{\rho g} + hf$$

$$P_1 - P_2 = \rho g h f \qquad \ldots\ldots\ldots (i)$$

Head loss is due to friction and the intensity of pressure is in the direction of flow. Solving for frictional resistance where Frictional force is equal to frictional resistance per unit wetted area per unit velocity x wetted area x velocity squared.

$$F_f = f'.\pi dL\,.v^2 \qquad (2.1—8)$$

Where:

F_f - Frictional force (Nm)

f' - frictional resistance per unit wetted area per unit velocity

v - fluid velocity (m/s)

Since:

- Perimeter = πd = p

$$F_f = f'.p.L\,.v^2 \qquad \text{. . . . . (ii)}$$

If the fluid is moving at a constant velocity, the acceleration is equal to zero. Therefore, the sum of the vector forces must be equal to zero. Solving for forces in the horizontal plane:

$$\Sigma F_x = 0$$

$$F_1 - F_2 - F_f = 0$$

$$P_1A_1 - P_2A_2 = F_f \qquad \text{. . . . . (iii)}$$

Since:

- Uniform pipe diameter $\therefore A_1 = A_2 = A$

$$P_1A_1 - P_2A_2 = F_f$$

$$(P_1 - P_2)A = F_f = f'.p.L\,.v^2 \qquad \text{. . . . . sub (ii) into (iii)}$$

$$P_1 - P_2 = \frac{f'.p.L\,.v^2}{A} \qquad \text{. . . . . (iv)}$$

$$\rho ghf = \frac{f'.p.L\,.v^2}{A}$$

$$hf = \frac{f'.p.L\,.v^2}{A.\rho.g}$$

In equation above:

$$\frac{p}{A} = \frac{wetted\ perimeter}{Area} = \frac{\pi d}{\frac{\pi d^2}{4}} = \frac{4}{d}$$

$$\therefore \qquad hf = \frac{4.f'.L.v^2}{\rho.g.d}$$

Since:

- Uniform pipe diameter $\therefore \frac{f'}{\rho g} = \frac{f}{2}$

Where:

f - co-efficient of friction

$$hf = \frac{4.f.L.v^2}{2.g.d} \qquad (2.1—9)$$

The Darcy-Weisbach equation above is dependent on the friction factor of the pipe.

Pipe friction factor

Experimental studies were performed by many researchers to determine the relationship between the friction factor, Reynolds number, and internal roughness of the pipe.

Nikuradse performed experiments by sticking grains of sand at constant size onto the inside of the pipe wall. He recorded the flow resistance at different grain sizes. Moody, Blasius, and Colebrook also performed experiments to determine the function of friction in terms of Reynolds number and the internal roughness of the pipe. The most useful is the moody diagram which is a function of friction versus Reynolds number. Moody's experiment compared commercial pipe to sand-covered pipe and determined the equivalence thereof.

There are various equations and charts formulated to determine the value off. The most useful of these methods are the Moody diagram and the Colebrook en White formula for fluid in the turbulent region.

$$\frac{1}{\sqrt{f}} = -4\,log_{10}\{\frac{1.255}{Re\sqrt{f}} + \frac{\epsilon}{3.71\,d}\} \qquad (2.1—10)$$

Where:

ϵ - surface roughness (m)

Equation 2.1-10 is implicit for f, therefore, an initial value for f must be guessed and inserted into the right side of the equation. The result must be substituted into the right of the formula. This process must be repeated until the result remains constant.

2.1.5. Minor Losses

Pipe friction losses are categorised into two categories namely Major losses and Minor losses. Major losses are due to friction in straight lengths of pipe and Minor losses are due to the sudden change of velocity of the fluid. The following cases result in Minor losses:

a) Sudden expansion/reduction of the pipe diameter
b) Bends in piping routes
c) Pipe fittings etc.

These effects cause disturbances in the fluid flow. Separation of the flow also occurs which results in the change of Kinetic energy of the fluid into internal energy. The equation below is used to calculate minor losses in piping systems.

$$h_{minor} = \frac{kV^2}{2g} \qquad (2.1—11)$$

Experimental tests were conducted to determine *k* loss coefficients which are generally dependent on the nominal diameter and design of the component. The *k* values for the different minor loss cases are detailed below.

A decrease in pipe diameter:

Table 2.1-1: *k values for the decrease in pipe diameter (Meyer, Applications of Fluid Mechanics Part I, 1995)*

A_2/A_1	k
1.0	0
0.7	0.14
0.5	0.24
0.3	0.34
0.1	0.41

Increase in pipe diameter:

$$\mathrm{h_l} = \frac{(\mathrm{V_1} - V_2)^2}{2\mathrm{g}}$$

Sharp outlet from tank:

$$k = 0.5$$

Inlet to tank:

$$k = 1$$

Pipe bends or elbow:

***Table 2.1-2**: k values for pipe bends or elbows (Meyer, Applications of Fluid Mechanics Part I, 1995)*

$\boldsymbol{Pipe\ diameter\ (inch)}$	$\boldsymbol{k}$	
	90° degree bend	**45° degree bend**
6	0.45	0.45
4	0.51	0.51
3	0.53	0.53
2	0.57	0.57
1	0.69	0.69

Non-full bore valves:

***Figure 2.1-5:** k-values for non-full bore valves (Meyer, Applications of Fluid Mechanics Part I, 1995)*

Valve type	**k**
Foot valve with strainer	2.5
Globe valve completely open	10
Angle valve completely open	5
One way valve swing type	2.5
Ball valve	70
Gate valve completely open	0.19
Gate valve ¾ open	1.15
Gate valve ½ open	5.6
Gate valve ¼ open	24

The results obtained from a single minor loss could be negligible, but studies have shown that the accumulation of minor losses especially in short lengths of pipe, has been detrimental.

2.1.6. Water Hammer

Water hammer is a case of infrequent load occurrence that could result in high-stress results during the operation of piping systems. Rapid disruption of the flow of change in velocity in a pipe causes a pressure surge or wave which will cycle upstream and downstream at the velocity of sound. This instantaneous pressure shock generally occurs when a valve is closed suddenly along with the piping system. The shock wave is revealed by multiple hammer banging-like sounds. Another term for this phenomenon is a hydraulic shock. Unlike primary and secondary stresses which could lead to failure after multiple occurrences, a single occurrence could damage piping and equipment in the system.

<u>A practical explanation of water hammer:</u>

Consider a tank containing fluid at a height H that is connected to a long pipe AB with a valve at the end.

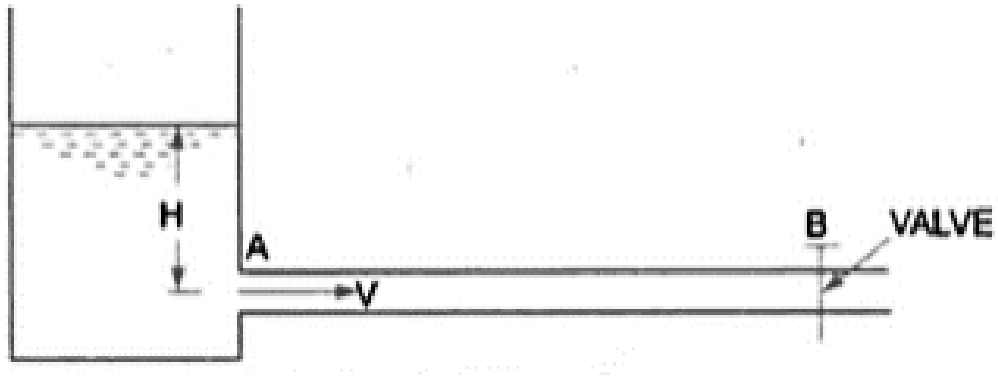

Figure 2.1-6: *Pipe water hammer (Meyer, Applications of Fluid Mechanics Part I, 1995)*

When the valve is open the gravitational force on the fluid will cause the fluid to flow out of the tank through the pipe. If the valve is suddenly closed, the momentum of the fluid will be affected causing a pressure wave. The pressure wave will be conveyed along the pipe at a velocity equal to the velocity of sound. The pressure wave will reflect between the tank and the closed valve. The wave will either superimpose the previous wave or reflect as a low-pressure wave depending on the number of reflections, length of pipe, and frictional effects of the pipe surface. As the wave travels along the pipe it causes a hammering action on the surface of the pipe.

Preventative measures should be included in the design of piping to avoid water hammer. The following methods can be used:

I. Air vessels or accumulators – Acts as air cushions that inject air into the system when a drop in pressure is experienced. This will gradually diminish the pressure wave.
II. Relieve valves – Response to a sudden increase in pressure. Relieves the pressure back to the tank or over the closed system.
III. Air valves – Introduces air into the system when the pressure drops below atmospheric pressure. The air is slowly released when the pressure in the system returns to normal.

The velocity of the pressure surge is expressed as:

$$a = \sqrt{\frac{K_e}{\rho}} \qquad (2.1—12)$$

Where:

K_e - the equivalent bulk modulus of the pipe
ρ - density of the fluid

Also:

$$\frac{1}{K_e} = \frac{1}{K_f} + \frac{kd}{tE} \qquad (2.1—13)$$

Where:

K_f - bulk modulus of the liquid, K_{oil} = 1.8 GPa
d - internal diameter of the pipe
t - wall thickness
E - elasticity modulus of the pipe material

The factor k is related to the Poissons ratio of the piping material and the method in which the pipe is supported. For typical piping applications, this value is approximately 0.9

Typical values for the velocity of sound in piping are:

Thin-walled steel pipe = 850 m/s
Plastic pipes = 200 m/s

A wave that is propagated along the length of the pipe to one end is then reflected to the initiation point. The time taken to travel this length L is referred to as the critical period.

$$t_p = \frac{2L}{a} \qquad (2.1—14)$$

Where:

t_p - critical period

For:

Time is taken for a change of flow < $\frac{2L}{a}$ - Described as a sudden change, therefore, water hammer occurred

Time is taken for a change of flow > $\frac{2L}{a}$ - Described as gradual change, therefore, water surge occurred

The increase in pressure head experienced by water hammer is expressed using the Joukowsky law:

$$\Delta h_{hammer} = \frac{a\Delta V}{g} \qquad (2.1—15)$$

Where:

ΔV - change in velocity

From equation 2.1-15, the increase in pressure head due to water hammer is not dependent on the pipe length. However, the pressure increase due to water surging is dependent on the pipe length. The pipe length is used to calculate the volume of water that shall be brought to a halt in time t.

$$\Delta h_{surge} = \frac{\Delta p}{\rho g} = \frac{pressure\ increase}{\rho g} = \frac{\frac{force}{area}}{\rho g}$$

$$= \frac{\frac{mass\ x\ deceleration}{area}}{\rho g}$$

$$= \frac{\frac{\rho L \frac{\pi}{4} d^2\ x\ \frac{\Delta V}{t}}{\frac{\pi d^2}{4}}}{\rho g}$$

$$\Delta h_{surge} = \frac{L \Delta V}{g t} \qquad (2.1—16)$$

A piping system shall be designed to withstand stresses due to internal pressure from frictional effects, change in kinetic energy, gravitational forces, and pressure surges due to water hammer.

2.2 Primary Stresses due to Internal Pressure

The next step in the design process of a piping system is to determine the stresses experienced from internal pressure. A piping system shall be designed to operate within the allowable stress limits of the piping material. The allowable stress limit S_A is based on a function of the tensile or yield strength of the material at low temperatures, and on creep rates for elevated temperatures. The Allowable stresses are tabulated in Appendix D, extracted from the ASME B31.3 design code, for various materials used in the Petroleum industry. The stress values in Table A are based on the lowest of (i) one-third of the minimum tensile strength at room temperature; and (ii) two-thirds of the yield strength at room temperature.

The stresses experienced by a piping system are categorized into two types namely Primary stresses and Secondary stresses. Where Primary stresses (sustained loads) are based on the internal pressure, deadweight, and dynamic loadings of the system; and Secondary stresses are of cyclic nature due to thermal displacement. This subsection shall focus on the primary stresses generated on the piping system from internal pressure. The pressure calculated using the previous subsections equations shall be used to determine the Primary stress in piping. The following subsection focuses on the stresses and strains experienced on a system due to deadweight and dynamic loadings. Secondary stresses will be discussed in a subsequent subsection in this chapter.

In the simplest problems, a structural system or part of a structure fails when a certain function of stress or strain reaches a critical value. Therefore, the basic knowledge needed by a designer is to understand: (i) how to calculate stresses and strains from the applied load on a system; (ii) the critical combinations of stress and strain that cause failure.
The first statement relates to the field of applied mechanics – elasticity and the mathematical theory of the plastic field, mathematical rheology.
The second statement relates to the mechanical properties of solids – physics of solids.

Failure can occur on a structural part by:

a) Elastic deformation
b) Non-elastic deformation (plastic)
c) Fracture

When a structure suffers excessive deformation, it reaches its end of serviceable life. The deformation causing failure could be either elastic or non-elastic deformation.

Moderate deformations in a structure can be advantageous in that stress redistribution occurs, resulting in dislocations in the metal which increases the strength. Though in many cases the deformation leads to the change in the shape of the structure which increases the resultant stress of the applied load. If this increased load is not counterbalanced by strain hardening, rapid disruption is faced.

The fundamentals of the Mechanics of Materials shall first be described. These principles and theories form the basis of the equations developed to calculate stresses from internal pressure in piping.

2.2.1. Plasticity

A non-elastic type of deformation which is not time-dependent is defined as pure plasticity. Plastic strain (ε) is the deformation that takes place due to the value of stress (σ).

$$\sigma = f(\varepsilon) \qquad (2.2\text{—}1)$$

Where:

σ - stress (pascals)
ε - strain (mm)

Elastic deformations obey a similar law barring the fact that they are reversible. For plastic deformation, the relationship is only effective for increasing stress. Plastic deformation occurs at yield stress. In other words yield, stress means the stress required for plastic deformation to occur in a metal. The relationship between stress and strain of metals is represented on a stress-strain curve.

Carbon steels represent the so-called "yield phenomenon". At the value of the "yield point" plastic deformation occurs. Once this point is reached, the stress required for further deformation remains constant for a period, or decrease to a lower stress value ("lower yield point").

A very important point of interest to a designer is the maximum permissible plastic strain value. On the stress-strain curve, the value at which the yield stress is reached is called the "yield strength" or "proof stress".

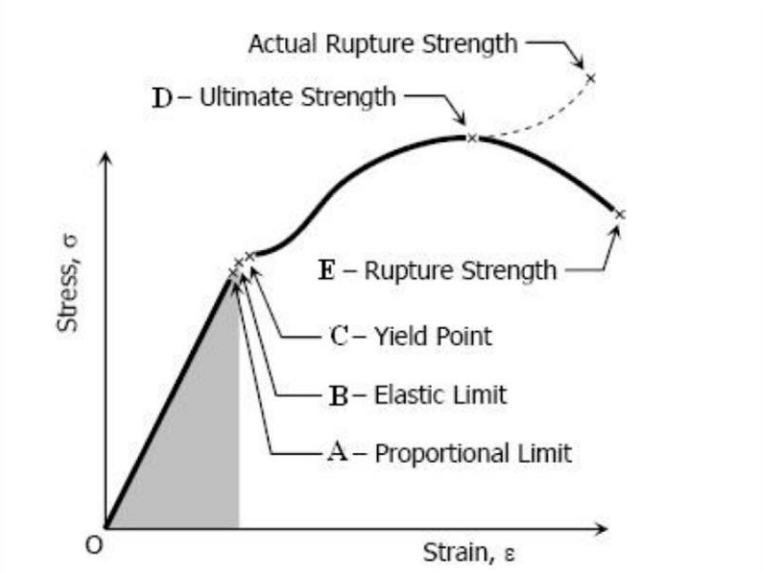

Figure 2.2-1: *Stress-Strain curve* (Kassimali, 1999)

2.2.2. Triaxial Stress

Piping systems experience Triaxial stress. If triaxial stress is experienced by a structure, with principle stresses $\sigma 1 \geq \sigma 2 \geq \sigma 3$, yielding occurs when the principle stresses reach a critical value. The most compatible and practical yield conditions that express triaxial yield conditions are:

I. Tresca (maximum shear stress) condition
II. von Mises (maximum octahedral stress) condition

2.2.2.1. Tresca

The Tresca yield criterion theory assumes that yielding occurs when the maximum shear stress, equal to one-half of the difference between the algebraically greatest and smallest principle stresses, reaches a critical value.

$$\sigma_1 - \sigma_2 = Y \qquad (2.2—2)$$

Where:

Y - yield stress in uniaxial tension or compression (Pa)

The intermediate principle stress does not affect yielding when applying the Tresca condition.

2.2.2.2. von Mises

The von Mises condition assumes that yielding occurs when the "effective" shear stress reaches the critical value of the yield stress in pure shear.

$$\tau_{eff} = \frac{1}{2\sqrt{2}} \sqrt{(\sigma_1 - \sigma_2)^2 + (\sigma_2 - \sigma_3)^2 + (\sigma_3 - \sigma_1)^2} \qquad (2.2—3)$$

Where:

τ_{eff} - effective shear stress (Pa)

In terms of yield stress Y, von Mises can be expressed as:

$$\sigma_y = \frac{1}{\sqrt{2}} \sqrt{(\sigma_1 - \sigma_2)^2 + (\sigma_2 - \sigma_3)^2 + (\sigma_3 - \sigma_1)^2} \qquad (2.2—4)$$

The major difference between the Tresca and von Mises failure criteria is the intermediate principle stress influences the occurrence of yielding. The two conditions will only coincide if the intermediate principle stress is equal to the highest or lowest principle stress.

The highest variance occurs between the two conditions when the intermediate principle stress is the mean of the highest and lowest principle stresses. At this occurrence, the von Mises condition results in approximately 15% higher yield stress than the Tresca condition.

Experiments conducted on metals produced results that were intermediate between the Tresca and von Mises condition.

2.2.2.3. Stress-Strain Relationships for Triaxial Stress

An important question is how the resulting strains are determined by the applied state of stress if yielding occurs. The complication with this problem is if the deformation of the structure depends on the sequence of application of the stress components. The deformation of one plane could damage the isotropy of the material and cause reverse deformation rather than continued deformation.

A solution has been determined by Levy and Mises only for the simple case of ideally isotropic material. The solution states that the increment of plastic strain is directly related to the applied stress. All increments should be added to the plastic strains from previous actions of stress.

$$\epsilon_1 = \lambda \left[\sigma_1 - \frac{1}{2}(\sigma_2 + \sigma_3) \right] \qquad (2.2—5)$$

$$\epsilon_2 = \lambda \left[\sigma_2 - \frac{1}{2}(\sigma_3 + \sigma_1) \right]$$

$$\epsilon_3 = \lambda \left[\sigma_3 - \frac{1}{2}(\sigma_1 + \sigma_2) \right]$$

Where:

ϵ - strain (mm)

2.2.3. Ultimate Stress and Working Stress

The two types of failure caused by plastic deformation are (i) distortion to the structure making it unserviceable; (ii) plastic disruption. In most cases, the second possibility is ignored because the distortion on the structure is much more significant. In piping, a plastic disruption could lead to bursting.

To prevent failure by distortion special attention must be paid to the maximum permissible stress value (yield strength). To prevent failure from plastic disruption the working stress must

be determined from the applied load or pressure at which instability sets in. The piping is then designed where the design load or design pressure is a percentage of the bursting pressure.

For a rod specimen under uniaxial tension load, the working stress is the ultimate tensile strength divided by a factor of safety. For piping, the maximum pressure occurs at stress different from the ultimate stress. Therefore, the maximum stress or pressure cannot be determined from the ultimate tensile stress but must be calculated based on the stress-strain curve. The relationship between the ultimate tensile stress and proof stress gives no clear indication of the fracture strain. The fracture could occur at the maximum load or multiple times more than the maximum load.

2.2.4. Creep

If a material experiences progressive deformation when under constant stress, it is said to show properties of creep. A type of deformation that relates to this definition is viscosity creep. A purely viscous material rate of straining is a direct function of stress which does not depend on the deformation already undergone. The material is said to show Newtonian viscosity.

$$d\gamma/dt = f(\tau) \qquad (2.2—6)$$

The creep behaviour of metals is different than pure viscosity materials.

2.2.5. Primary Stresses on Piping

Primary stresses are direct, shear, or bending stresses created by the applied load which satisfy the laws of equilibrium of internal and external moments and forces. The primary stresses consist of direct longitudinal and circumferential stresses from internal pressure; bending and torsional stresses due to dead load and environmental loading (snow, ice, wind, earthquake). In addition, stresses are created from restrained thermal loading due to fixed supports along with the piping.

Stress is defined as the ratio of Force to Area or Moments divided by the Pipe section modulus. A pipe analysis is done by constructing a three-dimensional, mutually perpendicular Principle Axis system. Each force acting on a plane can be trigonometrically reduced to force components represented by vectors, acting along each of the principle axes.

The principle stress acting along the centreline of the pipe is called the Longitudinal principle stress. This stress is caused by longitudinal bending, axial force loading, or pressure.

Radial principle stress acts on a line from the centre of the pipe radially through the pipe wall. This stress is compressive stress acting on the pipe inter diameter caused by internal pressure or tensile stress caused by external forces or vacuum.

Circumferential principle stress often referred to as Hoop or Tangential stress acts on a line perpendicular to the Longitudinal and the Radial stress.

When two or more Principle stresses act at a point on a pipe, shear stress will be generated.

2.2.6. A pipe under Internal Pressure

The analysis of piping meets the requirements of thin-walled cylinders. For the analysis of thin-walled cylinders, the assumption is made that the radial plans do not change, and the thickness of the cylinder remains constant. The criterion for a thin-wall cylinder is a large variance in size between the cylinder's internal diameter and the thickness of the cylinder. The general equation for classifying thin-wall cylinders is:

$$t/d_i = \frac{1}{20} \qquad (2.2—7)$$

Where:

t - pipe thickness (m)
d_i - pipe internal diameter (m)

The following co-ordinate system shall be used to determine the different stresses acting on a pipe.

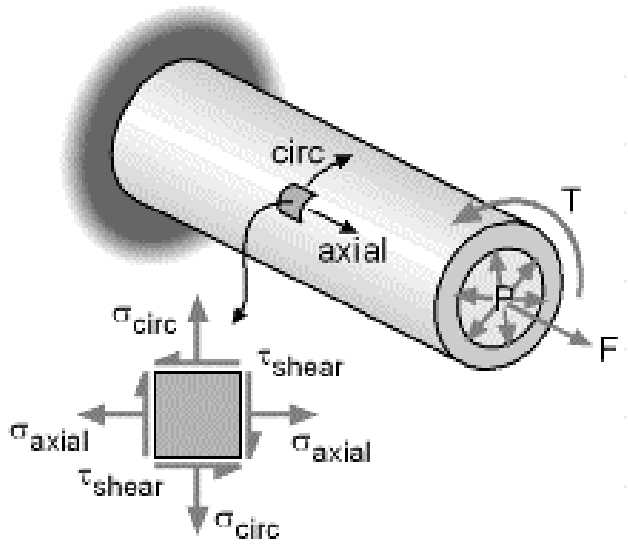

Figure 2.2-2: *Pipe stress analysis (Beam Elements, 2018)*

The failure of piping occurs when subjected to exceptionally high internal pressure. The pipe could burst along the circumference (axial stress) or parallel to the axis (hoop stress).

The major contributor to Triaxial stress is fluid pressure.

2.2.7. Longitudinal Stress

To determine the longitudinal stress along the Z-axis acting on the pipe, the law of equilibrium is applied. The pressure is acting on the internal of the pipe and to satisfy the law of equilibrium an equal but opposite force exists in the pipe. Where the stress of the material is the resistance to deformation by the applied load per unit area.

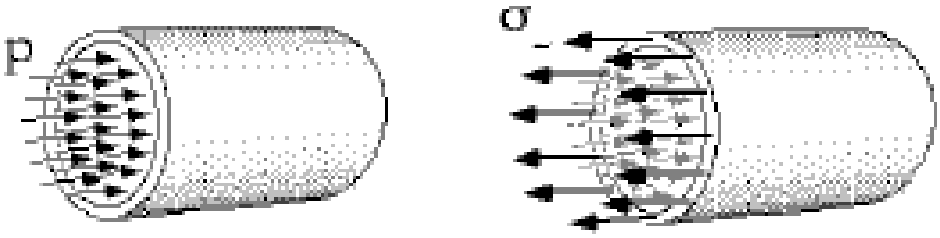

Figure 2.2-3: *Longitudinal stress (About beam modeling, 2018)*

Where:

P - internal pressure (Pa)
σ_L - longitudinal stress (Pa)

$$\sum F_Z = 0 \qquad (2.2\text{—}8)$$

$$F_P - F_N = 0$$

$$P \,.\, \pi r^2 - \sigma_L \,.\, 2\pi r t = 0$$

$$\sigma_L = \frac{P.r}{2.t}$$

Where:

F_P - force due to pressure $(N.m)$
F_N - normal force acting in a pipe $(N.m)$

2.2.8. Hoop or Circumferential Stress

The same principle is applied when calculating longitudinal stress for calculating hoop stress. The law of equilibrium is applied for the forces acting in the Y axis.

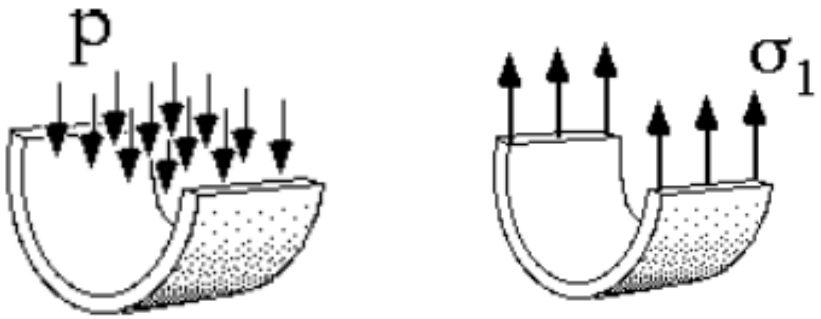

***Figure 2.2-4**: Hoop / Circumferential stress (About beam modeling, 2018)*

Where:

P - internal pressure (Pa)
σ_C - circumferential/hoop stress (Pa)

$$\sum F_Y = 0 \qquad (2.2—9)$$

$$F_P - F_N = 0$$

$$P \,.\, 2r \,.\, \Delta l - \sigma_C \,.\, 2t \,.\, \Delta l = 0$$

$$\sigma_C = \frac{P.r}{t}$$

Where:

F_P - force due to pressure ($N.m$)
F_N - normal force acting in a pipe ($N.m$)

The analysis of Primary stress due to deadweight and dynamic loading is done using computer program software. The analysis requires a full specification of all properties of the system to conduct the analysis. The initial piping material and thicknesses specification is done using the results of longitudinal and circumferential stresses.

2.3 Primary Stresses due to Dead Weight and Dynamic Loading

This subsection focuses on the analysis of forces, moments, stresses, and strains experienced by a piping system due to deadweight and dynamic loadings. The previous calculations are used by the piping designer to determine the dimensions and material specifications of the system. Although it is not practical to calculate the subsequent stresses and strains on the system manually. The development of the principles, theories, and equations is detailed to aid in the understanding of how these stresses and strains are calculated using computer programs.

The results from the analysis of dead weight and dynamic loadings generally require the designer to relook at the dimensional and material specification done using the results from the previous subsections. Where all results are to be within the Allowable stress limits of the system.

Finite Element Analysis (FEA) programs can be used to analysis forces, moments, stresses, and strains on a piping system from various types of loadings. The method used by FEA is to approximate solutions to differential equations. The majority of the cases are equations based on differential equations, constitutive relations, kinematics, and the relating boundary conditions.

The software selected for the analysis of dead weight and dynamic loading in piping systems is CAESAR II combined with FEATools which has the advantage of built-in code evaluations. The analysis of forces, moments, stresses, and strains are calculated using the classical beams theories, and either Tresca or von Mises failure theories. The results of the analysis are evaluated against the criteria of the statutory design requirements in the ASME code.

The introduction of beam theories applies assumptions that simplify formulation. The most applicable beam theories used for the analysis of piping systems are the Euler-Bernoulli beam theory and the Timoshenko beam theory. The following subsection will detail the basis of Finite Element Analysis and the Classical beam theories used for the analysis of piping systems.

2.3.1. Equations of Equilibrium for Three Dimensional Beams

The analysis of piping systems is an analytical method performed to determine how the system behaves based on its material properties and applied loadings. Typical primary loads are due to the dead weight of the pipe including internal fluid and pressure. Simple piping systems can be analysed using one-dimensional beams elements. Higher complexity piping systems shall be analysed by a series of three-dimensional elements created as a depiction of the piping geometry. This being the most efficient method of modelling piping systems. Each pipe is modelled as a uni-axial element having tension, compression, torsion, and bending capabilities. Each element has six degrees of freedom at each node: translations and rotations in the x, y, z axes. The Euler-Bernoulli's or Timoshenko's beam theory is applied to each element. Where the main difference between the two beam theories is Timoshenko's theory considers shear

deformation effects. Although analytical analysis cannot account for everything, with good safety factors history has shown this is a good approximation.

The finite element method involves the application of three basic concepts – equilibrium of forces, compatibility of displacements, and stress-strains relationships. These basics concepts shall be discussed thereafter the equations of beam theories will be developed.

The piping system is static therefore the equilibrium of motion laws shall apply.

$$\sum F = 0 \qquad (2.3—1)$$

Where:

F - the sum of all forces about any point

$$\sum M = 0 \qquad (2.3—2)$$

Where:

M - the sum of the moments of all forces about any point

The forces that develop at the piping supports or connections are referred to as reactions. Depending on the type of support that constrains the piping at a specific point, reactions or moments will be experienced. The support can be used to anchor (fixed), guide (roller), or absorb shock (spring) at a specific point on the piping system. A general rule of reactions, if the translation is prevented by the support in a certain direction, then a reacting force will develop on the pipe in that direction. Similarly, if the support prevents rotation, then a couple moment will be exerted on the pipe. The computer analysis for dead weight and dynamic loading requires the location and type of support to be determined before the analysis is performed. The initial positions and types of supports shall be specified using the experiential knowledge of the designer.

Successful application of the equations of equilibrium necessitates the full specification of all forces acting on a piping system, be it known or unknown. The initials steps before computer software analysis are firstly drawing the structure's free-body diagram. All applied loads and reactions, known or unknown, shall be highlighted on the free-body diagram. All process parameters and material properties are then specified for the analysis. Although the software used performs the calculations, incorrect set up of the analysis will produce false results. If the designer does not understand the basic theories, assumptions, boundary conditions, and applied equations used for the analysis, discrepancies will not be picked up in the results.

SUPPORT CLASSIFICATION (FUNCTIONS)	BASIC CONSTRUCTION	* SYMBOL	RESTRAINTS
LOOSE SUPPORT			(+) Y
LONGITUDINAL GUIDE			(±) Y & (±) X
TRANSVERSE GUIDE			(+) Y & (±) X
FIXED POINT (NON-WELDED TYPE)	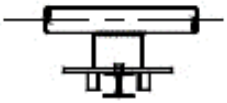		(±) X,(±) Y & (±) Z
FIXED POINT (ANCHOR) (WELDED TYPE)			ALL DISPLACEMENT ALL ROTATIONS
LIMIT STOP	SPECIAL DETAILS.	NOT APPLICABLE	ANY DIRECTION AS DESIRED.
SPECIAL SUPPORT	SPECIAL DETAILS	NOT APPLICABLE	ANY DIRECTION AS DESIRED

Figure 2.3-1: *Typical pipe supports (base, 2018)*

Pipe Boundary Conditions

To help understand the physics and develop the boundary conditions of a piping model, a straight pipe is considered. When no loading is applied to the pipe, the pipe is said to be in its referential state. The pipe has a length l with a uniform cross-section along the length. The origin 0 is placed at the left end of the pipe, with the displacement and rotation of the pipe referenced from an x, y, z coordinate system having base unit vectors i, j, k. The y-axis is centralised and runs parallel to the pipe. If the pipe is loaded by a uniformly distributed load (UDL) along the y-axis define by the vector field $q = q(y)$, with a corresponding moment load vector per unit length $m = m(y)$. This results in a differential beam element with a length dy, an external force vector qdy, and an external moment vector mdy. Due to the applied UDL, the system has the following load vectors per unit length in the x, y, z coordinate system.

$$q = \begin{bmatrix} qx \\ qy \\ qz \end{bmatrix} \quad (2.3—3)$$

Where:

q - distributed load per unit length

$$m = \begin{bmatrix} mx \\ my \\ mz \end{bmatrix} \quad (2.3—4)$$

Where:

m - distributed moment load vector per unit length

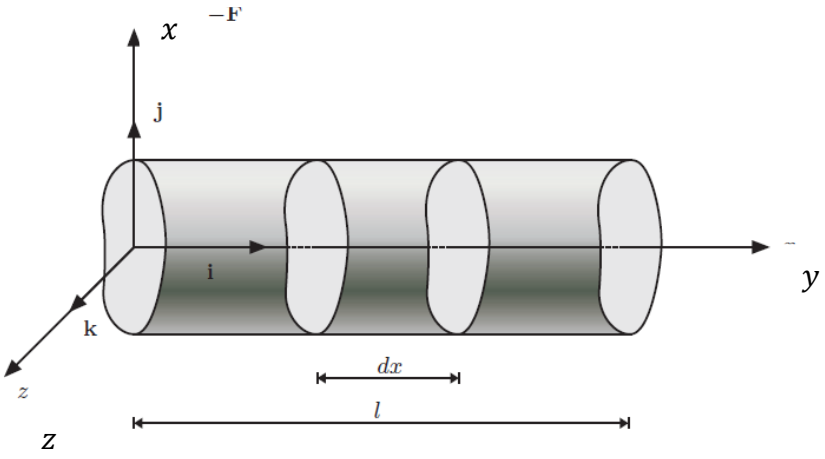

***Figure 2.3-2**: Pipe referential state*

As a result of the applied loads, the pipe deforms into a state where an internal section force vector $F = F(y)$ and an internal section moment vector $M = M(y)$ balances the externally applied loads. A base unit i normal vector in the outward direction of the y-axis acts on the cross-section of the pipe. The F and M components in the x, y, z coordinate system are as follows:

$$F = \begin{bmatrix} N \\ Qx \\ Qz \end{bmatrix} \quad (2.3—5)$$

Where:

F - internal section force vector

$$M = \begin{bmatrix} Mx \\ My \\ Mz \end{bmatrix} \quad (2.3—6)$$

Where:

M - internal section moment vector

Since the applied load acts along the y-axis, $N = N(y)$ is an axial force, and the corresponding components $Qx = Qy(y)$ and $Qz = Qz(y)$ are shear force components in the y and z axis. The moment resulting from the axial component is denoted the torsional moment. The corresponding $My = My\,(x)$ and $Mz = Mz\,(x)$ in the y-axis and z-axis denote bending moments. The two-dimensional beam theory ignores the torsional moment. Whereas the analysis of three-dimensional frame structures, the torsional behaviour of beams is imperative.

2.3.2. Section Forces and Stresses in a Beam

Following the example above with an outward-directed unit vector acting along the y-axis, the resulting stress σ_{yy} and shear stresses τ_{yx} ; τ_{yz} act on the pipe. The stresses and shear stresses are statically equivalent to the applied force vector *F* and section moment vector *M* as described in the following equations:

$$N = \int_A \sigma_{yy} dA \;\; ; \quad Q_x = \int_A \sigma_{yx} dA \quad ; \quad Q_z = \int_A \sigma_{yz} dA \qquad (2.3\text{—}7)$$

$$M_y = \int_A (\sigma_{yz} y - \sigma_{yx} z) dA \;\; ; \; M_x = \int_A z\sigma_{yy} dA \; ; M_z = -\int_A x\sigma_{yy} dA \qquad (2.3\text{—}8)$$

The stresses that act on sections orthogonal to the x-axis and z-axis are as follows:

x-axis - $\{\sigma_{xx}\,,\, \sigma_{xy}\,,\, \sigma_{xz}\}$

z-axis - $\{\sigma_{zz}\,,\, \sigma_{zy}\,,\, \sigma_{zx}\}$

The first stress index represents the coordinate axis in the same direction as the outward normal vector of the section. The second index represents acting in the direction of the stress component. The stresses described in the x, y, z coordinate system formulate the components of the stress tensor as shown below:

$$\sigma = \begin{bmatrix} \sigma_{xx} & \sigma_{yx} & \sigma_{zx} \\ \sigma_{xy} & \sigma_{yy} & \sigma_{zy} \\ \sigma_{xz} & \sigma_{yz} & \sigma_{zz} \end{bmatrix} \qquad (2.3\text{—}9)$$

Where:

σ - stress

For moment equilibrium of the cube, the following holds true:

$\sigma_{xy} = \sigma_{yx}$ $\qquad$ $\sigma_{xz} = \sigma_{zx}$ $\qquad$ $\sigma_{yz} = \sigma_{zy}$

Therefore the σ tensor is symmetrical.

2.3.3. Kinematics and Deformations of a Beam

The main assumption made in the classical beam theory is that the cross-section at right angles to the y-axis at the y coordinate remains plane and maintains its shape during deformation. This means the cross-sections act as a rigid body during translations and rotations. More importantly, this means that the Poisson's contractions in the transverse direction resulting from axial strains are ignored. A position vector $w = w(y)$ and rotation vector $\theta = \theta(y)$ describes the deformed position of the cross section in the x, y, z coordinate system with the following components:

$$w = \begin{bmatrix} w_x \\ w_y \\ w_z \end{bmatrix} \qquad (2.3—10)$$

Where:

w - position vector

$$\theta = \begin{bmatrix} \theta_x \\ \theta_y \\ \theta_z \end{bmatrix} \qquad (2.3—11)$$

Where:

θ - rotation vector

The displacement components (w_x, w_y, w_z) and rotation components $\theta_x, \theta_y, \theta_z$ are negligible therefore the linear beam theory will be considered.

$\sin\theta \approx \tan\theta \approx \theta$

Where the rotation components are represented as θ, measured in radians.

2.3.4. Beam Theories

As previously mentioned the two-beam theories that are used in the analysis of piping is the Euler-Bernoulli beam theory and Timoshenko beam theory. The equations used in CAESAR II for the analysis of piping systems shall be detailed in this subsection. Each pipe is modelled as a uni-axial beam element. Each node of the element has six degrees of freedom: translations in the x, y, z directions, and rotations about the x, y, z axis. The element formulation is based on Euler-Bernoulli's beam theory. A more rigorous analysis using the beam theory method is achieved by applying the Timoshenko's beam theory with the major difference being shear-deformation effects included.

A flexibility factor is applied to some of the piping components for the analysis. Flexibility factors shall be described in the next subsection.

The key equations of interest shall be described in the beam theory notes that are used to calculate forces, moments, stresses, and strains using CAESAR II software.

2.3.4.1 Euler-Bernoulli Beam Theory

The following assumptions were used to derive the Euler-Bernoulli model:

I. the cross-section of the beam remains rigid along its plane;
II. the cross-section of the beam rotates about the neutral axis remaining plane;
III. the cross-section remains perpendicular to the neutral axis during deformation.

A. Displacement Field

The figure above shows a beam before and after deformations with a plane section normal to the y-axis. Points A, O, B, and C in Figure 2.3-3 move to Point A', 0', B' and C' after deformation. According to Bernoulli's assumption, the plane defined by A', 0', B', and C' remains normal to the beam axis after deformation.

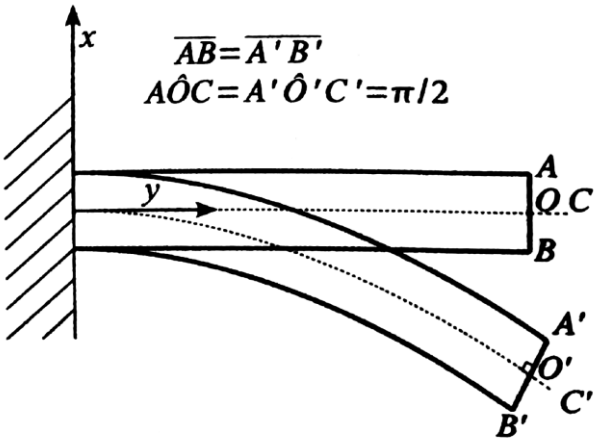

Figure 2.3-3: *Bending of a beam according to the Euler-Bernoulli beam theory (Carrera, 2011)*

According to the first assumption, in-plane deformations are not accounted for therefore the in-plane displacements u_x and u_z depend on the axial y coordinate only:

$$\varepsilon_{xx} = \frac{\partial u_x}{\partial_x} = 0$$

$$\varepsilon_{zz} = \frac{\partial u_z}{\partial_z} = 0 \qquad \Rightarrow \quad \begin{matrix} u_x(x,y,z) = u_{x1}(y) \\ u_z(x,y,z) = u_{z1}(y) \end{matrix} \quad (2.3\text{—}12)$$

$$\gamma_{xz} = \frac{\partial u_x}{\partial_z} + \frac{\partial u_z}{\partial_x} = 0$$

Based on the second hypothesis, the out-of-plane or axial displacement U_y is linear to the in-plane coordinates:

$$u_y(x,y,z) = u_{y1} + \emptyset_z(y)x + \emptyset_x(y) \qquad (2.3\text{—}13)$$

Where:

$\emptyset_z$ - Rotation angle along the z-axis

$\emptyset_x$ - Rotation angle along the x-axis

According to the third assumption shear deformations are disregarded:

$$y_{yz} = y_{yx} = 0 \qquad (2.3\text{—}14)$$

The rotational angles are obtained as functions of the derivatives of in-plane displacements from equations 2.3-12, 2.3-13 and 2.3-14:

$$\varepsilon_{xy} = \frac{\partial u_x}{\partial_x} + \frac{\partial u_x}{\partial_y} = \emptyset_z + \frac{\partial u_{x1}}{\partial_y} = 0 \qquad \emptyset_z = -\frac{\partial u_{x1}}{\partial_y}$$

$$\Rightarrow \qquad (2.3\text{—}15)$$

$$\varepsilon_{yz} = \frac{\partial u_y}{\partial_z} + \frac{\partial u_z}{\partial_y} = \emptyset_x + \frac{\partial u_{x1}}{\partial_y} = 0 \qquad \emptyset_x = -\frac{\partial u_{z1}}{\partial_y}$$

The displacement field is, therefore:

$$\begin{aligned} \mathrm{u}_x &= u_{x1} \\ u_y &= u_{y1} - \frac{\partial u_{x1}}{\partial_y} x - \frac{\partial u_{z1}}{\partial_y} z \\ \mathrm{u}_z &= u_{z1} \end{aligned} \qquad (2.3\text{—}16)$$

B. Strains

Following the Kinematic hypothesis the Euler-Bernoulli's theory accounts only for the axial strain:

$$\varepsilon_{yy} = \frac{\partial u_y}{\partial y} = \frac{\partial u_{y1}}{\partial y} - \frac{\partial^2 u_{x1}}{\partial y^2} x - \frac{\partial^2 u_{z1}}{\partial y^2} z = k_y^y + k_{yy}^x x + k_{yy}^z z$$

$$\Downarrow \quad \Downarrow \quad \Downarrow$$

$$k_y^y \quad k_{yy}^x \quad k_{yy}^z \qquad (2.3\text{—}17)$$

Where:

k_y^y - Membrane deformation

k_{yy}^x and k_{yy}^z are the second-order derivatives of the beams transverse displacements. These represent the curvatures of tiny deformations and rotations.

C. Stresses and Stress Resultants

The axial stress σ_{yy} experienced by the beam is obtained from the axial strain as a result of constitutive equations:

$$\sigma_{yy} = E\varepsilon_{yy} = E(k_y^y + k_{yy}^x x + k_{yy}^z z \qquad (2.3\text{—}18)$$

The stress resultants are calculated by integrating the axial stress along the cross-section of the beam:

(i) Axial force $N(y)$:

$$N(y) = \int_\Omega \sigma_{yy}\, d\Omega = \int_\Omega E\left(k_y^y + k_{yy}^x x + k_{yy}^z z\right) d\Omega$$

$$= E(k_y^y \int_\Omega d\Omega + k_{yy}^x \int_\Omega x\, d\Omega + k_{yy}^z \int_\Omega z\, d\Omega)$$

$$\Downarrow \quad \Downarrow \quad \Downarrow$$

$$A \quad S_x \quad s_z \qquad (2.3\text{—}19)$$

(ii) Bending moment along the z-axis:

$$M_z(y) = \int_\Omega \sigma_{yy} z\, d\Omega = \int_\Omega E\left(k_y^y + k_{yy}^x x + k_{yy}^z z\right) x d\Omega$$

$$= E(k_y^y \int_\Omega x d\Omega + k_{yy}^x \int_\Omega x^2\, d\Omega + k_{yy}^z \int_\Omega xz\, d\Omega)$$

$$\Downarrow \quad \Downarrow \quad \Downarrow$$

$$S_x \quad I_{zz} \quad I_{xz} \qquad (2.3\text{—}20)$$

(iii) Bend moment along the x-axis:

$$M_x(y) = -\int_\Omega \sigma_{yy} z \, d\Omega = \int_\Omega E\left(k_y^y + k_{yy}^x x + k_{yy}^z z\right) z d\Omega$$

$$= -E\left(k_y^y \int_\Omega z d\Omega + k_{yy}^x \int_\Omega xz \, d\Omega + k_{yy}^z \int_\Omega z^2 \, d\Omega\right) \qquad (2.3\text{—}21)$$

$$\Downarrow \qquad \Downarrow \qquad \Downarrow$$

$$S_z \qquad I_{xz} \qquad I_{xx}$$

The forces above are statically equivalent to the stress distribution of the beam. The negative moment in equation 2.3-21 results from the moment directed positively in the x-axis creating a negative rotation angle $\emptyset_x$.

Where:

A - Area of the cross-section, measured of the geometric entity Ω

S_x; S_z - Static moment

I_{xx}; I_{xz}; I_{zz} - Moment of inertia of the cross-section

The resultant forces equation 2.3-19 and 2.3-20 can be expressed in the following matrix:

$$\begin{Bmatrix} N \\ M_z \\ -M_x \end{Bmatrix} = E \begin{bmatrix} A & S_x & S_z \\ S_x & I_{zz} & I_{xz} \\ S_z & I_{xz} & I_{xx} \end{bmatrix} \begin{Bmatrix} k_1 \\ k_2 \\ k_3 \end{Bmatrix} \qquad (2.3\text{—}22)$$

Where the matrix below shows the fourth-order tensor of inertia

$$I_\Omega = \begin{bmatrix} A & S_z & S_x \\ S_z & I_{zz} & I_{xz} \\ S_x & I_{xz} & I_{xx} \end{bmatrix} \qquad (2.3\text{—}23)$$

D. Elastica

The vertical displacement and the rotation of the cross-section are described by uncoupled differential equations defined as elastica:

$$\frac{\partial^2 u_{x_{c1}}}{\partial y_c^2} = \frac{M_{z_c}}{EI_{z_c z_c}}$$

$$\frac{\partial^2 u_{z_{c1}}}{\partial y_c^2} = \frac{M_{x_c}}{EI_{x_c x_c}}$$

$$\emptyset_{z_c} = -\frac{\partial u_{x_{c1}}}{\partial y_c} \qquad (2.3\text{—}24)$$

$$\emptyset_{x_c} = -\frac{\partial u_{z_{c1}}}{\partial y_c}$$

2.3.4.2 Timoshenko Beam Theory

The major difference between the Euler-Bernoulli beam theory and the Timoshenko beam theory is that the beam is not constrained to remain perpendicular. Therefore, shear deformations ($\varepsilon_{xy}, \varepsilon_{yz}$) are accounted for.

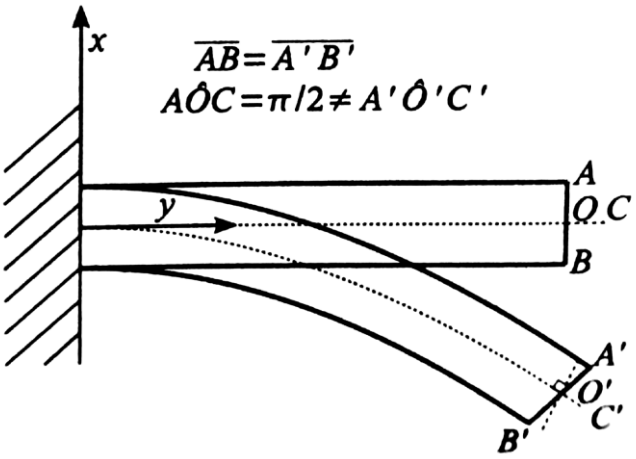

Figure 2.3-4: *Bending of a beam according to the Timoshenko beam theory (Carrera, 2011)*

A. Displacement Field

The displacement field is then:

$$\begin{aligned} u_x(x,y,z) &= u_{x1}(y) \\ u_y(x,y,z) &= u_{y1}(y) + \emptyset_z(y)x + \emptyset_x(y)z \\ u_z(x,y,z) &= u_{z1}(y) \end{aligned} \qquad (2.3\text{—}25)$$

B. Strains

To obtain the strain components the displacement field above is substituted into the geometrical relations that are valid under the assumption of linearity:

$$\varepsilon_{yy} = \frac{\partial u_y}{\partial_y} = \frac{\partial u_{y_1}}{\partial_y} + \frac{\partial \phi_z}{\partial_y} x + \frac{\partial \phi_z}{\partial_y} z$$

$$\gamma_{xy} = \frac{\partial u_y}{\partial_x} + \frac{\partial u_x}{\partial_y} = \emptyset_z + \frac{\partial u_{x1}}{\partial_y} \qquad (2.3—26)$$

$$\gamma_{yz} = \frac{\partial u_y}{\partial_z} + \frac{\partial u_z}{\partial_y} = \emptyset_x + \frac{\partial u_{z1}}{\partial_y}$$

C. Stresses and Stress Resultants

The axial stress and shear stress are calculated using constitutive relations:

$$\sigma_{yy} = E\varepsilon_{yy} = E\left(\frac{\partial u_{y1}}{\partial_y} + \frac{\partial \phi_z}{\partial_y} x + \frac{\partial \phi_x}{\partial_y} z\right)$$

$$\sigma_{xy} = \kappa G\left(\phi_z + \frac{\partial u_{x1}}{\partial y}\right) \qquad (2.3—27)$$

$$\sigma_{yz} = \kappa G\left(\phi_x + \frac{\partial u_{z1}}{\partial y}\right)$$

Where:

k - Shear correction factor

The stress resultants are determined by integrating the axial stress along the cross-section on the beam:

(i) Axial force *N*:

$$N = \int_\Omega \sigma_{yy}\, d\Omega = E \int_\Omega \left(\frac{\partial u_{y1}}{\partial_y} + \frac{\partial \phi_z}{\partial_y} x + \frac{\partial \phi_x}{\partial_y} z\right) d\Omega \qquad (2.3—28)$$

(ii) Bending moment along the *z*-axis:

$$M_z = \int_\Omega \sigma_{yy} z\, d\Omega = E \int_\Omega \left(\frac{\partial u_{y1}}{\partial_y} z + \frac{\partial \phi_z}{\partial_y} xz + \frac{\partial \phi_x}{\partial_y} z^2\right) d\Omega \qquad (2.3—29)$$

(iii) Bend moment along the *x*-axis:

$$M_x = -\int_\Omega \sigma_{yy} z\, d\Omega = -E \int_\Omega \left(\frac{\partial u_{y1}}{\partial_y} x + \frac{\partial \phi_z}{\partial_y} x^2 + \frac{\partial \phi_x}{\partial_y} xz\right) d\Omega$$

(2.3—30)

(iv) Shear force along the x-axis

$$V_x = \int_\Omega \sigma_{xy}\, d\Omega = \int_\Omega \kappa G \left(\phi_z + \frac{\partial u_{x1}}{\partial_y}\right) d\Omega = \kappa G \left(\phi_z + \frac{\partial u_{x1}}{\eth y}\right) A$$

(2.3—31)

(v) Shear force along the z-axis:

$$V_z = \int_\Omega \sigma_{yz}\, d\Omega = \int_\Omega \kappa G \left(\phi_x + \frac{\partial u_{z1}}{\partial_y}\right) d\Omega = \kappa G \left(\phi_x + \frac{\partial u_{z1}}{\eth y}\right) A$$

(2.3—32)

D. Elastica

The following coupled differential equations shall be solved to obtain the elastica equations:

$$\frac{\partial \emptyset_{z_c}}{\partial y_c} = \frac{M_{z_c}}{EI_{z_c z_c}} \qquad \frac{\partial \emptyset_{x_c}}{\partial y_c} = \frac{M_{x_c x_c}}{EI_{x_c x_c}}$$

(2.3—33)

$$\frac{\partial u_{x_{c1}}}{\partial y_c} = \frac{V_{x_c}}{\kappa GA} - \emptyset_{z_c} \qquad \frac{\partial u_{z_{c1}}}{\partial y_c} = \frac{V_{z_c}}{\kappa GA} - \emptyset_{x_c}$$

2.3.5. Stress due to Sustained Loads

The beam theories detailed in this subsection are used to calculate forces, moments, stresses, and strains in the piping system due to sustained loading. The CAESAR II analysis of the piping system focuses on three particular stresses that are due to sustained bending moments, sustained torsional moments, and sustained longitudinal forces. The stress due to sustained loadings shall not exceed the Allowable stress range of the system. Similar equations have been developed for the analysis of thermal displacement stresses in the next subsection.

$$S_L = \sqrt{(S_a + S_b)^2 + (2S_t)^2}$$

(2.3—34)

Where:

S_a - axial stress range due to sustained longitudinal force = $\frac{I_a F_a}{A_p}$

A_p - the cross-sectional area of pipe – Nominal thicknesses and outside diameters are to be used for analysis

F_a - the axial force between due to sustained loads – pressure and weight

I_a - sustained longitudinal force index = 1.0

S_t - torsional stress range due to displacement strains = $\frac{I_t M_t}{2Z}$

I_t - sustained torsional moment index = 1.0

M_t - torsional moment due to sustained loading – pressure and weight

Z - sustained section modulus of the pipe

The stress due to sustained bending moments is calculated using the following equation:

$$S_b = \frac{\sqrt{(I_i M_i)^2 + (I_o M_o)^2}}{Z} \qquad (2.3—35)$$

Where:

I_i - sustained in-plane moment index

I_o - sustained out-plane moment index

M_i - in-plane bending moment due to sustained loads

M_o - out-plane bending moment due to sustained loads

The sustained force as a result of internal pressure is included in the sustained longitudinal force, F_a. Piping systems with expansion joints along the run can compensate for this force although good practice will be to include it in the calculation as an additional factor of safety.

2.4 Secondary Stresses on Piping Systems

Secondary stresses are typical of a bending nature, ranging from positive to negative across the pipe wall thickness. The general cause of secondary forces, mainly fatigue, is the differential radial deflection experienced by the pipe wall. One of the most important examples of secondary stresses is the circumferential stresses on piping that is subjected to bending. A system will experience dimensional changes with any change in temperature. The cyclic displacement in piping is a result of a high variation in temperature of the pipe. The generation of secondary stresses from a single load application on ductile materials does not cause failure. When a piping system experiences stress above the yield strength of the material, local deformation occurs which results in the redistribution of the loading and the reduction of stress in the operating condition. If the stress is cyclic, a local strain range is established corresponding to the full magnitude. This initiates a potential source of failure through fatigue.

An initial overstress (during system tests) in the plastic region of a pipe could alter the contour to make it stronger. This would result in the lowering of local strain during subsequent load applications and the fatigue resistance would be accordingly increased. This does, however, pose the risk at initial overstress of propagating flaws in the base material, especially in welds. This could also initiate cracks in heat-affected zones adjacent to welds.

Piping under cyclic loading will experience fatigue damage, the level of damage relates to the stress amplitude and several cycles undergone during operation. The assumption is made that the damage incurred is permanent and cycles at different stress amplitudes in sequence results in the accumulation of damage equal to the sum of the damage increments at individual stress levels. Failure occurs when the sum of the damage increments reaches a critical value.

This section will focus on the following:

a) the understanding of cyclic loading experienced by piping systems
b) the utilization of inherent flexibility of the piping system acting as a spring in bending and torsion

2.5.1. Flexibility Analysis

A piping flexibility analysis involves the calculation of forces, moments, and stresses in a tubular structure frame at all critical locations under the effects of thermal expansion. The understanding of the allowable stress limits of the material of construction is of utter importance for the analysis.

Flexibility analysis of piping systems aims to prevent:

I. failure of piping or supports due to overstress and fatigue
II. leakage at joints
III. Overstress or distortion of connected equipment (pumps, valves, turbines, etc.) from excessive moments and forces

Piping components besides straight pipe particularly bends, show increased flexibility usually proportional to the intensification of stresses. Flexibility factors are determined in relation to a straight pipe. This is defined as the ratio of the rotation per unit length of a component produced by a moment to the rotation per unit length of straight pipe produced by the same moment. Components with the same properties are used for determining Flexibility factors (nominal size, thickness, and material).

A piping system shall be suitably designed to not exceed the allowable stress range due to displacements. All movements of piping systems due to thermal expansion needs to be determined during the design phase and duly accounted for. If the secondary stress analysis shows that a piping system does not have sufficient flexibility to allow for thermal expansion, the design needs to be altered accordingly. A flexibility analysis gives special consideration to strains (displacements) of the piping system and the resultant axial, torsional, and bending displacement stress ranges.

The following equations formulated to determine displacement stresses and reactions tend to be extremely complex due to the calculation of appropriate shape factors. Before the development of computer stress analysis programs, to allow the above equations to be more practical to designers, the following rules and assumptions were applied without causing too much inaccuracy or invalidity of the theory.

i. Dividing the system into nodes, the centre of gravity of each element is at its midpoint.
ii. Replacing square corners for curved members. This approximation ignores the increased flexibility of elbows and results in an overestimation of reactions and stress.
iii. The assumption that both bending and torsional rigidity are identical. The shear modulus is equal to half the elasticity modulus.
iv. In-plane and out-of-plane bending stress-intensification factors are identical

The flexibility analysis shall be performed using CAESAR II software. The major difference between the analysis of Primary stresses and Secondary stresses is the application of Stress Intensification Factors (SIF). SIF's are a multiplier of bending and torsional stresses of a piping component to that of straight pipe. CAESAR II models piping as beam elements and applies the classical beam theories to determine forces, moments, stresses, and strains. The beam theories do not apply to piping components except for straight pipe. The geometry of piping components creates great difficulty in analysing. For this reason, SIF's have been developed to approximate the bending and torsional stresses on piping components.

2.5.2. Allowable Stress Range, S_A

The allowable stress range is defined as the maximum allowable stress that a system can withstand before failure commences. The resistance to fatigue is measured by the endurance limit or endurance strength of the material. Two different types of loading are accommodated for in the calculation of the allowable stress: (i) single loading and (ii) cyclic loadings. Stresses due to single loadings are calculated in the previous subsections on Primary stresses. This study will focus on the cyclic loadings experienced by the piping system. A systems cyclic range is

calculated from the lowest possible operating temperature to the highest possible operating temperature.

$$S_A = f(1.25S_c + 0.25S_h) \qquad (2.4—1)$$

Where:

S_c - allowable stress of the system at low operating temperature

S_h - allowable stress of the system at high operating temperature

f - stress range factor

Appendix D Table A-1 extracted from the ASME B31.3 code lists material properties with allowable stresses at various temperatures.

The stress range factor f is based on the number of temperature cycles a piping system will experience during its serviceable life. The value for f can be determined from Figure 2.4-1 below or using the following equation:

$$f = 6.0(N)^{-0.2} \qquad (2.4—2)$$

Where:

N - Equivalent number of full displacement cycles during the service life of the piping system

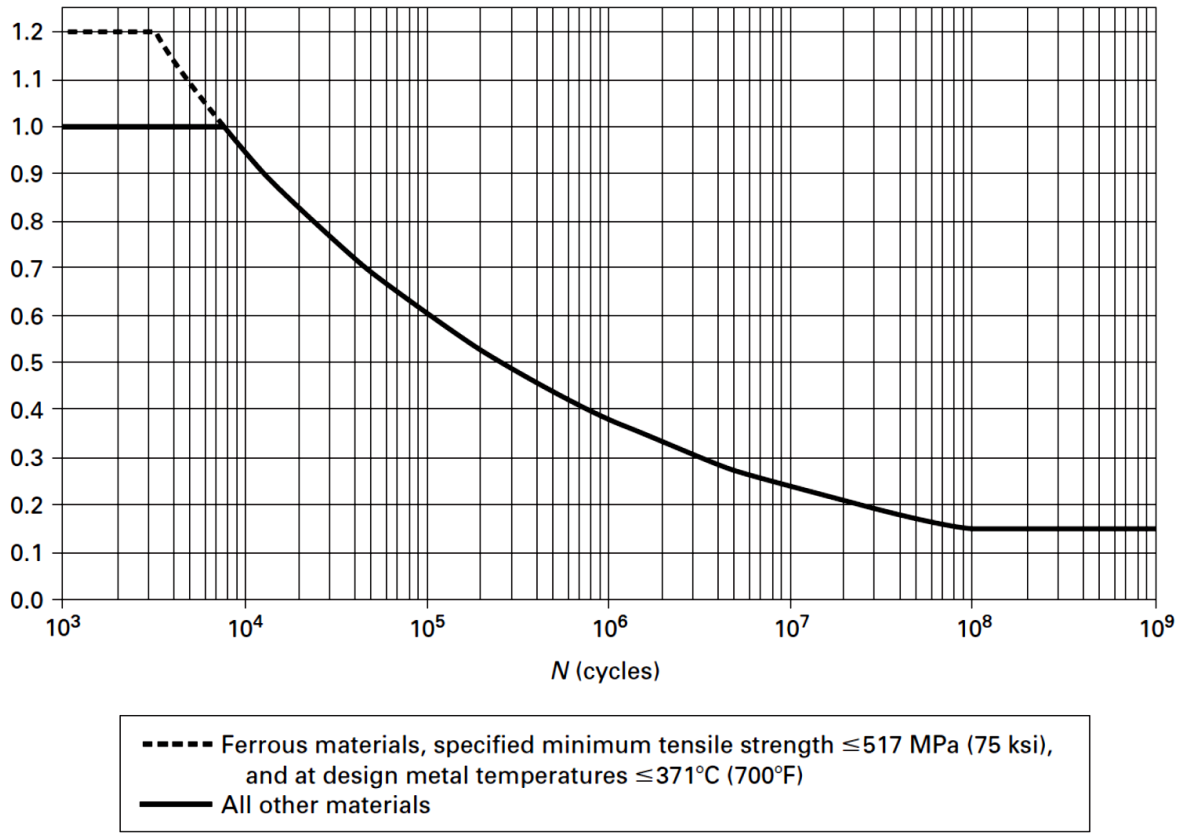

Figure 2.4-1: *Stress range factor (Engineers, 2014)*

2.5.3. Component Flexibility Factors

Flexibility factors are unitless numbers determined on the nominal wall thickness and mean radius of the pipe fitting. Curved elbows have the most flexibility due to its ability to ovalize when it experiences bending moments. K-factors are the multiple of the increased flexibility of the component compared to a straight pipe.

Curved Elbows –The flexibility is achieved from the flattening on the component along with one of its axis. The flexibility factor was determined using a Fourier-series solution by von Karman in 1911 and later redeveloped by Hovgaard in 1926. The following equation is used to calculate the flexibility factor of elbows:

$$\mathrm{k} = \frac{12h^2+10}{12h^2+1} \qquad \textit{(2.4—3)}$$

Where:

k - flexibility factor

h - $\frac{tR}{r^2}$

t - pipe wall thickness (m)

r - mean radius (m)

R - radius of curvature (m)

Mitre Bends – The flexibility properties of Mitre bends are similar to that of curved elbows. The mitre angle is usually small which resembles a curved elbow. From tests performed the flexibility factor approaches approximately 80 percent to that of the curved elbows. The following equation is used to calculate the flexibility factor of Mitre bends:

$$\mathrm{k} = \frac{1.52}{h^{\frac{3}{6}}} \qquad \textit{(2.4—4)}$$

Where:

R_e - equivalent radius

- $\frac{s}{2}cot\alpha$ $\quad for\ s \leq r\ (1 + tan\alpha)$
- $\frac{r}{2}(1 + cot\alpha)$ $\quad for\ s \geq r\ (1 + tan\alpha)$

s - mitre spacing at the centerline

r - pipe wall radius

α - one half of the angle between adjacent mitre axes

2.5.4. Stress Intensification Factors

Stress Intensification Factors are used to intensify the bending stresses in piping components resulting from thermal expansion. The magnitude of SIF's depends on the geometry of the piping component. Where the minimum SIF is 1.0. Components with smooth transition radii have low SIF's compared to components with sharp geometrical changes that have higher SIF's. The theory of stress intensification factors is based on ideal homogenous notch-free material although the results of fatigue tests are done using commercials products joined by butt welding. This causes surface imperfections from stress raisers in heat-affected zones. For this reason, stress intensification factors obtained from fatigue tests are usually lower than those predicted by theory or measured during strain-gage testing.

Since the straight pipe is the primary constituent of piping systems and most piping failures occur from the effects of cyclic loading, stress-intensification factors will be defined as the ratio of fatigue failure caused by bending moment for a given number of cycles in a straight pipe to that of other piping components. From this definition the S-N curves for straight pipe and piping components are parallel. The following expression has been determined to represent this:

$$\mathrm{i}SN^{0.2} = C \qquad (2.4—5)$$

Where:

i - Stress-intensification factor
S - Bending stress
N - number of stress cycles to failure
C - material constant

Tests performed by Rossheim determined material constants (C) for commercial piping material grades. The following results were achieved:

Carbon steel grade B - 245 000

Stainless steel 316 - 245 000

Stainless steel 347 - 245 000

Stress intensification factors for two straight lengths of pipe welded together – As previously discussed tests are done on butt welded pipe therefore this forms the basis of all testing.

∴ Stress intensification = 1

An important discovery by AC Markl proved that fatigue failure does not only transpire at high number of cycles. Tests performed on commercial piping proved fatigue failure can occur at 20 cycles or 2 000 000 cycles depending on the stress amplitude.

Stress intensification factors for Piping Components - The outcome of the fatigued tests performed by AC Markl showed similarities in the behaviour of bending fatigue for all piping components. Therefore a common empirical expression for the stress-intensification factor could be derived:

$$\mathrm{i} = \frac{0.9}{{h_e}^{2/3}} \geq 1 \qquad (2.4—6)$$

Where:

h_e - effective flexibility characteristic = $c\ (\frac{t_e R_e}{r^2})$

c - section-modulus correction factor = $\left(\frac{t_e}{t}\right)^{1.5}$

t_e - effective fitting thickness = pipe thickness

t - pipe thickness

r - mean radius of pipe

R_e - effective bend radius

Stress intensification factors for Flanged connections - Bolted flange connections present dual problems in piping flexibility analysis. The first being the extreme failure by rupture and the second joint displacement causing gasket blowouts. A paper published by Markl and George predicted ultimate rupture in bolted joints that occurred at around 275 MPa, with leakage in joints initiating well below the rupture stress. In conclusion, a stress intensification factor of 1.5 was predicted for bolted flanged joints.

Stress intensification factors, i, and flexibility factors, k, shall not be less than 1. Appendix E lists the flexibility factors and stress intensification factors for all piping components. CAESAR II software used for the flexibility analysis of piping systems automatically calculates SIF's and flexibility factors. The modelling of piping components is critical to obtain accurate results.

2.5.5. General Process for Flexibility Analysis

A piping system is a tubular-frame structure therefore the analysis of stresses, forces, and moments shall be evaluated with the principles and theories thereof. Although theoretical calculations are valid for any number of restraints, the computation increases drastically with the number of unknowns. For this reason, stress analysis software programs are used for the Flexibility analysis of piping systems.

The following steps are taken for the flexibility analysis of any piping systems for a given line size, system configuration, and material with a predetermined stress amplitude and several temperature cycles.

1. The first step in the analysis is to determine the physical properties of the material such as – thermal coefficient of expansion, modulus of elasticity, Poisson's ratio, endurance strength, yield stress, creep, and allowable stresses.
2. The piping system is modelled on CAESAR II. SIF's and Flexibility factors are automatically loaded by the software program.
3. Forces and moments are to be calculated at restraints. Restraints are classified as either end restraints, major or secondary restraints. The resistance to free movement from guides, solid hangers, and braces are of most importance.
4. A method of analysis is to be adopted to solve for stresses and strains – Tresca or von Mises.
5. The final step is to compare the calculated results to the allowable stresses and strains of the system.

Thermal coefficient - The value for the Thermal coefficient of expansion can be determined from Appendix F. The value used for analysis is the algebraic difference between the systems minimum and maximum operating temperature.

Poisson's ratio - taken as 0.3 for all metals at all operating temperatures.

Modulus of Elasticity – Reference modulus of elasticity is taken at room temperature, E_a. Modulus of elasticity at minimum, E_c, or maximum, E_m, room temperature is taken from Appendix F.

Reactions

The reaction forces and moments at all piping restraints shall be calculated on the maximum loading from operating conditions, dead weight, pressure, dynamic loadings, and thermal displacements. The modulus of elasticity shall be taken at maximum or minimum operating temperature, E_m.

The fatigue stress analysis of a piping system is broken down into the different points of the temperature range in actual practice. The two critical points being the initial install temperature called the Cold-spring and the design temperature of the system called Hot-spring. Cold Spring is the intentional deformation of piping to reduce stresses on the system during operation. Adding cold spring to a piping system is the removal of pipe length to allow for expansion at design temperature. A factor is introduced in stress and reaction force calculations for the variance in the temperature range called the cold-spring factor (c). The factor ranges from 0 for no cold spring to 1 for 100 percent cold spring.

If a system is installed with no cold spring, high stresses are initially experienced. The system will cycle from zero stress at initial install condition to max stress at max operating temperature. Laboratory tests performed on a system with no cold spring initially added, relaxed over time causing "self-sprung".

The diagram below shows the stress cycling of a system with an initial 50 percent cold spring and one of no cold spring.

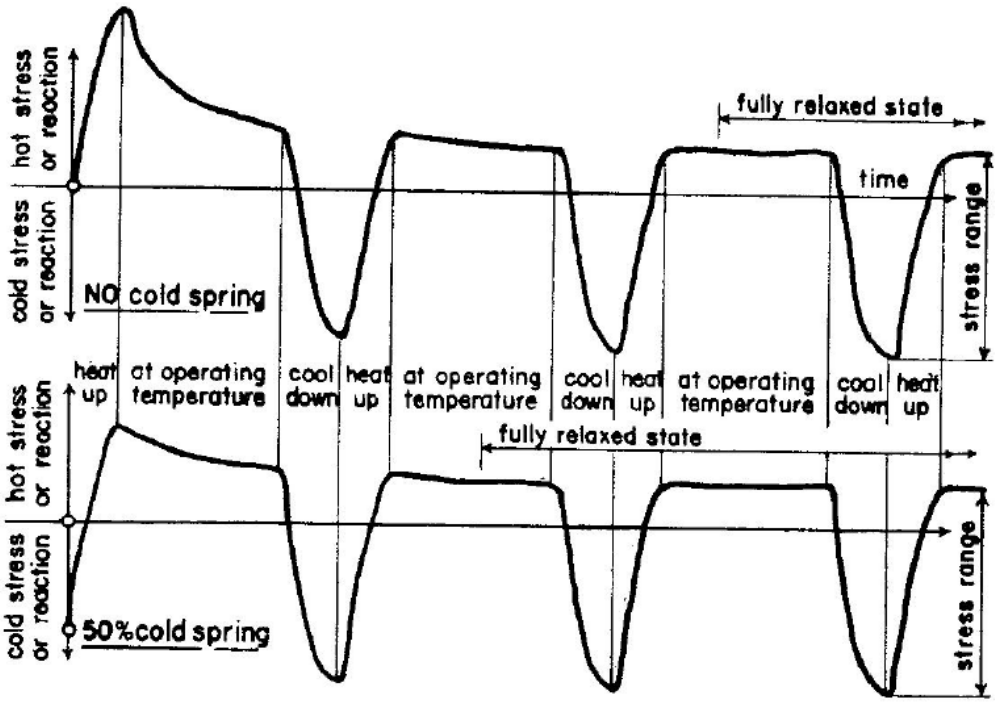

Figure 2.4-2: *Initial no cold spring vs 50% cold spring (Markl, 1955)*

The study of a system can be isolated to the stress variation from changing temperature conditions.

$$s'_C = cS_E \qquad (2.4—7)$$

Where:

s'_C - initial cold stress

As temperature increases, the stress decreases, reaching zero stress if the installation dimensions allowed for full expansion of the pipe at design temperature.

$$s'_h = (1 - c)\,\frac{E_h}{E_c}\,S_E \qquad (2.4—8)$$

Where:

s'_h - Initial hot stress

E_h - Young's modulus at max operating temperature

If yielding or creep does not occur in either the hot or cold condition, the stress experienced by the system due to fatigue will alternate between the hot stress and cold stress during thermal cycles.

The extreme hot and cold stress conditions are expressed as follows:

$$s_h'' = S_r \qquad (2.4—9)$$

Where:

s_h'' - ultimate hot stress

$$s_c'' = S_E - \frac{E_c}{E_h} S_r \qquad (2.4—10)$$

Where:

s_c'' - ultimate hot stress

The previous four equations describe the extreme stress conditions experienced by a piping system during the service life. These equations hold true for the system with and without cold spring.

The reaction forces at nodes on the piping structure are calculated using the following equation:

$$\mathrm{R} = eE_c I F_r = \frac{ZF_r}{tF_s} S_E = FS_E \qquad (2.4—11)$$

Where:

e - coefficient of thermal expansion

E_c - Young's modulus at the initial installation temperature

I - moment of inertia

i - stress-intensification factor

$\frac{F_r}{F_S}$ - Shape factors

F - composition factor

The reactions and stresses of a system for the temperature range are interrelated by a factor F, which is constant for any line of given shape and dimensions.

A system shall be designed to withstand the maximum reaction forces and moments experienced during the temperature range. From the above equations for reaction forces for a temperature cycle, the following equation has been derived for the Maximum reaction including a factor of safety of 3. The maximum reaction is calculated at extreme displacement conditions using the following equation:

$$\mathrm{R}_m = R\left(1 - \frac{2C}{3}\right)\frac{E_m}{E_a} \qquad (2.4—12)$$

Where:

C - cold spring factor

2.5.6. Displacement Stress Range

The displacement stress range, S_E, is the range of secondary stress a piping system experiences due to thermal expansion and contraction. Primary stresses due to pressure and weight are excluded from this evaluation. The combination of axial, bending, and torsional displacement stress ranges are used to calculate the displacement stress range. This value shall not exceed the Allowable stress range of the system.

Axial stress, S_a, is a result of axial thermal forces over the cross-section of the pipe.

Bending stress, S_b, is a result of in-plane and out-plane bending stresses due to thermal expansion.

Torsional stress, S_t, is a result of torsional stress in the piping component.

$$S_E = \sqrt{(S_a + S_b)^2 + (2S_t)^2} \qquad (2.4\text{—}13)$$

Where:

S_a - axial stress range due to displacement strains = $\frac{i_a F_a}{A_p}$

A_p - cross-sectional area of pipe – Nominal thicknesses and outside diameters are to be used for analysis

F_a - axial force between two nodes

i_a - axial stress intensification factor = 1.0 for pipe bend, mitre bends or i

S_t - torsional stress range due to displacement strains = $\frac{i_t M_t}{2Z}$

i_t - torsional stress intensification factor = 1.0 for pipe bend, mitre bends or i

M_t - torsional moment range between two nodes

Z - section modulus of the pipe

The bending stress range is calculated using the following equation:

$$S_b = \frac{\sqrt{(i_i M_i)^2 + (i_o M_o)^2}}{Z}$$

Where:

i_i - in-plane stress intensification factor

i_i - out-plane stress intensification factor

M_i - in-plane bending moment range between two nodes

M_o - out-plane bending moment range between two nodes

An in-plane bending moment can be described as the bending moment that causes the component to open or close in its reference planes. Whereas out-plane bending moments cause the component to bend out of its reference plane. Figures 2.4-3 and 2.4-4 show the in-plane and out-plane bending moments of a pipe bend and branch connection respectively.

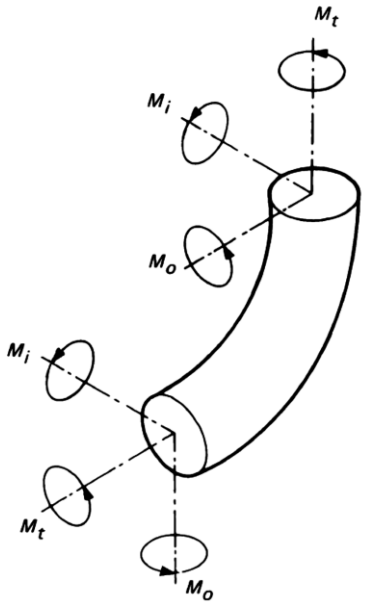

Figure 2.4-3: *Moment in bends (Engineers, 2014)*

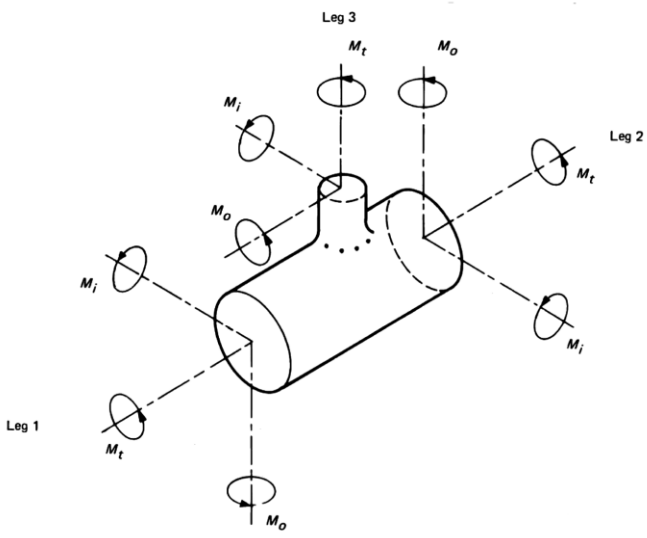

Figure 2.4-4: *Moment in branch connections (Engineers, 2014)*

CHAPTER 3

3.0 Practical Analysis

The apparent need for piping systems stress analysis at Indy Oils blending plant became eminent after the occurrence of piping failures. These failures included cracks on pipe walls, gasket blowouts, damage to equipment as a result of piping failures and the failure of piping supports. Following these failures, thorough investigations were done on the systems to try and determine the root cause. This study identifies the shortfalls of the original design. The knowledge gained through research and analysis of similar piping systems is used to determine the failure modes of the Plants failed piping systems. The results of a comprehensive analysis of Indy Oils Tank Farm piping will be used to predict failure modes of similar systems. These results are used in conjunction with the review and understanding of historical literature.

A major project was initiated to install a bulk holding Tank Farm at Indy Oil for the storage of Petroleum products. The product range stored in the Tank Farm is petroleum base oils and additives. A total of 17 tanks were installed with a total holding capacity of 2.25 million litres. Dedicated piping systems are required from each of the bulk holding tanks to the blending tanks in the plant. The area that was available for the Tank Farm is very confined, making the routing of piping very difficult. The radial distance between each Tank is only 1 meter apart. Figure 3.1-1 below shows the layout view of the Tank Farm tanks. The high complexity of this design and analysis increases its suitability to predict failures on other systems.

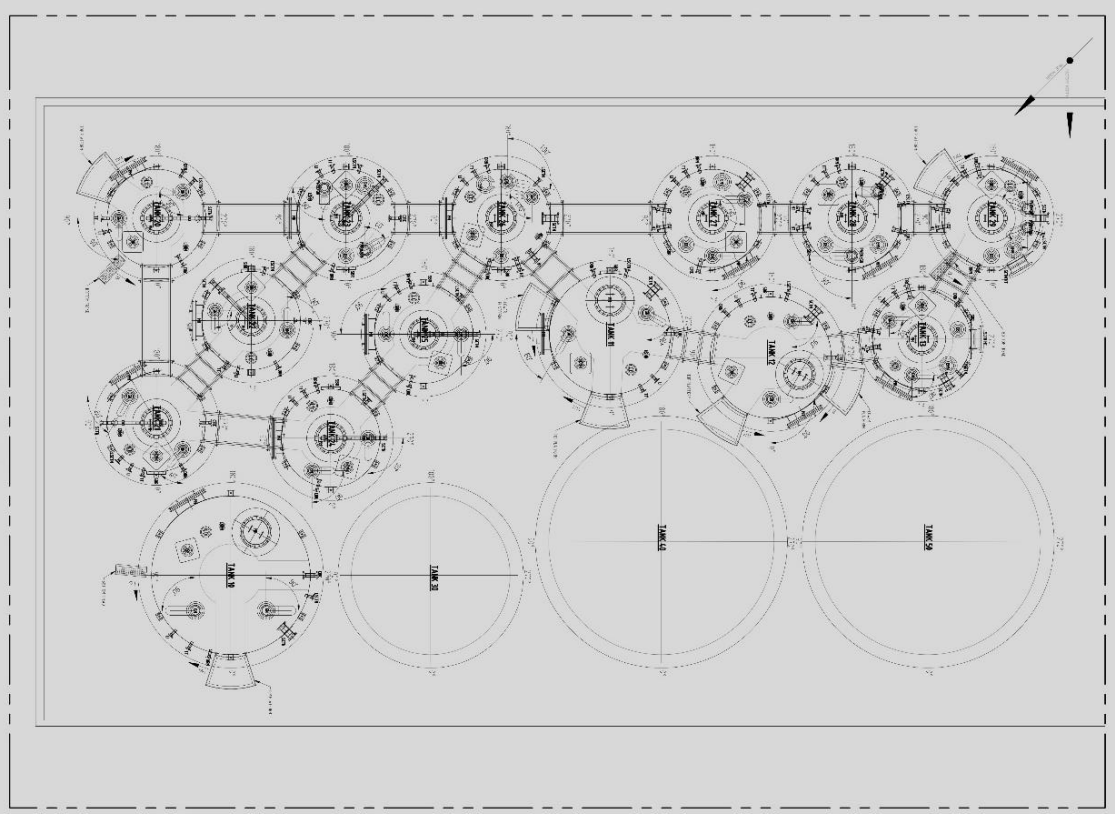

Figure 2.4-1: *Tank Farm Layout*

This study shall focus on the full stress analysis of one of the piping routes from the Indy Oil Tank Farm to the blending plant. The same principles will be applied in the analysis of the other 16 pipe routes. The modelling of all 17 pipe routes was done to ensure there is sufficient space in the Tank Farm bund for all piping systems. Process and Instrumentation diagrams were done to determine the optimum process flow. The piping system shall be broken up into two sections. The first section is the route from the Tank Farm bulk holding tank to the pump and will be referred to as the Suction line route. The second section is the route from the pump to the blending plants tank, and this route will be referred to as the Discharge line route.

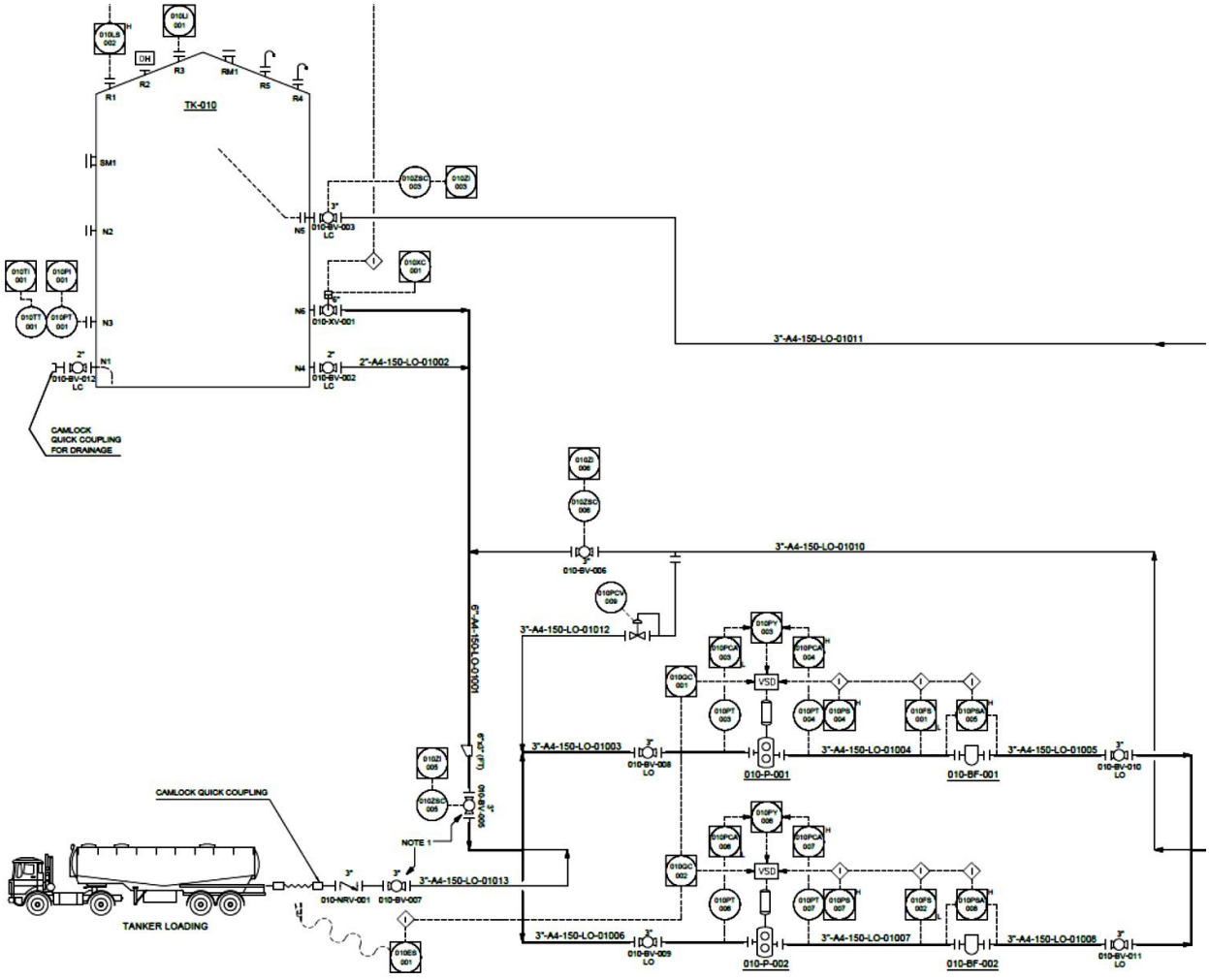

Figure 2.4-2: *Typical P&ID for all tanks*

Following the design steps described in this study, the first step of the design process is the use of Fluid Dynamics theories to calculate the piping's internal pressure. By doing so the dimensional properties are specified for the system.

3.1 Primary Stress Analysis

3.1.1. Fluid Dynamics in Piping Systems

The most basic function of a piping system is to deliver fluid from one point to another in the quickest possible time. The driving force required for the transfer of fluid is done by using a pump. An industrial process's fluid flow rate is reliant on the balance between the transfer pump size and the size of the piping.

The most common types of pumps used for the transfer of petroleum product is categorised into two groups — positive displacement pumps and dynamic (centrifugal) pumps. Positive displacement pumps work by a mechanical means that vary the size of the fluid chamber which causes the fluid to flow. Centrifugal pumps create fluid flow by using centrifugal force from a rotating impeller. Each pump has different torque and flows characteristics. Positive displacement pumps have constant torque, whereas centrifugal pump torque varies according to flow resistance at the discharge of the pump. A pump has to overcome the pressure in the piping system to achieve fluid flow. Low-pressure industrial pumps (not pressure generating) that are manufactured for the transfer of fluid at high flow rates can withstand a maximum pressure of 5 to 16 bar. Therefore, the maximum pump pressure is one of the limiting factors in the design of piping systems.

As discussed in the notes of Fluid Dynamics, the pressure is created from frictional forces between the pipes surface and the fluid; change in kinetic energy; and from the change in elevation of the piping to the pump. Where pipe frictional forces are dependent on fluid flow rate, the viscosity of the fluid, and pipe diameter.

The Fluid Dynamics calculations in the design of piping systems are critical to the process requirements of the Plant. The selection of pump size and pipe diameters is limited to the available budget of the project. The floor space available for the system also plays a role in decision making.

The higher the flow rate achievable for the transfer of fluid from the Tank Farm to the blending tanks at Indy Oil, the higher the production output. This, in turn, results in a quicker delivery to customers, therefore, higher turnover for the business. Space constraints at Indy Oil's Tank Farm are also faced, limiting the diameter size of the piping. For this reason, all piping routes are to be modelled in the Tank Farm before the stress analysis is performed to ensure efficient size and space utilization.

The industry standard for the transfer of petroleum products between process equipment is 1000 l/min. This flow rate shall be used as the basis for the Fluid dynamics design. All products stored in the Tank Farm are petroleum base oils and additives with a viscosity range of 23 – 33554 cSt at 20°C.

The piping model can only be completed once the optimal transfer flow rate to the pipe dimension is determined. The limiting factor in determining these two variables is pipe internal pressure. The length of pipe and pipe fittings (bends, reducers, tees, etc.) will be estimated in

the worst-case situation i.e. longest pipe length, maximum pipe fittings, highest viscosity fluid, etc. The piping model is done based on the results of the Fluid Dynamics analysis.

The table below details the process parameters for Fluid Dynamics analysis.

Table 3.1-1: *Process parameters*

PROCESS PARAMETER	**UNITS**
Flow rate	$1000\ l/\min = 0.0167\ \frac{m^3}{s}$
Viscosity	$23 – 33554\ cSt$ $= 0.000023 – 0.033554\ \frac{m^2}{s}$
Operating temperature	5 – 100 °C

As discussed the piping route is broken up into two sections namely the Suction line and Discharge line. The maximum pressure in the piping system is at the pump and decreases along the length of the pipe.

Suction Line:

Pipe suction properties are estimated as follows, to determine the pressure at the suction line:

- Length = 45 m
- Pipe diameter = 6 in = 152.4 mm = 0.1541 m – See Appendix G
- Number of 90° bends = 8
- Number of 45° bends = 4
- Number of pipe reductions = 1 reduction to 3 in
- Length of reduction = 4 m
- Number of valves according to P&ID = 2 (Full bore, therefore, no minor losses)

The reduction in pipe diameter prevents air pockets at the suction of the pump. This shall ensure full diameter flow is delivered to the pump.

To calculate the pressure in the suction line Bernoulli's equation (2.1.4-2) is applied from the Tank Farm bulk holding tank to the pumps suction side:

Point 1 is located at the outlet of the Tank Farm bulk holding tank and Point 2 is located at the pump suction.

$$\frac{P_1}{\rho g} + \frac{{V_1}^2}{2g} + Z_1 = \frac{P_2}{\rho g} + \frac{{V_2}^2}{2g} + Z_2 + \sum h_f$$

Where:

P_1	- the pressure at Tank Farm outlet (Pa)
P_2	- pressure at pump suction (Pa)
ρ	- density of fluid (kg/m^3)
V_1	- fluid velocity at Tank Farm outlet $\left(\frac{m}{s}\right)$
V_2	- fluid velocity at pump suction $\left(\frac{m}{s}\right)$
z_1	- elevation at Tank Farm outlet (m)
z_2	- elevation at pump suction (m)
$\sum h_f$	- the sum of losses (m)

It is a process requirement for the pump to completely empty the Bulk holding tank. Therefore the analysis will be based on the worst-case for the pump where hydrostatic pressure is ignored; $P_1 = 0$. The velocity at the Tank Farm tank outlet is equal to the velocity at the pump suction; $\frac{{V_1}^2}{2g} = \frac{{V_2}^2}{2g}$. Datum is set at the pump. The elevation difference between the pump and bulk holding tank is taken as 0 metres for worst-case analysis, $z_1 = z_2 = 0$. $\sum h_f$ is the sum of friction losses (before and after reduction in pipe diameter) and minor losses due to pipe bends, diameter reductions, valves, etc.

$$\therefore \quad \frac{P_1}{\rho g} = \sum h_f$$

Applying equation (2.1-9) to calculate pipe Frictional losses:

$$hf = \frac{4.f.L.v^2}{2.g.d}$$

Where:

f	- friction factor
P_2	- the pressure at pump suction (Pa)

$$\therefore \quad hf = \frac{(4)(f)(15)(0.894^2)}{(2)(9.81)(0.1541)}$$

Pipe length is estimated at 45 metres. Fluid velocity, $V = \frac{4Q}{\pi d^2}$, where $Q = 0.0167 \frac{m^3}{s}$. The friction factor is calculated using the Colebrook en White formula (2.1-10).

$$\frac{1}{\sqrt{f}} = -4\, log_{10}\{\frac{1.255}{Re\sqrt{f}} + \frac{\epsilon}{3.71\, d}\}$$

The initial analysis will be based on commercial carbon steel piping with a surface roughness of 0.000046 m.

$$\therefore \qquad \frac{1}{\sqrt{\mathrm{f}}} = -4\log_{10}\left\{\frac{1.255}{R_e\sqrt{f}} + \frac{0.000046}{3.71(0.1541)}\right\}$$

The Reynolds number is determined using equation (2.1-5):

$$\mathrm{R_e} = \frac{\mathrm{V_{avg}D}}{\mathrm{v}}$$

$$\therefore \qquad \mathrm{R_e} = \frac{\mathrm{V_{avg}D}}{\mathrm{v}}$$

The density range of Petroleum base oils is $700 - 1000\frac{kg}{m^3}$, Viscosity range is $0.000023 - 0.33554\frac{m^2}{s}$.

$$\therefore \qquad \mathrm{R_e} = \frac{(0.894)(0.1541)}{0.000023}$$

$$\therefore \qquad \mathrm{R_e} = 5989.8$$

For the above situation, the flow is turbulent.

As described earlier Equation 2.1-10 is implicit for f, therefore, an initial value for f must be guessed and inserted into the right side of the equation. The result must be substituted into the right of the formula. This process must be repeated until the result remains constant.

0.033 shall be used as the initial guess for f

$$\therefore \qquad \frac{1}{\sqrt{\mathrm{f}}} = -4\log_{10}\{\frac{1.255}{5989.8\sqrt{0.033}} + \frac{0.000046}{3.71(0.1541)}\}$$

$$\therefore \qquad f = 0.007387$$

Inserting the solved answer for f back into equation 2.1-10:

Sub. 2 – f = 0.009253

Sub. 3 – f = 0.008926

Sub. 4 – f = 0.008977

Sub. 5 – f = 0.008969

Sub. 6 – f = 0.008970

Sub. 7 – f = 0.008970

Sub. 8 – f = 0.008970

The answer for f remains constant after the sixth substitution.

The pressure loss due to friction is therefore:

$$\therefore \quad hf = \frac{(4)(0.008970)(15)(0.894^2)}{(2)(9.81)(0.1541)}$$

$$\therefore \quad hf = \frac{(4)(0.008970)(15)(0.894^2)}{(2)(9.81)(0.1541)}$$

$$\therefore \quad hf = 0.4268\, m$$

The same procedure is applied as above to calculate friction loss for the length of a pipe after the reduction in pipe diameter. Where: $L = 4\, m$; $d = 0.07793\, m$

$$hf = 0.9748\, m$$

Minor losses are determined using equation (2.1-11)

$$\mathrm{h_{minor}} = \frac{\mathrm{kV^2}}{\mathrm{2g}}$$

Where coefficients are as follows:

Pipe reduction to 3 inch = 0.34; 6 inch 90° pipe bend = 0.24; 6 inch 45° bend = 0.24
Velocity is calculated at $3.494\frac{m}{s}$ for the reduced pipe diameter of 3 inches.

Pipe reduction:

$$\therefore \quad \mathrm{h_{minor}} = \frac{0.34(3.494^2)}{2(9.81)}$$

$$\therefore \quad \mathrm{h_{minor}} = 0.2116\, m$$

Pipe 90° bend:

$$\therefore \quad \mathrm{h_{minor}} = \frac{0.24(0.894^2)}{2(9.81)}$$

$$\therefore \quad \mathrm{h_{minor}} = 0.00978\, m$$

The *k* coefficient for 45° and 90° bends of the same diameter are equal therefore losses for the same system are equal.

The pressure at the pump suction is, therefore:

$$\therefore \quad \frac{P_1}{\rho g} = 0.4268 + 0.9748 + 0.2116 + (8 \times 0.00978) + (4 \times 0.00978)$$

$$\therefore \quad \frac{P_1}{\rho g} = 1.73056\, m$$

$$\therefore \quad P_1 = 16.977\, kPa = 0.17\, bar$$

The following table shows the calculated pipe pressures at various fluid viscosities and flow rates. All other estimated system properties are kept constant as per the workings above. The optimum pipe diameter and fluid flow rate are selected using this data.

The following pipe diameter reductions are made before the pump:

- 6 inch to 3 inch
- 3 inch to 2 inch
- 2 inch to 1 inch

Table 3.1-2: *Suction length pipe internal pressure*

Pipe Diameter (in)	**Pipe Internal Pressure (Bar) at Flow Rate (l/min)**											
	Viscosity = $0.000023\ \frac{m^2}{s}$			Viscosity = $0.000102\ \frac{m^2}{s}$			Viscosity = $0.002681\ \frac{m^2}{s}$			Viscosity = $0.033554\ \frac{m^2}{s}$		
	500	750	1000	500	750	1000	500	750	1000	500	750	1000
6 in	0.05	0.1	0.17	0.08	0.12	0.24	1.76	2.64	3.53	21.8	32.83	43.78
3 in	0.59	1.21	2.03	0.69	1.38	2.86	16.28					
2 in	2.42	5.01	8.45	2.36	7.08	11.68	55.23					

The above table is calculated for the longest length pipeline in the Tank Farm. The tank's closet to the locations of the pumps is within 10 metres. The product allocations will therefore be based on the viscosities of the products stored in the tanks. The maximum pressure at the suction side of the pump is governed by atmospheric pressure (101.325 kPa / 1.01325 Bar). All values above 1 bar will cause the pump to cavitate. Cavitation causes damage to the pump and could also promote the ignition properties of Petroleum products. It is not necessary to calculate the pressures in the table above at high viscosities and small pipe diameters.

From the results in the table above it can be noticed that if a Fluid dynamics analysis is not performed it can be detrimental to the entire piping system.

Discharge Line:

Pipe discharge properties are estimated as follows, to determine the pressure at the discharge line:

- Length = 80 m
- Pipe diameter = 4 in = 102.26 mm = 0.10226 m - See Appendix H
- Number of 90° bends = 16
- Number of 45° bends = 8
- Number of pipe reductions = 1 reduction to 3 in
- Length of reduction = 4 m
- Number of valves according to P&ID = 2

To calculate the pressure in the Discharge line Bernoulli's equation (2.1.4-2) is applied from the pump discharge to the inlet of the blending tank:

Point 1 is located at the pump discharge and Point 2 is located at the blending tank inlet.

$$\frac{P_1}{\rho g} + \frac{{V_1}^2}{2g} + Z_1 = \frac{P_2}{\rho g} + \frac{{V_2}^2}{2g} + Z_2 + \sum h_f$$

Where:

P_1	- the pressure at the pump (Pa)
P_2	- pressure at pipe discharge (Pa)
ρ	- density of fluid (kg/m^3)
V_1	- fluid velocity at pump $\left(\frac{m}{s}\right)$
V_2	- fluid velocity at pipe discharge $\left(\frac{m}{s}\right)$
z_1	- elevation at pump (m)
z_2	- elevation at pipe discharge(m)
$\sum h_f$	- the sum of losses (m)

The discharge pipe is routed to the top of the blend tank, therefore, vented to the atmosphere; $P_2 = 0$. The velocity at the pump is equal to the velocity at the pipe discharge; $\frac{{V_1}^2}{2g} = \frac{{V_2}^2}{2g}$. Datum is set at the pump; $z_1 = 0$. The elevation difference between the pump and top of the tank is 7 metres. $\sum h_f$ is the sum of friction losses and minor losses due to pipe bends, diameter reductions, valves, etc.

$$\therefore \quad \frac{P_1}{\rho g} = 7 + \sum h_f$$

Pressure loss due to friction is calculated using the same theories and procedures as done to determine losses in the Suction line. Only final results for pressure will be described.
The following table shows the calculated pipe pressure at various fluid viscosities and flow rates. The optimum pipe diameter and fluid flow rate are selected using this data.

The following pipe diameter reductions are made before the pump:

- 4 inch to 3 inch
- 3 inch to 2 inch
- 2 inch to 1 inch

Table 3.1-3: *Discharge length pipe internal pressure*

Pipe Diameter (in)	**Pipe Pressure (Bar) at Flow Rate (l/min)**											
	Viscosity = $0.000023\ \frac{m^2}{s}$			Viscosity = $0.000102\ \frac{m^2}{s}$			Viscosity = $0.002681\ \frac{m^2}{s}$			Viscosity = $0.033554\ \frac{m^2}{s}$		
	500	750	1000	500	750	1000	500	750	1000	500	750	1000
4 in	0.9	1.1	1.4	1.0	1.2	1.5	8.4	12.2	16.1	96.4	144.3	192.2
3 in	1.6	2.5	3.7	1.7	2.7	4.9	25.3	37.8	50.2	307.9	416.6	615.4
2 in	5.0	9.6	15.7	4.9	13.2	21.3	97.06					

The results in the table above are calculated for the longest length pipeline from the pump's discharge to the plant's blend tank. The maximum pressure at the discharge side of the pump is governed by the maximum allowable pressure specified by the pump manufacturer (1600 kPa = 16 Bar). Although piping can be specified to withstand high internal pressure, industrial pumps maximum pressure is inversely proportional to flow rate. In other words, pumps that run at high flow rates have a low maximum pressure capacity. From the results in the table above it can be noticed that incorrectly specifying a pipe diameter can be detrimental to the piping system. Pressure increases exponentially in a matter of seconds which could lead to failure of the pump. This increase in pressure will also cause overstress in the piping system and can result in piping failures.

Water Hammer

Sudden closure of a valve along the Suction line or Discharge line will result in Water Hammer which is described as a rapid increase in the pipe's internal pressure.

The first analysis will be done on the Suction Line. Where $P = 0.17\ bar$, $d\ =\ 154.1\ mm$, $t\ =\ 7.112mm$, $V\ =\ 0.894\ m/s$

The velocity by which a pressure wave is propagated in the pipe is calculated using equation (2.1-12):

$$\mathrm{a} = \sqrt{\frac{\mathrm{K_e}}{\rho}}$$

Where the density of Petroleum base oil is taken as $890\ kg/m^3$, k is related to Poissons ratio = 0.9, $\mathrm{K_e}$ is calculated using the following equation (2.1-13)

$$\frac{1}{\mathrm{K_e}} = \frac{1}{\mathrm{K_f}} + \frac{\mathrm{kd}}{\mathrm{tE}}$$

The bulk modulus of the oil is 1.8 GPa, Equivalent bulk modulus of carbon steel at 20 degrees Celsius is interpolated from Appendix D = $203.46\ GPa$

$$\therefore \qquad \frac{1}{\mathrm{K_e}} = \frac{1}{1.8 \times 10^9} + \frac{(0.9)(0.1541)}{(0.00711)(203.46 \times 10^9)}$$

$$\therefore \qquad K_e = 1.54 \times 10^9$$

Velocity in the pipe is, therefore:

$$\therefore \qquad \mathrm{a} = \sqrt{\frac{1.54 \times 10^9}{890}}$$

$$\therefore \qquad \mathrm{a} = 1315.42 \frac{m}{s}$$

This will result in a rapid increase in pressure calculated using equation (2.1-15)

$$\Delta \mathrm{h_{hammer}} = \frac{\mathrm{a}\Delta \mathrm{V}}{\mathrm{g}}$$

$$\therefore \qquad \Delta \mathrm{h_{hammer}} = \frac{(1315.42)(0.894)}{9.81}$$

$$\therefore \qquad \Delta \mathrm{h_{hammer}} = 119.88\ m = 1175.985\ kPa = 11.76\ bar$$

The analysis of water hammer is repeated for the discharge line Where $P = 1.4\ bar$, $d\ =\ 102.3\ mm$, $t\ =\ 6.02\ mm$, $V\ =\ 2.03\ m/s$

The equivalent bulk modulus of the discharge line:

$$\frac{1}{\mathrm{K_e}} = \frac{1}{1.8 \times 10^9} + \frac{(0.9)(0.1023)}{(0.00602)(203.46 \times 10^9}$$

$$\therefore \quad K_e = 1.585 \times 10^9$$

Velocity in the discharge pipe is, therefore:

$$\mathrm{a} = \sqrt{\frac{1.585 \times 10^9}{890}}$$

$$\therefore \quad \mathrm{a} = 1334.7 \frac{m}{s}$$

The rapid increase in pressure due to water hammer:

$$\therefore \quad \Delta \mathrm{h_{hammer}} = \frac{(1334.7)(2.03)}{9.81}$$

$$\therefore \quad \Delta \mathrm{h_{hammer}} = 276.19\, m = 2709.448\, kPa = 27.09\, bar$$

3.1.2. Primary Stresses On Piping Due To Internal Pressure

As a minimum, the piping system shall withstand the stresses developed from internal pressure. The optimum pipe size calculated is 6 inches on the suction side of the pump and 4 inches on the discharge side. The maximum internal pressures were calculated as follows:

- Frictional forces between the pipes surface and the fluid; change in kinetic energy, and from the change in elevation of the piping to the pump = 16 Bar (based on the systems maximum design pressure).
- Water hammer = 27.09 Bar

The equations developed for the calculation of stresses due to internal pressure is based on the Thin wall cylinder principles and von Mises theory. Equation (2.2-7) is used to determine if the specified piping meets the requirements of Thin-wall cylinders:

$$\frac{t}{d_i} < \frac{1}{20}$$

$$\frac{7.112}{168.275} < \frac{1}{20} \qquad \text{for 6 in piping}$$

$$\frac{6.02}{102.3} < \frac{1}{20} \qquad \text{for 4 in piping}$$

<u>Suction Line:</u>

Longitudinal stresses are calculated using equation (2.2-8):

Due to Friction, Kinetic energy, and gravitational force –

$$\sigma_L = \frac{P.r}{2.t}$$

$$\sigma_L = \frac{(1600 \times 10^3)(0.07703)}{(2)(0.00711)}$$

$$\therefore \quad \sigma_L = 8.67\ MPa$$

Due to water hammer -

$$\therefore \quad \sigma_L = \frac{(2709 \times 10^3)(0.07703)}{(2)(0.00711)}$$

$$\sigma_L = 14.67\ MPa$$

Hoop / Circumferential stresses are calculated using equation (2.2-9):

Due to Friction, Kinetic energy, and gravitational force -

$$\sigma_C = \frac{(16000 \times 10^3)(0.07703)}{(0.00711)}$$

$$\therefore \quad \sigma_C = 17.33\ MPa$$

Due to water hammer -

$$\therefore \quad \sigma_C = \frac{(2709 \times 10^3)(0.07703)}{(0.00711)}$$

$$\therefore \quad \sigma_C = 29.35\ MPa$$

Discharge Line:

Longitudinal stresses:

Due to Friction, Kinetic energy, and gravitational force –

$$\sigma_L = \frac{(1600 \times 10^3)(0.05115)}{(2)(0.00602)}$$

$$\therefore \quad \sigma_L = 6.79\ MPa$$

Due to water hammer -

$$\therefore \quad \sigma_L = \frac{(2709 \times 10^3)(0.05115)}{(2)(0.00602)}$$

$$\sigma_L = 11.51\ MPa$$

Hoop / Circumferential stresses are calculated using equation (2.2-9):

Due to Friction, Kinetic energy, and gravitational force -

$$\sigma_C = \frac{(1600 \times 10^3)(0.05115)}{(0.00602)}$$

$$\therefore \quad \sigma_C = 13.59\ MPa$$

Due to water hammer -

$$\therefore \quad \sigma_C = \frac{(2709 \times 10^3)(0.05115)}{(0.00602)}$$

$$\therefore \quad \sigma_C = 23.02\ MPa$$

The Yield stress according to von Mises theory is calculated using equation (2.2-4):

Suction Line:

$$\sigma_y = \frac{1}{\sqrt{2}} \sqrt{(\sigma_1 - \sigma_2)^2 + (\sigma_2 - \sigma_3)^2 + (\sigma_3 - \sigma_1)^2}$$

Water hammer creates higher stresses in the suction line. Where $\sigma_1 = 14.47\ MPa$ and $\sigma_2 = 29.35\ MPa$

$$\therefore \quad \sigma_y = \frac{1}{\sqrt{2}} \sqrt{(14.47 - 29.35)^2 + (29.35 - 0)^2 + (0 - 14.47)^2}$$

$$\therefore \quad \sigma_y = 25.42\ MPa$$

Discharge Line:

Water hammer creates higher stresses in the discharge line. Where $\sigma_1 = 11.51\ MPa$ and $\sigma_2 = 23.02\ MPa$

$$\therefore \quad \sigma_y = \frac{1}{\sqrt{2}} \sqrt{(11.51 - 23.02)^2 + (23.02 - 0)^2 + (0 - 11.51)^2}$$

$$\therefore \quad \sigma_y = 19.94\ MPa$$

Material Specification

Piping dimensional and material properties are controlled by the ASME B31.3 code for Pressure piping design. The most readily available ASME schedule steel piping in South Africa are (See Appendix E):

I. A106 Grade A – Schedule 40
II. A106 Grade B – Schedule 40
III. A53 Grade A – Schedule 40
IV. A53 Grade B – Schedule 40

Piping specification A106 Grade B Schedule 40 shall be used as a basis for the piping stress analysis. The following table was extracted from Appendix E for A106 Grade B piping specification:

Table 3.1-4: *A106 Grade B Allowable Stresses*

Stress Type	**Stress** $(\boldsymbol{MPa})$
Minimum tensile strength	414
Minimum Yield strength	241
Basic Allowable stress at 0°C	138

The table below shows the summary of stresses experienced by the piping system due to internal pressure

Table 3.1-5: *Application Stress Summary*

Line Description	**Stress Type**	**Stress** $(\boldsymbol{MPa})$
Suction Line	Longitudinal stress	14.67
Suction Line	Circumferential stress	29.35
Suction Line	Yield Stress	25.42
Discharge Line	Longitudinal stress	11.51
Discharge Line	Circumferential stress	23.02
Discharge Line	Yield Stress	19.94

All applied stresses to the system due to internal pressure is within the allowable stress limits.

The minimum thickness of the piping components is calculated using equation (2.1-1):

$$t = \frac{PD}{2\,(SEW + PY)}$$

Internal pressure (P) due to water hammer is used to accommodate for the worst-case situation; Quality factors (E, W) are determined from Appendix A and B; Coefficient Y is determined from Appendix C

Suction Line:

$$t = \frac{(2709\times10^3)(0.154)}{2\,([(138\times10^6)(0.9)(1)]+[(2709\times10^3)(0.4)])}$$

$$t = 0.001665\,m = 1.665\,mm$$

Discharge Line:

$$t = \frac{(2709\times10^3)(0.1023)}{2\,([(138\times10^6)(0.9)(1)]+[(2709\times10^3)(0.4)])}$$

$$t = 0.00111\,m = 1.11\,mm$$

The suction and discharge minimum pipe thickness calculation is less than the specified pipe A106 Grade B Schedule 40 thickness.

3.1.3. Primary Stresses on Piping Due to Dead Weight and Dynamic Loading

Based on the dimensional and material specification done using the results of the Fluid Dynamics and Primary Stresses due to internal pressure calculations. A 3-dimensional model of the piping system was completed. The modelling of all 17 Bulk holding tanks was done to ensure there was sufficient space for all piping routes. Figures 3.1-1 to 3.1-9 show the complete piping system model design with a focus on one route from the bulk holding tank to the Plant's blend tank.

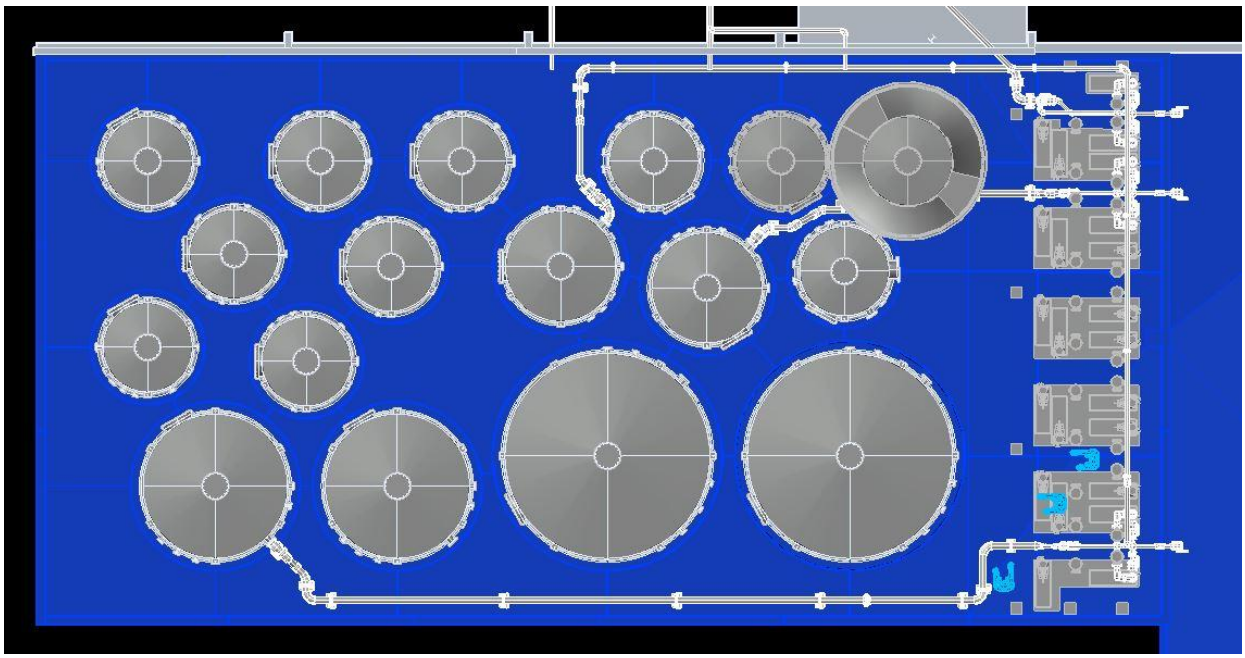

Figure 3.1-1: *Plan view of Tank Farm model*

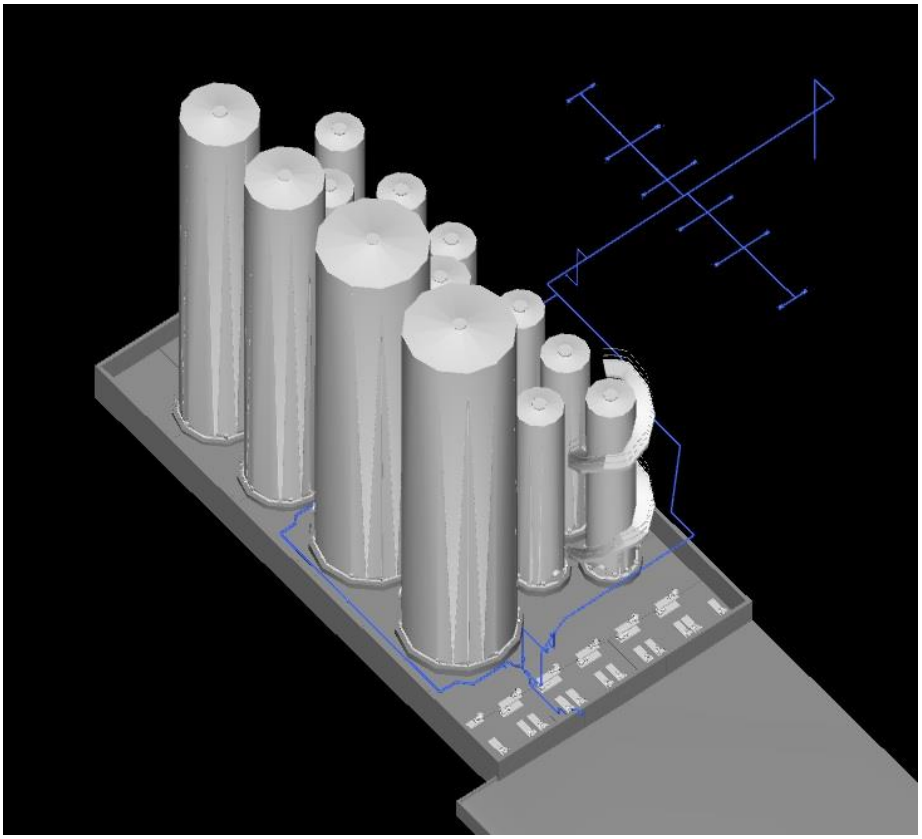

Figure 3.1-2: *Isometric view of a single piping model*

Figure 3.1-2 shows an isometric view of the single piping route that is being analysed. The model shows the confined space that the Tank Farm is situated in.

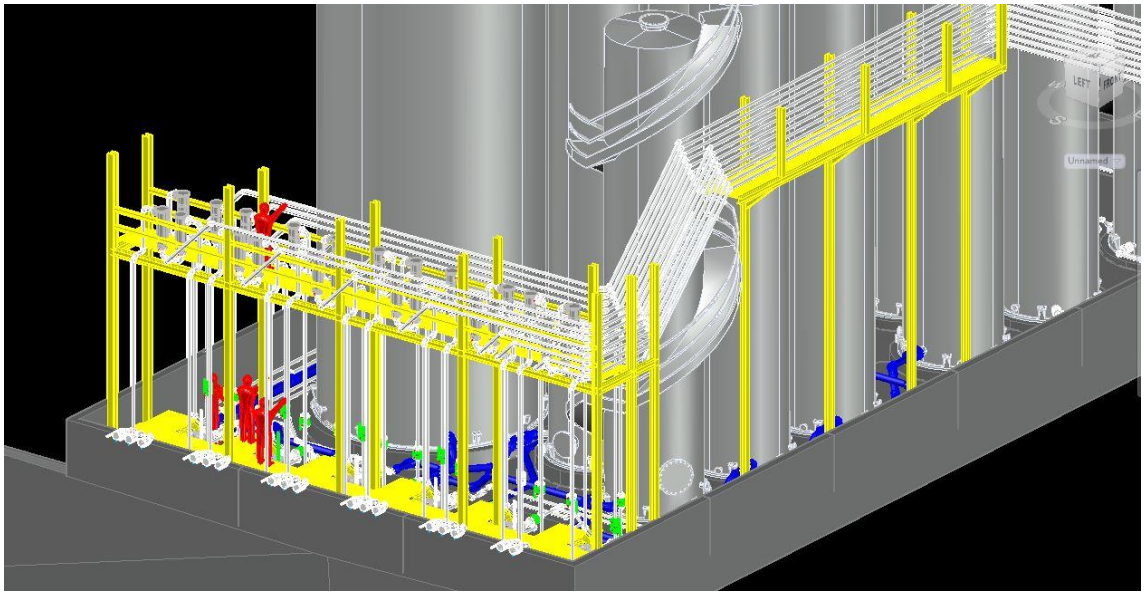

Figure 3.1-3: *Tank Farm model with all piping routes*

As previously discussed, to ensure all piping routes fit in the Tank Farm bund with the optimal utilization of space, all routes were modelled.

Suction Line:

The following figures show the Suction Line route from the bulk holding tank in the Tank Farm to the suction side of the pump:

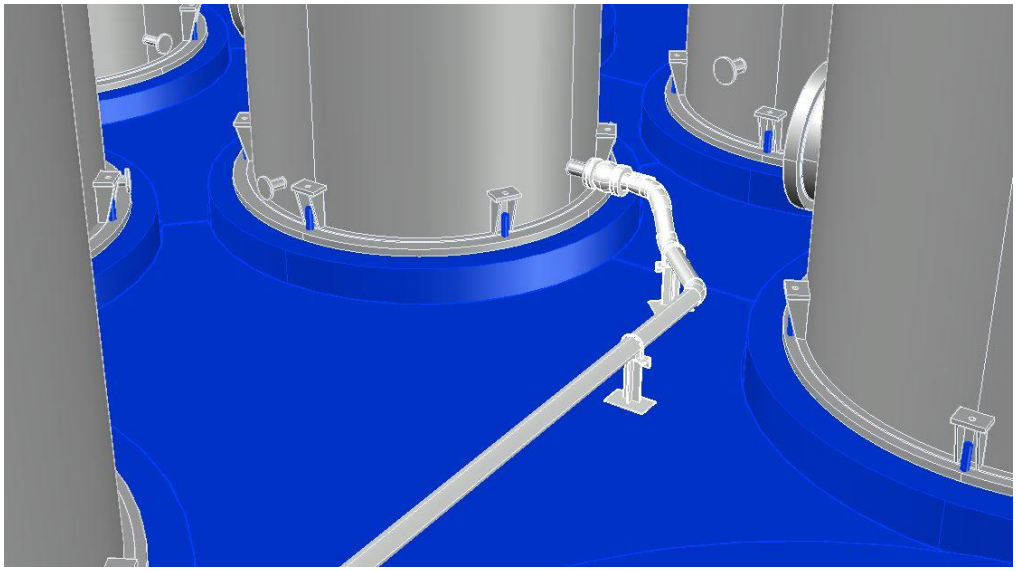

Figure 3.1-4: *Bulk holding tank outlet*

The outlet of the Tank Farm tank is shown in Figure 3.1-24 above. A valve is mounted directly on the Holdings tank. This is the first node (10) of the Suction line stress analysis model.

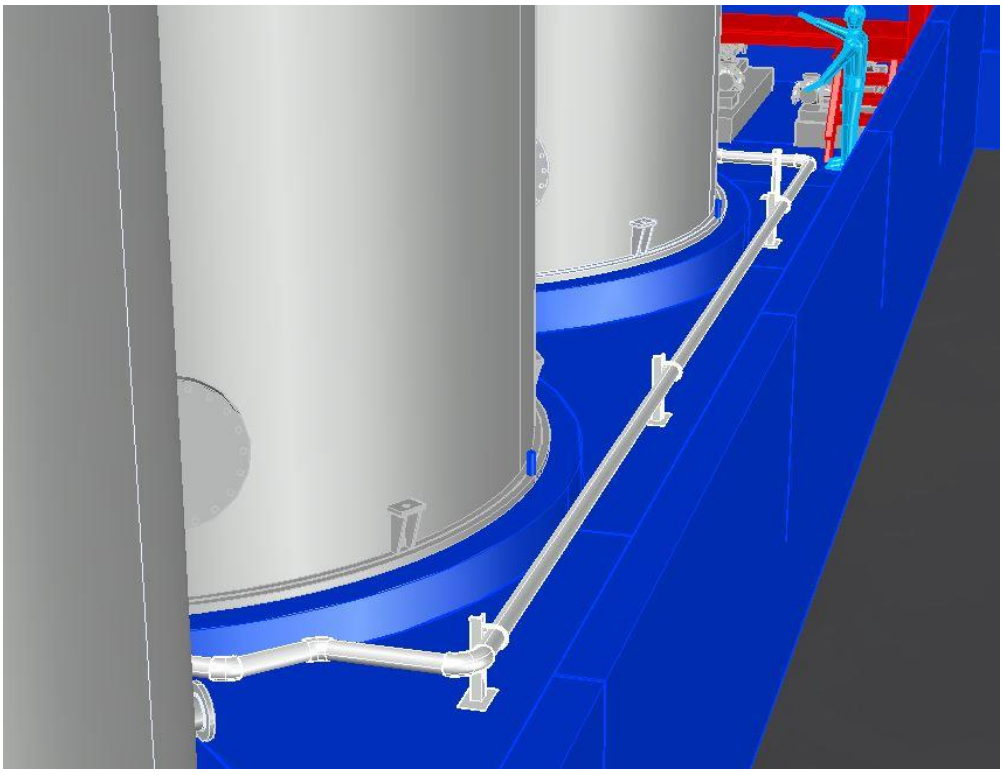

Figure 3.1-5: *Suction line*

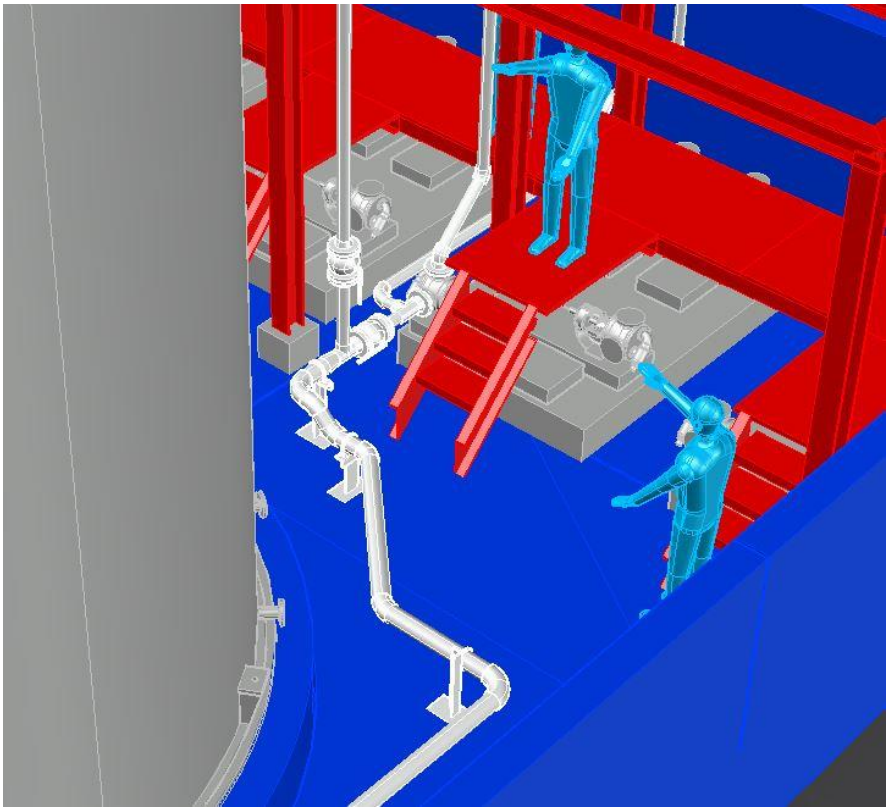

Figure 3.1-6: *Pump inlet*

Figure 3.1-5 shows the last node of the Suction line which is at the inlet to the pump.

Discharge Line:

The following figures show the Discharge line piping route from the pump's outlet to the inlet of the Plant's blend tank.

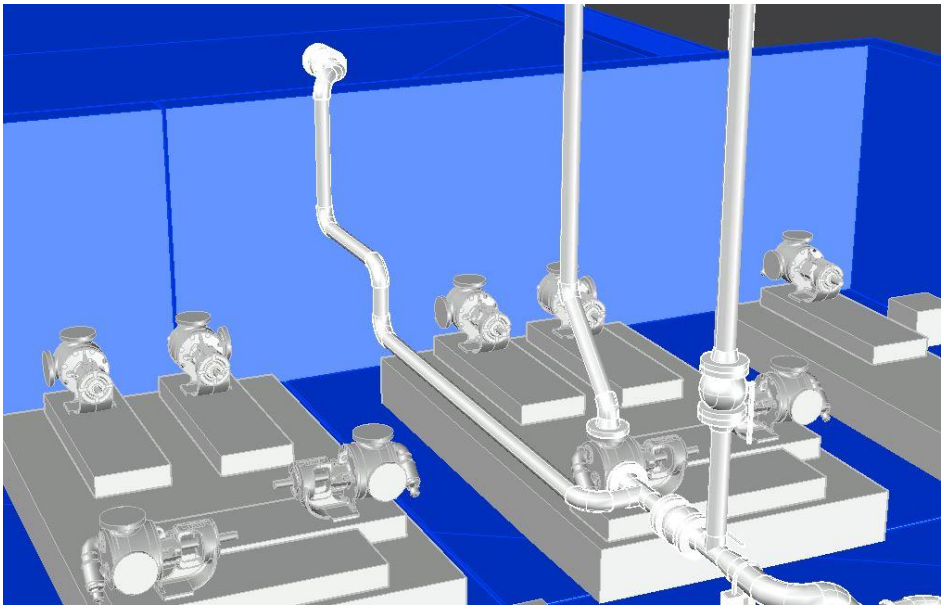

Figure 3.1-7: *Pump outlet*

The ideal route designed for the discharge line is vertically out of the pump. The discharge piping gains elevation by doing so. Although elevation increases pressure in the piping system, these routes are the most ergonomical in the Tank Farm and Plant.

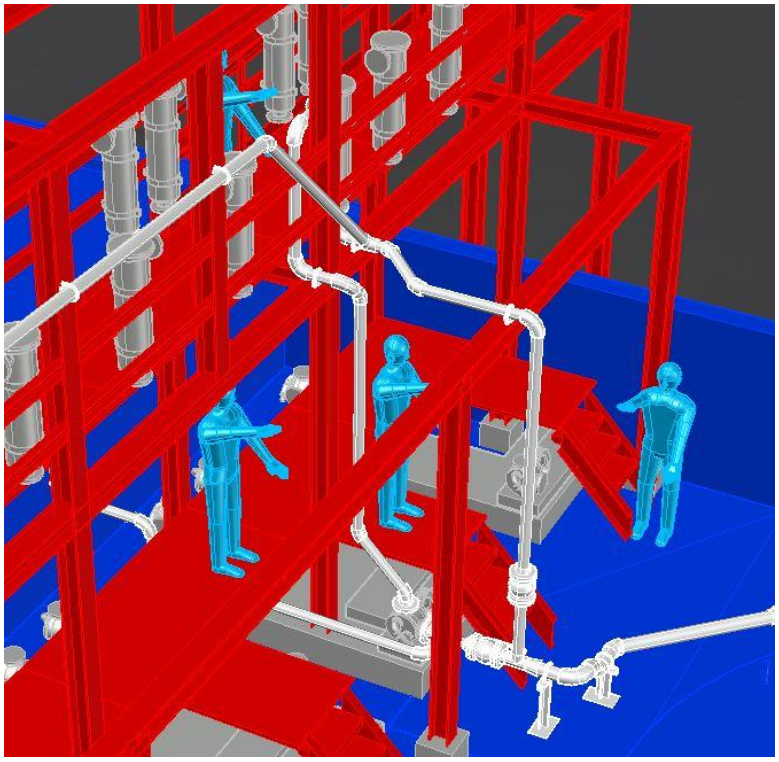

Figure 3.1-8: *Pipe route into plant*

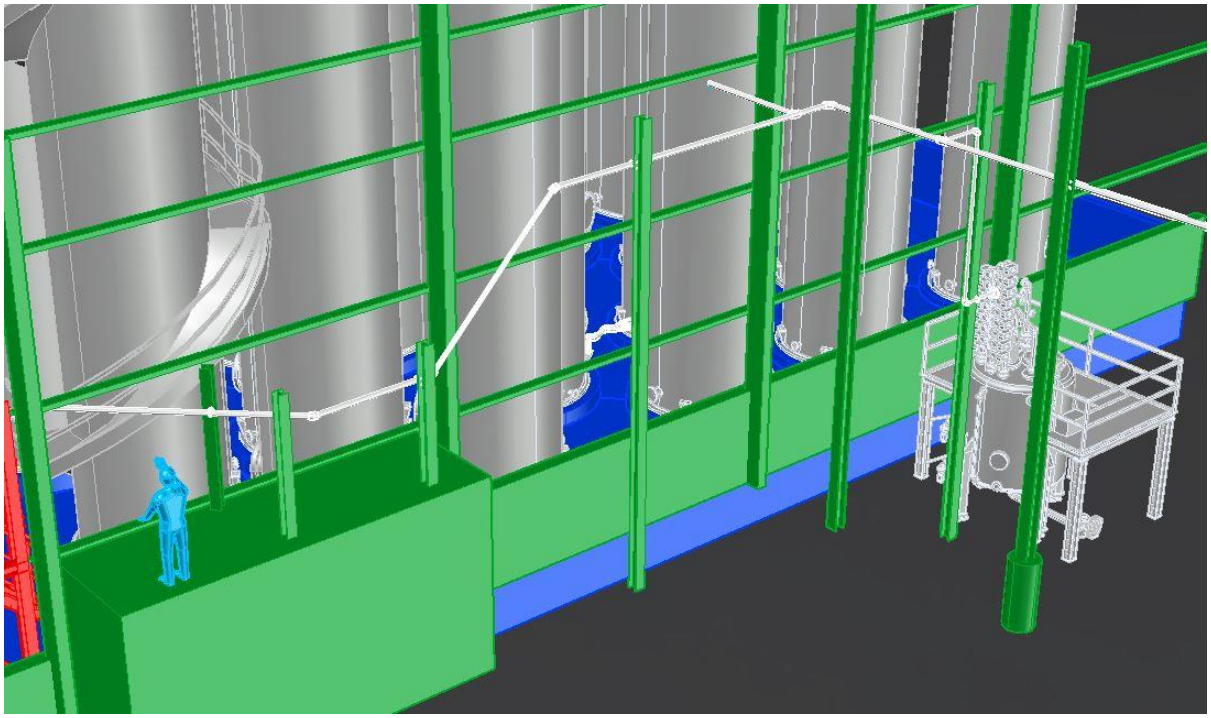

Figure 3.1-9: *Discharge pipe into top of the blending tank*

Sustained Loadings

The analysis of Primary stresses due to deadweight and dynamic loading is done using CAESAR II software. CAESAR models the piping system as beam elements then applies the classical beam theories as well as von Mises or Trescas Theory to determine forces, moments, stresses, and strains in the piping system. Element stiffness matrices and load vectors are created for the analysis of unknown reactions. The piping system will experience loading due to pressure, deadweight and thermal change. Primary loading and Secondary loading will be analysed separately thereafter combinational loadings will be analysed. Equation (2.3-34) is used to calculate stresses due to sustained loadings (Pressure and Deadweight):

$$S_L = \sqrt{(S_a + S_b)^2 + (2S_t)^2}$$

Where; $S_a = \frac{I_a F_a}{A_p}$, $S_t = \frac{I_t M_t}{2Z}$, $S_b = \frac{\sqrt{(I_i M_i)^2 + (I_o M_o)^2}}{Z}$

The table below shows the standard units of measurement for the CAESAR II analysis. SI units have been selected as default units.

ITEM	Internal Units		Constant		User Units	ITEM	Internal Units		Constant		User Units
Length	inches	*	2.54	=	cm	Fluid Den.	lbs./cu.in.	*	0.0276799	=	kg./cu.cm.
Force	pounds	*	4.44822	=	N.	Transl. Stiff.	lbs./in.	*	1.75127	=	N./cm.
Mass-dynamics	pounds	*	0.453592	=	Kg.	Rotl. Stiff.	in-lb/deg	*	0.112985	=	N.m./deg
Moment-input	in.-lb.	*	0.112985	=	N.m.	Unif. Load	lb./in.	*	1.75127	=	N./cm.
Moment-output	in.-lb.	*	0.112985	=	N.m.	G Load	g's	*	1	=	g's
Stress	lbs./sq.in.	*	6.89476	=	KPa	Wind Load	lbs./sq.in.	*	6.89476	=	KPa
Temp. Scale	degrees F	*	0.555556	=	C	Elevation	inches	*	0.0254	=	m.
Pressure	psig	*	6.89476	=	KPa	Cmpd Lng	inches	*	0.0254	=	m.
Elastic Modulus	lbs./sq.in.	*	6.89476	=	KPa	Diameter	inches	*	2.54	=	cm.
Pipe Density	lbs./cu.in.	*	0.0276799	=	kg./cu.cm.	Thickness	inches	*	2.54	=	cm.
Insulation Den.	lbs./cu.in.	*	0.0276799	=	kg./cu.cm.	Nominals				=	ON
Units File Label:			SI								

Figure 3.1-10: *Standard units of measure for CAESAR II*

Suction Line:

Figure 3.1-11 below shows the pipe suction line modelled on CAESAR II software.

The pipe route is anchored before the inlet at the pump. All other supports were guide type supports that allows movement in the axial direction of the pipe.

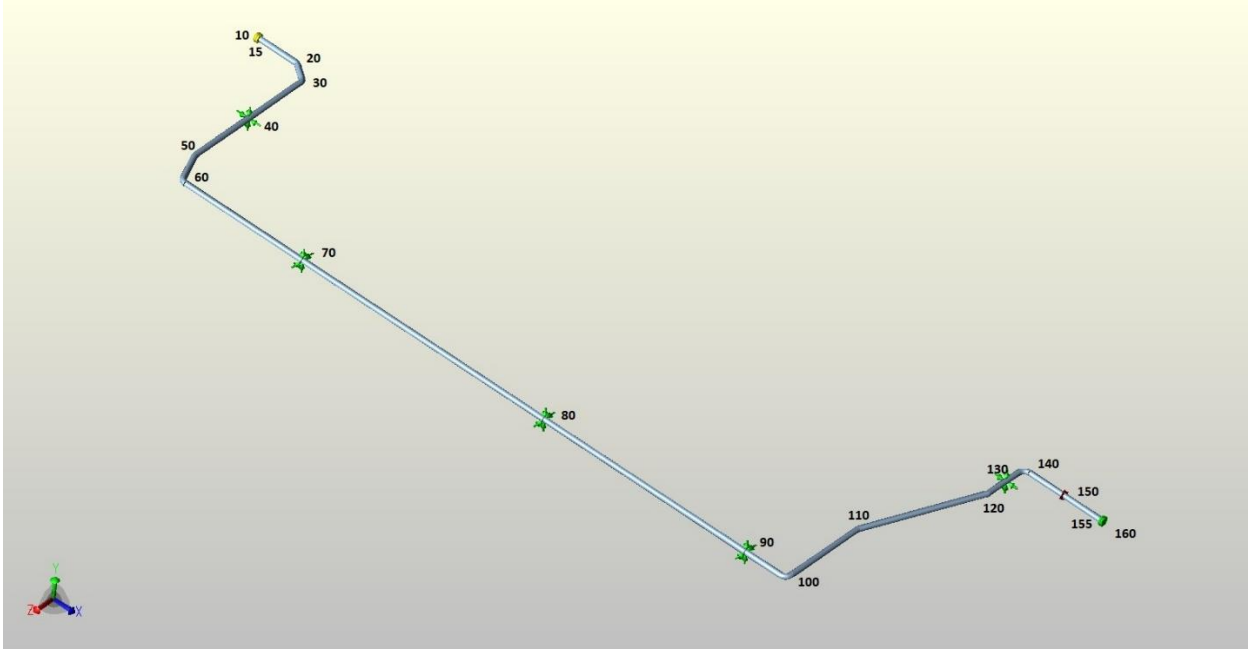

Figure 3.1-11: *Suction Line CAESAR II model*

CENTER OF GRAVITY REPORT

	Total Wght N.	X cg m.	Y cg m.	Z cg m.
Pipe :	4487.9	10.0	0.0	2.5
Insulation :	0.0	0.0	0.0	0.0
Refractory :	0.0	0.0	0.0	0.0
Fluid :	1991.6	10.0	0.0	2.6
Pipe+Ins+Rfrty :	4487.9	10.0	0.0	2.5
Pipe+Fluid :	6479.5	10.0	0.0	2.5
Pipe+Ins+Rfrty+Fld :	6479.5	10.0	0.0	2.5

Figure 3.1-12: *Suction line center of Gravity report*

The following results were obtained from the analysis done for sustained loadings:

Displacements:

Table 3.1-6: *Suction Line displacements due to Sustained loadings*

Node	DX cm.	DY cm.	DZ cm.	RX deg.	RY deg.	RZ deg.
10	0.0000	-0.7294	-0.0000	-0.0964	-0.0000	0.2210
15	0.0000	-0.6988	-0.0000	-0.0964	-0.0000	0.2210
18	0.0000	-0.3656	0.0000	-0.0964	-0.0000	0.2156
19	0.0000	-0.3463	0.0000	-0.0959	-0.0000	0.2118
20	0.0000	-0.3266	0.0000	-0.0946	-0.0000	0.2082
28	0.0000	-0.1833	0.0000	-0.0938	-0.0000	0.1995
29	0.0000	-0.1594	0.0000	-0.0879	-0.0000	0.1926
30	-0.0000	-0.1439	0.0000	-0.0822	0.0000	0.1888

Node	DX cm.	DY cm.	DZ cm.	RX deg.	RY deg.	RZ deg.
40	0.0000	-0.0000	0.0000	-0.0145	0.0000	0.1357
48	0.0000	-0.0775	0.0000	0.0555	0.0000	0.0808
49	0.0000	-0.0802	0.0000	0.0579	0.0000	0.0795
50	0.0000	-0.0819	0.0000	0.0607	0.0000	0.0776
58	0.0000	-0.1150	0.0000	0.0605	0.0000	0.0584
59	0.0000	-0.1167	0.0000	0.0621	0.0000	0.0539
60	0.0000	-0.1121	0.0000	0.0628	0.0000	0.0462
70	0.0000	-0.0000	0.0000	0.0364	0.0000	-0.0208
80	0.0000	-0.0000	-0.0000	-0.0185	-0.0000	0.0213
90	0.0000	-0.0000	-0.0000	-0.0642	0.0000	-0.0115
98	0.0000	-0.0351	-0.0000	-0.0719	0.0000	-0.0281
99	0.0000	-0.0459	-0.0000	-0.0723	0.0000	-0.0257
100	0.0000	-0.0615	-0.0000	-0.0722	0.0000	-0.0238
108	0.0000	-0.2322	-0.0000	-0.0217	0.0000	0.0017
109	0.0000	-0.2331	-0.0000	-0.0150	0.0000	0.0025
110	0.0000	-0.2336	-0.0000	-0.0083	0.0000	0.0044
118	0.0000	-0.0452	-0.0000	0.0601	0.0000	0.0088
119	0.0000	-0.0422	-0.0000	0.0572	0.0000	0.0076
120	0.0000	-0.0394	-0.0000	0.0542	0.0000	0.0069
130	0.0000	-0.0000	-0.0000	0.0386	0.0000	-0.0016
138	-0.0000	0.0190	-0.0000	0.0268	0.0000	-0.0079
139	0.0000	0.0220	-0.0000	0.0155	-0.0000	-0.0133
140	-0.0000	0.0198	-0.0000	0.0114	-0.0000	-0.0189
150	-0.0000	0.0000	0.0000	0.0000	-0.0000	-0.0000
155	-0.0000	-0.0070	0.0000	0.0000	-0.0000	-0.0061
160	-0.0000	-0.0079	0.0000	0.0000	-0.0000	-0.0061

Restraints:

Table 3.1-7: *Suction line restraints due to Sustained loadings*

Node	FX N.	FY N.	FZ N.	Resultant Force N.	MX N.m.	MY N.m.	MZ N.m.	Resultant Moment N.m.	
40	0	0	0	0	0	0	0	0	Rigid X
40	0	-1467	0	1467	0	0	0	0	Rigid Y
70	0	0	0	0	0	0	0	0	Rigid Z
70	0	-1163	0	1163	0	0	0	0	Rigid Y
80	0	0	-0	0	0	0	0	0	Rigid Z
80	0	-1284	0	1284	0	0	0	0	Rigid Y
90	0	0	-0	0	0	0	0	0	Rigid Z
90	0	-1263	0	1263	0	0	0	0	Rigid Y
130	0	0	0	0	0	0	0	0	Rigid X
130	0	-1537	0	1537	0	0	0	0	Rigid Y
150	-0	234	0	234	111	-0	-658	667	Rigid ANC

Global Element Forces:

Table 3.1-8: *Suction line global element forces due to Sustained loadings*

Node	Axial Force N.	Shear Force N.	Bending Moment N.m.	Torsion Moment N.m.	FX N.	FY N.	FZ N.	MX N.m.	MY N.m.	MZ N.m.
10	-0	0	0	0	-0	-0	0	0	-0	-0
15	0	77	3	0	0	77	-0	0	0	-3
15	0	77	3	0	0	-77	-0	0	-0	3
18	-0	276	157	-0	-0	276	0	-0	0	-157
18	0	276	157	0	0	-276	-0	0	-0	157
19	-0	287	162	-52	-0	287	0	2	0	-170
19	-0	287	162	52	-0	-287	-0	-2	-0	170
20	0	299	152	-103	0	299	0	9	0	-183
20	0	299	152	103	0	-299	-0	-9	-0	183
28	-0	384	279	-103	-0	384	0	85	0	-285
28	0	384	279	103	0	-384	-0	-85	-0	285
29	-0	400	230	-223	-0	400	-0	106	0	-302
29	-0	400	230	223	0	-400	-0	-106	-0	302
30	-0	416	134	-309	0	416	-0	134	0	-309
30	-0	416	134	309	-0	-416	-0	-134	-0	309
40	0	742	959	-309	0	742	0	959	-0	-309
40	-0	724	959	309	-0	724	-0	-959	0	309
48	0	388	142	-309	0	-388	0	142	-0	-309
48	-0	388	142	309	-0	388	-0	-142	0	309
49	0	381	189	-275	0	-381	0	130	-0	-307
49	-0	381	189	275	-0	381	0	-130	0	307
50	0	374	229	-233	0	-374	0	119	-0	-304
50	-0	374	229	233	-0	374	0	-119	0	304
58	0	230	39	-233	0	-230	-0	-56	-0	-229
58	-0	230	39	233	-0	230	0	56	0	229
59	0	209	142	-178	0	-209	0	-70	-0	-217
59	-0	209	142	178	-0	209	-0	70	0	217
60	0	189	200	-76	0	-189	0	-76	-0	-200

Node	Axial Force N.	Shear Force N.	Bending Moment N.m.	Torsion Moment N.m.	FX N.	FY N.	FZ N.	MX N.m.	MY N.m.	MZ N.m.
60	-0	189	200	76	-0	189	-0	76	0	200
70	0	475	615	-76	0	475	0	-76	-0	-615
70	-0	688	615	76	-0	688	-0	76	0	615
80	0	686	609	-76	0	686	0	-76	0	-609
80	-0	597	609	76	-0	597	-0	76	-0	609
90	0	548	485	-76	0	548	0	-76	0	-485
90	-0	715	485	76	-0	715	0	76	-0	485
98	0	521	39	-76	0	-521	-0	-76	-0	39
98	-0	521	39	76	-0	521	0	76	0	-39
99	0	494	29	-104	0	-494	-0	-53	-0	94
99	-0	494	29	104	-0	494	0	53	0	-94
100	0	467	1	-116	0	-467	-0	-1	-0	116
100	-0	467	1	116	-0	467	0	1	0	-116
108	0	50	468	-116	0	-50	-0	468	0	116
108	-0	50	468	116	-0	50	0	-468	-0	-116
109	0	44	483	-25	0	-44	-0	470	0	116
109	-0	44	483	25	-0	44	0	-470	-0	-116
110	0	37	480	67	0	-37	-0	471	0	116
110	-0	37	480	-67	-0	37	0	-471	-0	-116
118	0	566	217	67	0	566	-0	-176	0	-143
118	-0	566	217	-67	-0	-566	0	176	-0	143
119	0	573	217	108	0	573	-0	-192	0	-147
119	-0	573	217	-108	-0	-573	0	192	-0	147
120	0	579	209	149	0	579	-0	-209	0	-149
120	-0	579	209	-149	-0	-579	0	209	-0	149
130	0	687	507	149	0	687	-0	-507	0	-149
130	-0	850	507	-149	-0	850	0	507	-0	149
138	0	770	225	149	0	-770	-0	-225	0	-149
138	-0	770	225	-149	-0	770	0	225	-0	149
139	0	743	183	-20	0	-743	-0	-144	0	-115

Node	Axial Force N.	Shear Force N.	Bending Moment N.m.	Torsion Moment N.m.	FX N.	FY N.	FZ N.	MX N.m.	MY N.m.	MZ N.m.
139	-0	743	183	20	-0	743	0	144	-0	115
140	0	715	37	-111	0	-715	-0	-111	0	-37
140	-0	715	37	111	-0	715	0	111	-0	37
150	0	521	487	-111	0	-521	-0	-111	0	487
150	0	288	171	0	0	288	-0	0	0	171
155	-0	77	3	-0	-0	-77	0	-0	-0	-3
155	0	77	3	0	0	77	-0	0	0	3
160	-0	0	0	0	-0	-0	0	0	0	-0

Stresses:

Table 3.1-9: *Suction line stresses due to Sustained loadings*

Node	Axial Stress KPa	Bending Stress KPa	Torsion Stress KPa	Hoop Stress KPa	Max Stress Intensity KPa	SIF/ Index In Plane	SIF/ Index Out Plane	Code Stress KPa	Allowable Stress KPa	Ratio %	Piping Code
10	0.0	0.0	0.0	0.0	0.0	0.000	0.000	0.0	0.0	0.0	B31.3
15	0.0	0.0	0.0	0.0	0.0	0.000	0.000	0.0	0.0	0.0	B31.3
15	79.3	67.6	0.0	166.2	190.5	1.000	1.000	146.9	137895.1	0.1	B31.3
18	79.3	3470.1	-0.0	166.2	3549.3	1.000	1.000	3549.3	137895.1	2.6	B31.3
18	79.3	5644.9	0.0	166.2	5724.2	1.952	1.627	5724.2	137895.1	4.2	B31.3
19	79.3	5844.8	-572.9	166.2	6033.9	1.952	1.627	6033.9	137895.1	4.4	B31.3
19	79.3	5844.8	572.9	166.2	6033.9	1.952	1.627	6033.9	137895.1	4.4	B31.3
20	79.3	5464.6	-1136.8	166.2	5992.0	1.952	1.627	5992.0	137895.1	4.3	B31.3
20	79.3	3359.2	1136.8	166.2	4122.2	1.000	1.000	4122.2	137895.1	3.0	B31.3
28	79.3	6180.5	-1136.8	166.2	6659.9	1.000	1.000	6659.9	137895.1	4.8	B31.3
28	79.3	10054.2	1136.8	166.2	10385.4	1.952	1.627	10385.4	137895.1	7.5	B31.3
29	79.3	8302.5	-2468.3	166.2	9727.4	1.952	1.627	9727.4	137895.1	7.1	B31.3
29	79.3	8302.5	2468.3	166.2	9727.4	1.952	1.627	9727.4	137895.1	7.1	B31.3
30	79.3	4838.2	-3421.2	166.2	8426.2	1.952	1.627	8426.2	137895.1	6.1	B31.3
30	79.3	2974.2	3421.2	166.2	7492.8	1.000	1.000	7492.8	137895.1	5.4	B31.3
40	79.3	21258.5	-3421.2	166.2	22408.0	1.000	1.000	22408.0	137895.1	16.3	B31.3
40	79.3	21258.5	3421.2	166.2	22408.0	1.000	1.000	22408.0	137895.1	16.3	B31.3
48	79.3	3146.8	-3421.2	166.2	7564.9	1.000	1.000	7564.9	137895.1	5.5	B31.3
48	79.3	5119.1	3421.2	166.2	8593.2	1.952	1.627	8593.2	137895.1	6.2	B31.3
49	79.3	6827.7	-3048.3	166.2	9212.8	1.952	1.627	9212.8	137895.1	6.7	B31.3
49	79.3	6827.7	3048.3	166.2	9212.8	1.952	1.627	9212.8	137895.1	6.7	B31.3
50	79.3	8265.2	-2577.2	166.2	9808.0	1.952	1.627	9808.0	137895.1	7.1	B31.3

Node	Axial Stress KPa	Bending Stress KPa	Torsion Stress KPa	Hoop Stress KPa	Max Stress Intensity KPa	SIF/ Index In Plane	SIF/ Index Out Plane	Code Stress KPa	Allowable Stress KPa	Ratio %	Piping Code
50	79.3	5080.8	2577.2	166.2	7293.4	1.000	1.000	7293.4	137895.1	5.3	B31.3
58	79.3	866.2	-2577.2	166.2	5240.3	1.000	1.000	5240.3	137895.1	3.8	B31.3
58	79.3	1409.1	2577.2	166.2	5364.9	1.952	1.627	5364.9	137895.1	3.9	B31.3
59	79.3	5128.7	-1975.3	166.2	6536.8	1.952	1.627	6536.8	137895.1	4.7	B31.3
59	79.3	5128.7	1975.3	166.2	6536.8	1.952	1.627	6536.8	137895.1	4.7	B31.3
60	79.3	7217.5	-837.8	166.2	7486.7	1.952	1.627	7486.7	137895.1	5.4	B31.3
60	79.3	4436.8	837.8	166.2	4816.9	1.000	1.000	4816.9	137895.1	3.5	B31.3
70	79.3	13622.4	-837.8	166.2	13803.7	1.000	1.000	13803.7	137895.1	10.0	B31.3
70	79.3	13622.4	837.8	166.2	13803.7	1.000	1.000	13803.7	137895.1	10.0	B31.3
80	79.3	13511.2	-837.8	166.2	13693.4	1.000	1.000	13693.4	137895.1	9.9	B31.3
80	79.3	13511.2	837.8	166.2	13693.4	1.000	1.000	13693.4	137895.1	9.9	B31.3
90	79.3	10750.3	-837.8	166.2	10958.4	1.000	1.000	10958.4	137895.1	7.9	B31.3
90	79.3	10750.3	837.8	166.2	10958.4	1.000	1.000	10958.4	137895.1	7.9	B31.3
98	79.3	869.9	-837.8	166.2	1925.8	1.000	1.000	1925.8	137895.1	1.4	B31.3
98	79.3	1415.1	837.8	166.2	2245.2	1.952	1.627	2245.2	137895.1	1.6	B31.3
99	79.3	1043.2	-1153.3	166.2	2565.2	1.952	1.627	2565.2	137895.1	1.9	B31.3
99	79.3	1043.2	1153.3	166.2	2565.2	1.952	1.627	2565.2	137895.1	1.9	B31.3
100	79.3	52.1	-1282.0	166.2	2567.4	1.952	1.627	2567.4	137895.1	1.9	B31.3
100	79.3	32.0	1282.0	166.2	2566.5	1.000	1.000	2566.5	137895.1	1.9	B31.3
108	79.3	10382.8	-1282.0	166.2	10771.6	1.000	1.000	10771.6	137895.1	7.8	B31.3
108	79.3	16890.2	1282.0	166.2	17162.1	1.952	1.627	17162.1	137895.1	12.4	B31.3
109	79.3	17422.9	-275.6	166.2	17510.9	1.952	1.627	17510.9	137895.1	12.7	B31.3
109	79.3	17422.9	275.6	166.2	17510.9	1.952	1.627	17510.9	137895.1	12.7	B31.3
110	79.3	17320.0	743.2	166.2	17462.6	1.952	1.627	17462.6	137895.1	12.7	B31.3
110	79.3	10647.0	-743.2	166.2	10828.7	1.000	1.000	10828.7	137895.1	7.9	B31.3
118	79.3	4805.2	743.2	166.2	5105.6	1.000	1.000	5105.6	137895.1	3.7	B31.3
118	79.3	7817.0	-743.1	166.2	8034.9	1.952	1.627	8034.9	137895.1	5.8	B31.3
119	79.3	7810.6	1201.4	166.2	8247.6	1.952	1.627	8247.6	137895.1	6.0	B31.3
119	79.3	7810.6	-1201.4	166.2	8247.6	1.952	1.627	8247.6	137895.1	6.0	B31.3
120	79.3	7529.2	1651.3	166.2	8294.3	1.952	1.627	8294.3	137895.1	6.0	B31.3
120	79.3	4628.3	-1651.3	166.2	5750.6	1.000	1.000	5750.6	137895.1	4.2	B31.3
130	79.3	11236.7	1651.3	166.2	11788.0	1.000	1.000	11788.0	137895.1	8.5	B31.3
130	79.3	11236.7	-1651.3	166.2	11788.0	1.000	1.000	11788.0	137895.1	8.5	B31.3
138	79.3	4995.0	1651.3	166.2	6054.4	1.000	1.000	6054.4	137895.1	4.4	B31.3
138	79.3	8125.7	-1651.3	166.2	8844.7	1.952	1.627	8844.7	137895.1	6.4	B31.3
139	79.3	6607.7	-221.9	166.2	6701.7	1.952	1.627	6701.7	137895.1	4.9	B31.3

Node	Axial Stress KPa	Bending Stress KPa	Torsion Stress KPa	Hoop Stress KPa	Max Stress Intensity KPa	SIF/ Index In Plane	SIF/ Index Out Plane	Code Stress KPa	Allowable Stress KPa	Ratio %	Piping Code
139	79.3	6607.7	221.9	166.2	6701.7	1.952	1.627	6701.7	137895.1	4.9	B31.3
140	79.3	1331.4	-1230.1	166.2	2836.0	1.952	1.627	2836.0	137895.1	2.1	B31.3
140	79.3	818.4	1230.1	166.2	2618.9	1.000	1.000	2618.9	137895.1	1.9	B31.3
150	79.3	10800.1	-1230.1	166.2	11154.1	1.000	1.000	11154.1	137895.1	8.1	B31.3
150	79.3	3787.5	0.0	166.2	3866.7	1.000	1.000	3866.7	137895.1	2.8	B31.3
155	79.3	67.6	-0.0	166.2	190.5	1.000	1.000	146.9	137895.1	0.1	B31.3
155	0.0	0.0	0.0	0.0	0.0	0.000	0.000	0.0	0.0	0.0	B31.3
160	0.0	0.0	0.0	0.0	0.0	0.000	0.000	0.0	0.0	0.0	B31.3

The results of the analysis are within the allowable stress range therefore ASME code compliance is met. The highest stresses experienced by the Suction Line is as follows:

Highest Stresses:	(KPa)		
Ratio (%):	16.3	@Node 40	
Code Stress:	22408.0	Allowable Stress:	137895.1
Axial Stress:	79.3	@Node 18	
Bending Stress:	21258.5	@Node 40	
Torsion Stress:	3421.2	@Node 48	
Hoop Stress:	166.2	@Node 18	
Max Stress Intensity:	22408.0	@Node 40	

Discharge Line:

The figure 3.1-13 below shows the pipe discharge line modelled on CAESAR II software.

The pipe route is anchored before the inlet at the pump and the inlet to the Plant's blend tank. All other supports were guide type supports that allows movement in the axial direction of the pipe.

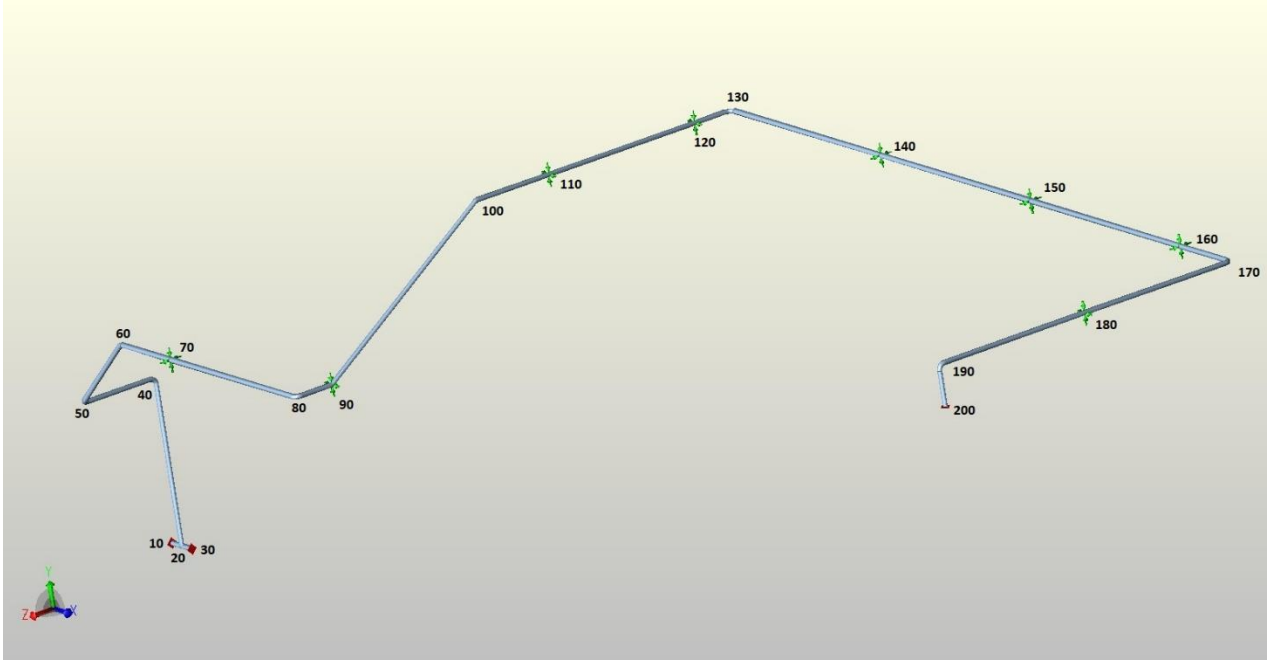

Figure 3.1-13: *Discharge Line CAESAR II model*

CENTER OF GRAVITY REPORT

	Total Wght N.	X cg m.	Y cg m.	Z cg m.
Pipe :	9196.8	14.0	7.3	-5.1
Insulation :	0.0	0.0	0.0	0.0
Refractory :	0.0	0.0	0.0	0.0
Fluid :	4190.8	14.0	7.3	-5.1
Pipe+Ins+Rfrty :	9196.8	14.0	7.3	-5.1
Pipe+Fluid :	13387.6	14.0	7.3	-5.1
Pipe+Ins+Rfrty+Fld:	13387.6	14.0	7.3	-5.1

Figure 3.1-14: *Discharge line centre of Gravity report*

The following results were obtained from the analysis done for sustained loadings:

Displacements:

Table 3.1-10: *Discharge line displacements due to Sustained loadings*

Node	DX cm.	DY cm.	DZ cm.	RX deg.	RY deg.	RZ deg.
10	0.0000	-0.0000	0.0000	0.0074	-0.0004	-0.0036
20	0.0000	-0.0018	-0.0000	0.0074	0.0013	0.0007
30	0.0000	-0.0000	-0.0000	0.0000	-0.0000	0.0000
38	-0.0688	-0.0029	0.4104	0.1414	0.0888	0.0269
39	-0.0673	-0.0157	0.4400	0.1755	0.0911	0.0310
40	-0.0520	-0.0519	0.4546	0.2068	0.0985	0.0315
48	0.2785	-0.7066	0.4545	0.2135	0.1235	0.0594
49	0.2991	-0.7414	0.4573	0.1943	0.1305	0.0648

Node	DX cm.	DY cm.	DZ cm.	RX deg.	RY deg.	RZ deg.
50	0.3008	-0.7462	0.4611	0.1778	0.1401	0.0751
58	0.0120	-0.4160	0.4050	0.1124	0.1342	0.1286
59	0.0056	-0.4054	0.3996	0.1114	0.1334	0.1317
60	0.0034	-0.3929	0.3891	0.1106	0.1312	0.1345
70	0.0034	-0.0000	0.0000	0.0755	0.0914	0.0625
78	0.0034	0.0621	-0.3220	-0.0123	0.0064	0.0290
79	0.0031	0.0662	-0.3230	-0.0164	0.0041	0.0251
80	0.0025	0.0640	-0.3233	-0.0266	0.0022	0.0212
88	0.0007	0.0101	-0.3233	-0.0561	0.0008	0.0143
89	0.0005	0.0053	-0.3240	-0.0694	0.0005	0.0138
90	-0.0000	-0.0000	-0.3265	-0.0834	-0.0000	0.0132
98	0.0199	-0.3613	-0.5671	0.0780	0.0054	-0.0271
99	0.0204	-0.3554	-0.5643	0.0866	0.0052	-0.0276
100	0.0204	-0.3484	-0.5633	0.0949	0.0052	-0.0280
110	-0.0000	-0.0000	-0.5633	0.0744	0.0069	-0.0430
120	0.0000	-0.0000	-0.5632	-0.0663	-0.0161	-0.0738
128	0.0321	-0.1232	-0.5632	-0.0919	-0.0276	-0.0804
129	0.0381	-0.1471	-0.5606	-0.0939	-0.0365	-0.0818
130	0.0412	-0.1699	-0.5529	-0.0937	-0.0452	-0.0820
140	0.0412	-0.0000	-0.0000	-0.0739	-0.0316	0.0304
150	0.0411	-0.0000	0.0000	-0.0535	0.0077	0.0022
160	0.0411	-0.0000	-0.0000	-0.0331	0.0007	-0.0391
168	0.0411	-0.2827	-0.0049	-0.0269	0.0004	-0.1065
169	0.0410	-0.3004	-0.0048	-0.0273	-0.0018	-0.1035
170	0.0405	-0.3031	-0.0046	-0.0287	-0.0041	-0.1016
180	0.0000	-0.0000	-0.0047	-0.0237	-0.0030	-0.0573
188	0.0071	-0.0025	-0.0047	-0.0107	0.0013	-0.0130
189	0.0064	-0.0006	-0.0040	-0.0081	0.0015	-0.0112
190	0.0049	-0.0001	-0.0028	-0.0043	0.0023	-0.0068
200	-0.0000	-0.0000	0.0000	-0.0000	0.0000	-0.0000

Restraints:

Table 3.1-11: *Discharge line restraints due to Sustained loadings*

Node	FX N.	FY N.	FZ N.	Resultant Force N.	MX N.m.	MY N.m.	MZ N.m.	Resultant Moment N.m.	
10	0	-602	0	602	0	0	0	0	Rigid Y
10	0	0	219	219	0	0	0	0	Rigid Z
30	31	-1191	-333	1237	152	-33	250	294	Rigid ANC
70	0	0	173	173	0	0	0	0	Rigid Z
70	0	-1564	0	1564	0	0	0	0	Rigid Y
90	-28	0	0	28	0	0	0	0	Rigid X
90	0	-1493	0	1493	0	0	0	0	Rigid Y
110	-39	0	0	39	0	0	0	0	Rigid X

Node	FX N.	FY N.	FZ N.	Resultant Force N.	MX N.m.	MY N.m.	MZ N.m.	Resultant Moment N.m.	
110	0	-1288	0	1288	0	0	0	0	Rigid Y
120	15	0	0	15	0	0	0	0	Rigid X
120	0	-1185	0	1185	0	0	0	0	Rigid Y
140	0	-1573	0	1573	0	0	0	0	Rigid Y
140	0	0	-101	101	0	0	0	0	Rigid Z
150	0	-1250	0	1250	0	0	0	0	Rigid Y
150	0	0	57	57	0	0	0	0	Rigid Z
160	0	-1508	0	1508	0	0	0	0	Rigid Y
160	0	0	-52	52	0	0	0	0	Rigid Z
180	38	0	0	38	0	0	0	0	Rigid X
180	0	-1195	0	1195	0	0	0	0	Rigid Y
200	-17	-538	37	540	-38	23	-79	90	Rigid ANC

Global Element Forces:

Table 3.1-12: *Discharge line global element forces due to Sustained loadings*

Node	Axial Force N.	Shear Force N.	Bending Moment N.m.	Torsion Moment N.m.	FX N.	FY N.	FZ N.	MX N.m.	MY N.m.	MZ N.m.
10	0	641	0	0	0	602	-219	0	0	-0
20	-0	555	239	-0	-0	-511	219	-0	88	223
20	31	1149	231	152	31	-1099	-333	152	100	-208
30	-31	1236	252	-152	-31	1191	333	-152	33	-250
20	1610	118	153	-188	-31	1610	114	-152	-188	-14
38	-729	118	607	188	31	-729	-114	592	188	132
38	729	118	607	-188	-31	729	114	-592	-188	-132
39	-577	416	574	228	31	-701	-114	573	187	135
39	577	416	574	-228	-31	701	114	-573	-187	-135
40	-114	674	536	136	31	-674	-114	504	183	136
40	114	674	536	-136	-31	674	114	-504	-183	-136
48	-114	287	336	136	31	-286	-114	-309	132	136
48	114	287	336	-136	-31	286	114	309	-132	-136
49	-185	216	386	-17	31	-258	-114	-335	125	146
49	185	216	386	17	-31	258	114	335	-125	-146
50	-129	225	351	-180	31	-231	-114	-338	114	168

Node	Axial Force N.	Shear Force N.	Bending Moment N.m.	Torsion Moment N.m.	FX N.	FY N.	FZ N.	MX N.m.	MY N.m.	MZ N.m.
50	129	225	351	180	-31	231	114	338	-114	-168
58	240	255	129	-180	31	330	-114	-154	-97	126
58	-240	255	129	180	-31	-330	114	154	97	-126
59	149	330	119	-177	31	342	-114	-151	-102	111
59	-149	330	119	177	-31	-342	114	151	102	-111
60	31	373	143	-150	31	355	-114	-150	-108	93
60	-31	373	143	150	-31	-355	114	150	108	-93
70	31	808	1080	-150	31	800	-114	-150	-330	-1029
70	-31	766	1080	150	-31	764	-59	150	330	1029
78	31	351	47	-150	31	346	59	-150	-44	-16
78	-31	351	47	150	-31	-346	-59	150	44	16
79	-20	379	160	-79	31	374	59	-166	-37	-55
79	20	379	160	79	-31	-374	-59	166	37	55
80	-59	402	210	72	31	401	59	-208	-31	-72
80	59	402	210	-72	-31	-401	-59	208	31	72
88	-59	585	603	72	31	584	59	-603	-6	-72
88	59	585	603	-72	-31	-584	-59	603	6	72
89	116	587	630	67	31	595	59	-629	-5	-71
89	-116	587	630	-67	-31	-595	-59	629	5	71
90	287	537	656	57	31	605	59	-654	-4	-71
90	541	706	656	-57	-2	888	-59	654	4	71
98	134	307	407	57	2	330	59	406	7	-64
98	-134	307	407	-57	-2	-330	-59	-406	-7	64
99	42	342	391	63	2	340	59	391	7	-64
99	-42	342	391	-63	-2	-340	-59	-391	-7	64
100	-59	350	376	64	2	350	59	375	7	-64
100	59	350	376	-64	-2	-350	-59	-375	-7	64
110	-59	798	746	64	2	798	59	-746	12	-64
110	59	492	746	-64	37	490	-59	746	-12	64

Node	Axial Force N.	Shear Force N.	Bending Moment N.m.	Torsion Moment N.m.	FX N.	FY N.	FZ N.	MX N.m.	MY N.m.	MZ N.m.
120	-59	427	631	64	-37	426	59	-617	-135	-64
120	59	760	631	-64	21	760	-59	617	135	64
128	-59	566	163	64	-21	-566	59	-55	-153	-64
128	59	566	163	-64	21	566	-59	55	153	64
129	-57	539	155	31	-21	-538	59	4	-153	-39
129	57	539	155	-31	21	538	-59	-4	153	39
130	-21	514	149	28	-21	-511	59	28	-148	17
130	21	514	149	-28	21	511	-59	-28	148	-17
140	-21	830	932	28	-21	828	59	28	197	-911
140	21	746	932	-28	21	745	42	-28	-197	911
150	-21	630	566	28	-21	629	-42	28	-57	-564
150	21	622	566	-28	21	621	-15	-28	57	564
160	-21	753	958	28	-21	753	15	28	32	-957
160	21	756	958	-28	21	755	37	-28	-32	957
168	-21	334	60	28	-21	-332	-37	28	-36	48
168	21	334	60	-28	21	332	37	-28	36	-48
169	-41	305	62	68	-21	-305	-37	14	-39	82
169	41	305	62	-68	21	305	37	-14	39	-82
170	-37	278	42	95	-21	-278	-37	-17	-38	95
170	37	278	42	-95	21	278	37	17	38	-95
180	-37	604	611	95	-21	604	-37	610	44	95
180	37	592	611	-95	-17	592	37	-610	-44	-95
188	-37	290	34	95	17	289	-37	28	-20	95
188	37	290	34	-95	-17	-289	37	-28	20	-95
189	-250	199	78	82	17	317	-37	59	-22	94
189	250	199	78	-82	-17	-317	37	-59	22	-94
190	-344	40	116	23	17	344	-37	69	-23	93
190	344	40	116	-23	-17	-344	37	-69	23	-93
200	-538	40	87	23	17	538	-37	38	-23	79

Stresses:

Table 3.1-13: *Discharge line stresses due to Sustained loadings*

Node	Axial Stress KPa	Bending Stress KPa	Torsion Stress KPa	Hoop Stress KPa	Max Stress Intensity KPa	SIF/Index In Plane	SIF/Index Out Plane	Code Stress KPa	Allowable Stress KPa	Ratio %	Piping Code
10	10865.1	0.0	0.0	23009.4	27148.2	1.000	1.000	10865.1	137895.1	7.9	B31.3
20	10865.1	14870.2	-0.0	23009.4	27148.2	3.169	3.892	25735.3	137895.1	18.7	B31.3
20	10850.2	14569.2	1446.6	23009.4	28206.4	3.169	3.892	25583.5	137895.1	18.6	B31.3
30	10850.2	4779.6	-1446.6	23009.4	27324.7	1.000	1.000	15895.3	137895.1	11.5	B31.3
20	10079.0	11293.5	-1785.3	23009.4	27892.3	3.169	3.892	21668.7	137895.1	15.7	B31.3
38	10509.3	11516.3	1785.3	23009.4	27751.3	1.000	1.000	22313.1	137895.1	16.2	B31.3
38	10509.3	21863.5	-1785.3	23009.4	33869.9	1.912	1.594	32569.1	137895.1	23.6	B31.3
39	10583.5	20822.3	2159.6	23009.4	32713.7	1.912	1.594	31701.4	137895.1	23.0	B31.3
39	10583.5	20822.3	-2159.6	23009.4	33110.8	1.912	1.594	31701.4	137895.1	23.0	B31.3
40	10809.3	19114.9	1294.7	23009.4	30970.7	1.912	1.594	30036.0	137895.1	21.8	B31.3
40	10809.3	10179.3	-1294.7	23009.4	27433.8	1.000	1.000	21147.7	137895.1	15.3	B31.3
48	10809.3	6380.7	1294.7	23009.4	27314.1	1.000	1.000	17383.9	137895.1	12.6	B31.3
48	10809.3	11844.6	-1294.7	23009.4	27551.7	1.912	1.594	22801.3	137895.1	16.5	B31.3
49	10774.9	13274.6	-161.4	23009.4	27159.8	1.912	1.594	24051.6	137895.1	17.4	B31.3
49	10774.9	13274.6	161.4	23009.4	27161.0	1.912	1.594	24051.6	137895.1	17.4	B31.3
50	10802.1	12299.9	-1704.7	23009.4	27846.5	1.912	1.594	23352.2	137895.1	16.9	B31.3
50	10802.1	6669.8	1704.7	23009.4	27444.8	1.000	1.000	17801.4	137895.1	12.9	B31.3
58	10982.4	2457.5	-1704.7	23009.4	27351.1	1.000	1.000	13865.5	137895.1	10.1	B31.3
58	10982.4	4664.1	1704.7	23009.4	27386.6	1.912	1.594	16013.6	137895.1	11.6	B31.3
59	10937.8	4242.0	-1681.0	23009.4	27375.8	1.912	1.594	15547.6	137895.1	11.3	B31.3
59	10937.8	4242.0	1681.0	23009.4	27372.6	1.912	1.594	15547.6	137895.1	11.3	B31.3
60	10880.0	4700.8	-1421.3	23009.4	27317.9	1.912	1.594	15837.9	137895.1	11.5	B31.3
60	10880.0	2707.5	1421.3	23009.4	27291.1	1.000	1.000	13881.6	137895.1	10.1	B31.3
70	10880.0	20508.4	-1421.3	23009.4	32253.9	1.000	1.000	31516.9	137895.1	22.9	B31.3
70	10880.0	20508.4	1421.3	23009.4	32225.8	1.000	1.000	31516.9	137895.1	22.9	B31.3
78	10880.0	893.1	-1421.3	23009.4	27273.6	1.000	1.000	12111.4	137895.1	8.8	B31.3
78	10880.0	1678.0	1421.3	23009.4	27280.5	1.912	1.594	12875.7	137895.1	9.3	B31.3
79	10855.3	4900.4	-748.2	23009.4	27196.6	1.912	1.594	15826.5	137895.1	11.5	B31.3
79	10855.3	4900.4	748.2	23009.4	27196.7	1.912	1.594	15826.5	137895.1	11.5	B31.3
80	10836.3	6384.2	679.6	23009.4	27194.7	1.912	1.594	17274.1	137895.1	12.5	B31.3
80	10836.3	3987.5	-679.6	23009.4	27185.1	1.000	1.000	14886.0	137895.1	10.8	B31.3
88	10836.3	11441.6	679.6	23009.4	27254.6	1.000	1.000	22319.3	137895.1	16.2	B31.3
88	10836.3	21879.5	-679.6	23009.4	33238.5	1.912	1.594	32744.0	137895.1	23.7	B31.3
89	10921.7	22850.7	635.4	23009.4	34120.8	1.912	1.594	33796.3	137895.1	24.5	B31.3

Node	Axial Stress KPa	Bending Stress KPa	Torsion Stress KPa	Hoop Stress KPa	Max Stress Intensity KPa	SIF/Index In Plane	SIF/Index Out Plane	Code Stress KPa	Allowable Stress KPa	Ratio %	Piping Code
89	10921.7	22850.7	-635.4	23009.4	34093.4	1.912	1.594	33796.3	137895.1	24.5	B31.3
90	11005.0	23792.1	540.4	23009.4	35029.6	1.912	1.594	34813.9	137895.1	25.2	B31.3
90	10600.7	12449.4	-540.4	23009.4	27250.9	1.000	1.000	23075.4	137895.1	16.7	B31.3
98	10930.4	7722.9	540.4	23009.4	27183.4	1.000	1.000	18684.6	137895.1	13.5	B31.3
98	10930.4	14756.7	-540.4	23009.4	27460.2	1.912	1.594	25709.9	137895.1	18.6	B31.3
99	10885.6	14202.4	598.3	23009.4	27407.2	1.912	1.594	25116.5	137895.1	18.2	B31.3
99	10885.6	14202.4	-598.3	23009.4	27399.6	1.912	1.594	25116.5	137895.1	18.2	B31.3
100	10836.3	13632.5	604.5	23009.4	27332.1	1.912	1.594	24498.6	137895.1	17.8	B31.3
100	10836.3	7129.2	-604.5	23009.4	27188.7	1.000	1.000	18006.1	137895.1	13.1	B31.3
110	10836.3	14160.8	604.5	23009.4	27395.7	1.000	1.000	25026.3	137895.1	18.1	B31.3
110	10836.3	14160.8	-604.5	23009.4	27406.1	1.000	1.000	25026.3	137895.1	18.1	B31.3
120	10836.3	11985.7	604.5	23009.4	27246.4	1.000	1.000	22854.0	137895.1	16.6	B31.3
120	10836.3	11985.7	-604.5	23009.4	27248.2	1.000	1.000	22854.0	137895.1	16.6	B31.3
128	10836.3	3092.0	604.5	23009.4	27175.1	1.000	1.000	13980.7	137895.1	10.1	B31.3
128	10836.3	5808.7	-604.5	23009.4	27183.0	1.912	1.594	16688.8	137895.1	12.1	B31.3
129	10837.3	5602.2	293.5	23009.4	27156.2	1.912	1.594	16450.0	137895.1	11.9	B31.3
129	10837.3	5602.2	-293.5	23009.4	27156.2	1.912	1.594	16450.0	137895.1	11.9	B31.3
130	10854.6	5381.8	266.6	23009.4	27154.6	1.912	1.594	16245.2	137895.1	11.8	B31.3
130	10854.6	2820.1	-266.6	23009.4	27153.3	1.000	1.000	13685.1	137895.1	9.9	B31.3
140	10854.6	17697.8	266.6	23009.4	29422.3	1.000	1.000	28557.4	137895.1	20.7	B31.3
140	10854.6	17697.8	-266.6	23009.4	29442.9	1.000	1.000	28557.4	137895.1	20.7	B31.3
150	10854.6	10754.0	266.6	23009.4	27162.5	1.000	1.000	21615.2	137895.1	15.7	B31.3
150	10854.6	10754.0	-266.6	23009.4	27162.5	1.000	1.000	21615.2	137895.1	15.7	B31.3
160	10854.6	18184.7	266.6	23009.4	29857.5	1.000	1.000	29044.2	137895.1	21.1	B31.3
160	10854.6	18184.7	-266.6	23009.4	29874.6	1.000	1.000	29044.2	137895.1	21.1	B31.3
168	10854.6	1131.3	266.6	23009.4	27152.7	1.000	1.000	11997.8	137895.1	8.7	B31.3
168	10854.6	1941.1	-266.6	23009.4	27153.0	1.912	1.594	12806.8	137895.1	9.3	B31.3
169	10845.0	2026.0	644.9	23009.4	27176.3	1.912	1.594	12935.5	137895.1	9.4	B31.3
169	10845.0	2026.0	-644.9	23009.4	27176.4	1.912	1.594	12935.5	137895.1	9.4	B31.3
170	10847.1	1482.0	903.9	23009.4	27201.2	1.912	1.594	12460.9	137895.1	9.0	B31.3
170	10847.1	795.8	-903.9	23009.4	27198.9	1.000	1.000	11782.4	137895.1	8.5	B31.3
180	10847.1	11606.3	903.9	23009.4	27340.5	1.000	1.000	22526.0	137895.1	16.3	B31.3
180	10847.1	11606.3	-903.9	23009.4	27342.4	1.000	1.000	22526.0	137895.1	16.3	B31.3
188	10847.1	652.0	903.9	23009.4	27198.2	1.000	1.000	11640.3	137895.1	8.4	B31.3
188	10847.1	1179.4	-903.9	23009.4	27200.3	1.912	1.594	12161.6	137895.1	8.8	B31.3
189	10743.0	2636.6	781.6	23009.4	27191.1	1.912	1.594	13470.6	137895.1	9.8	B31.3

Node	Axial Stress KPa	Bending Stress KPa	Torsion Stress KPa	Hoop Stress KPa	Max Stress Intensity KPa	SIF/Index In Plane	SIF/Index Out Plane	Code Stress KPa	Allowable Stress KPa	Ratio %	Piping Code
189	10743.0	2636.6	-781.6	23009.4	27192.1	1.912	1.594	13470.6	137895.1	9.8	B31.3
190	10697.0	3767.3	215.6	23009.4	27151.7	1.912	1.594	14470.8	137895.1	10.5	B31.3
190	10697.0	2197.0	-215.6	23009.4	27151.4	1.000	1.000	12901.3	137895.1	9.4	B31.3
200	10602.3	1657.1	215.6	23009.4	27151.2	1.000	1.000	12267.0	137895.1	8.9	B31.3

The results of the analysis are within the allowable stress range therefore ASME code compliance is met. The highest stresses experienced by the Discharge Line due to Sustained loading is as follows:

Highest Stresses:	(KPa)		
Ratio (%):	25.2	@Node 90	
Code Stress:	34813.9	Allowable Stress:	137895.1
Axial Stress:	11005.0	@Node 90	
Bending Stress:	23792.1	@Node 90	
Torsion Stress:	2159.6	@Node 39	
Hoop Stress:	23009.4	@Node 20	
Max Stress Intensity:	35029.6	@Node 90	

The following table shows the summary of stresses experienced by the Discharge line compared to the Allowable stress of the system. Column 5 shows the percentage relationship between the two stresses.

Table 3.1-14: *Discharge line code compliance comparison due to Sustained loadings*

Load Case	From Node	Code Stress KPa	Allowable Stress KPa	Ratio %	To Node	Code Stress KPa	Allowable Stress KPa	Ratio %	Piping Code
3(SUS)	10	10865.1	137895.1	7.9	20	25735.3	137895.1	18.7	B31.3
3(SUS)	20	25583.5	137895.1	18.6	30	15895.3	137895.1	11.5	B31.3
3(SUS)	20	21668.7	137895.1	15.7	38	22313.1	137895.1	16.2	B31.3
3(SUS)	38	32569.1	137895.1	23.6	39	31701.4	137895.1	23.0	B31.3
3(SUS)	39	31701.4	137895.1	23.0	40	30036.0	137895.1	21.8	B31.3

Load Case	From Node	Code Stress KPa	Allowable Stress KPa	Ratio %	To Node	Code Stress KPa	Allowable Stress KPa	Ratio %	Piping Code
3(SUS)	40	21147.7	137895.1	15.3	48	17383.9	137895.1	12.6	B31.3
3(SUS)	48	22801.3	137895.1	16.5	49	24051.6	137895.1	17.4	B31.3
3(SUS)	49	24051.6	137895.1	17.4	50	23352.2	137895.1	16.9	B31.3
3(SUS)	50	17801.4	137895.1	12.9	58	13865.5	137895.1	10.1	B31.3
3(SUS)	58	16013.6	137895.1	11.6	59	15547.6	137895.1	11.3	B31.3
3(SUS)	59	15547.6	137895.1	11.3	60	15837.9	137895.1	11.5	B31.3
3(SUS)	60	13881.6	137895.1	10.1	70	31516.9	137895.1	22.9	B31.3
3(SUS)	70	31516.9	137895.1	22.9	78	12111.4	137895.1	8.8	B31.3
3(SUS)	78	12875.7	137895.1	9.3	79	15826.5	137895.1	11.5	B31.3
3(SUS)	79	15826.5	137895.1	11.5	80	17274.1	137895.1	12.5	B31.3
3(SUS)	80	14886.0	137895.1	10.8	88	22319.3	137895.1	16.2	B31.3
3(SUS)	88	32744.0	137895.1	23.7	89	33796.3	137895.1	24.5	B31.3
3(SUS)	89	33796.3	137895.1	24.5	90	34813.9	137895.1	25.2	B31.3
3(SUS)	90	23075.4	137895.1	16.7	98	18684.6	137895.1	13.5	B31.3
3(SUS)	98	25709.9	137895.1	18.6	99	25116.5	137895.1	18.2	B31.3
3(SUS)	99	25116.5	137895.1	18.2	100	24498.6	137895.1	17.8	B31.3

Load Case	From Node	Code Stress KPa	Allowable Stress KPa	Ratio %	To Node	Code Stress KPa	Allowable Stress KPa	Ratio %	Piping Code
3(SUS)	100	18006.1	137895.1	13.1	110	25026.3	137895.1	18.1	B31.3
3(SUS)	110	25026.3	137895.1	18.1	120	22854.0	137895.1	16.6	B31.3
3(SUS)	120	22854.0	137895.1	16.6	128	13980.7	137895.1	10.1	B31.3
3(SUS)	128	16688.8	137895.1	12.1	129	16450.0	137895.1	11.9	B31.3
3(SUS)	129	16450.0	137895.1	11.9	130	16245.2	137895.1	11.8	B31.3
3(SUS)	130	13685.1	137895.1	9.9	140	28557.4	137895.1	20.7	B31.3
3(SUS)	140	28557.4	137895.1	20.7	150	21615.2	137895.1	15.7	B31.3
3(SUS)	150	21615.2	137895.1	15.7	160	29044.2	137895.1	21.1	B31.3
3(SUS)	160	29044.2	137895.1	21.1	168	11997.8	137895.1	8.7	B31.3
3(SUS)	168	12806.8	137895.1	9.3	169	12935.5	137895.1	9.4	B31.3
3(SUS)	169	12935.5	137895.1	9.4	170	12460.9	137895.1	9.0	B31.3
3(SUS)	170	11782.4	137895.1	8.5	180	22526.0	137895.1	16.3	B31.3
3(SUS)	180	22526.0	137895.1	16.3	188	11640.3	137895.1	8.4	B31.3
3(SUS)	188	12161.6	137895.1	8.8	189	13470.6	137895.1	9.8	B31.3
3(SUS)	189	13470.6	137895.1	9.8	190	14470.8	137895.1	10.5	B31.3
3(SUS)	190	12901.3	137895.1	9.4	200	12267.0	137895.1	8.9	B31.3

3.2 Secondary Stress Analysis

3.2.1. Secondary Stresses on Piping Systems

A major requirement in the design of piping systems is to ensure adequate flexibility along the piping route to absorb thermal expansion and contraction. The pipe route could be either too stiff or too flexible. The thermal expansion analysis is performed for the extreme temperature ranges experienced at the Indy Oil site. The number of temperature cycles is estimated based on previous ambient temperature statics at yearly periods and production throughput requirements. To demonstrate the effects of thermal loadings, the stress analysis was performed on the discharge pipe route.

The following results were obtained from the analysis done for thermal loadings:

Discharge Line:

Displacements:

Table 3.2-1: *Discharge line displacements due to thermal expansion*

Node	DX cm.	DY cm.	DZ cm.	RX deg.	RY deg.	RZ deg.
10	-0.0349	-0.0000	-0.0000	-0.0088	0.0005	-0.0016
20	-0.0175	-0.0004	-0.0002	-0.0088	-0.0008	0.0027
30	-0.0000	0.0000	0.0000	-0.0000	-0.0000	-0.0000
38	-0.2916	0.1673	-0.1447	-0.0138	-0.0499	0.0469
39	-0.3038	0.1726	-0.1446	-0.0047	-0.0501	0.0408
40	-0.3165	0.1745	-0.1400	0.0041	-0.0525	0.0385
48	-0.4736	0.1483	-0.0661	0.0066	-0.0473	0.0048
49	-0.4803	0.1490	-0.0589	0.0011	-0.0369	0.0010
50	-0.4789	0.1517	-0.0528	-0.0049	-0.0262	-0.0072
58	-0.3331	0.1469	-0.0480	-0.0177	-0.0076	-0.0372
59	-0.3292	0.1450	-0.0482	-0.0175	-0.0078	-0.0398
60	-0.3262	0.1416	-0.0478	-0.0174	-0.0081	-0.0423
70	-0.2415	0.0000	0.0000	-0.0136	-0.0254	-0.0320
78	-0.0303	-0.0003	0.3522	-0.0040	-0.0330	0.0171
79	-0.0234	0.0027	0.3557	-0.0036	-0.0244	0.0178
80	-0.0177	0.0035	0.3527	-0.0029	-0.0161	0.0181
88	-0.0006	-0.0006	0.3178	-0.0033	-0.0100	0.0185
89	-0.0000	-0.0005	0.3158	-0.0039	-0.0095	0.0186
90	0.0000	-0.0000	0.3139	-0.0044	-0.0092	0.0187
98	-0.0319	0.0495	0.0684	-0.0151	-0.0075	0.0146
99	-0.0318	0.0493	0.0662	-0.0154	-0.0078	0.0144
100	-0.0314	0.0484	0.0641	-0.0158	-0.0080	0.0143
110	0.0000	0.0000	-0.0211	-0.0097	-0.0107	0.0109
120	-0.0000	-0.0000	-0.1955	0.0045	0.0253	0.0038
128	-0.0429	0.0065	-0.2324	0.0043	0.0270	0.0024
129	-0.0451	0.0075	-0.2387	0.0041	0.0158	0.0020
130	-0.0414	0.0081	-0.2423	0.0039	0.0027	0.0013

Node	DX cm.	DY cm.	DZ cm.	RX deg.	RY deg.	RZ deg.
140	0.2130	0.0000	-0.0000	0.0036	-0.0141	-0.0012
150	0.4740	0.0000	0.0000	0.0033	-0.0189	0.0009
160	0.7350	-0.0000	-0.0000	0.0031	0.0897	-0.0025
168	0.8154	-0.0097	-0.3122	0.0030	0.0601	-0.0026
169	0.8220	-0.0103	-0.3168	0.0028	0.0049	-0.0019
170	0.8192	-0.0109	-0.3110	0.0024	-0.0518	-0.0015
180	0.0000	0.0000	-0.1439	-0.0093	-0.0874	0.0061
188	-0.0182	0.0477	0.0231	0.0087	0.0276	0.0137
189	-0.0126	0.0432	0.0267	0.0176	0.0207	0.0120
190	-0.0091	0.0370	0.0246	0.0231	0.0170	0.0094
200	-0.0000	-0.0000	0.0000	0.0000	0.0000	0.0000

Restraints:

Table 3.2-2: *Discharge line restraints due to thermal expansion*

Node	FX N.	FY N.	FZ N.	Resultant Force N.	MX N.m.	MY N.m.	MZ N.m.	Resultant Moment N.m.	
10	0	-576	0	576	0	0	0	0	Rigid Y
10	0	0	-171	171	0	0	0	0	Rigid Z
30	-138	423	84	453	-183	-4	-11	183	Rigid ANC
70	0	0	155	155	0	0	0	0	Rigid Z
70	0	193	0	193	0	0	0	0	Rigid Y
90	133	0	0	133	0	0	0	0	Rigid X
90	0	-88	0	88	0	0	0	0	Rigid Y
110	63	0	0	63	0	0	0	0	Rigid X
110	0	68	0	68	0	0	0	0	Rigid Y
120	-509	0	0	509	0	0	0	0	Rigid X
120	0	-24	0	24	0	0	0	0	Rigid Y
140	0	4	0	4	0	0	0	0	Rigid Y
140	0	0	-126	126	0	0	0	0	Rigid Z
150	0	2	0	2	0	0	0	0	Rigid Y
150	0	0	184	184	0	0	0	0	Rigid Z
160	0	-18	0	18	0	0	0	0	Rigid Y
160	0	0	-929	929	0	0	0	0	Rigid Z
180	685	0	0	685	0	0	0	0	Rigid X
180	0	74	0	74	0	0	0	0	Rigid Y
200	-234	-59	803	838	631	166	217	688	Rigid ANC

Global Element Forces:

Table 3.2-3: *Discharge line global element forces due to thermal expansion*

Node	Axial Force N.	Shear Force N.	Bending Moment N.m.	Torsion Moment N.m.	FX N.	FY N.	FZ N.	MX N.m.	MY N.m.	MZ N.m.
10	-0	601	0	-0	-0	576	171	-0	-0	0

Node	Axial Force N.	Shear Force N.	Bending Moment N.m.	Torsion Moment N.m.	FX N.	FY N.	FZ N.	MX N.m.	MY N.m.	MZ N.m.
20	0	601	240	0	0	-576	-171	0	-69	230
20	-138	431	162	-183	-138	423	84	-183	-37	158
30	138	431	12	183	138	-423	-84	183	4	11
20	153	164	429	106	138	153	88	183	106	-388
38	-153	164	211	-106	-138	-153	-88	155	-106	-143
38	153	164	211	106	138	153	88	-155	106	143
39	-170	145	163	-182	-138	-153	-88	158	-100	-158
39	170	145	163	182	138	153	88	-158	100	158
40	-88	206	168	-164	-138	-153	-88	145	-85	-164
40	88	206	168	164	138	153	88	-145	85	164
48	-88	206	188	-164	-138	-153	-88	-114	149	-164
48	88	206	188	164	138	153	88	114	-149	164
49	-207	86	239	-108	-138	-153	-88	-128	161	-163
49	207	86	239	108	138	153	88	128	-161	163
50	-204	91	260	9	-138	-153	-88	-128	160	-160
50	204	91	260	-9	138	153	88	128	-160	160
58	-204	91	102	9	-138	-153	-88	13	-1	-101
58	204	91	102	-9	138	153	88	-13	1	101
59	-183	129	99	12	-138	-153	-88	15	-5	-98
59	183	129	99	-12	138	153	88	-15	5	98
60	-138	176	92	16	-138	-153	-88	16	-10	-91
60	138	176	92	-16	138	153	88	-16	10	91
70	-138	176	274	16	-138	-153	-88	16	-181	206
70	138	79	274	-16	138	-40	-68	-16	181	-206
78	-138	79	147	16	-138	40	68	16	147	11
78	138	79	147	-16	138	-40	-68	-16	-147	-11
79	-145	64	149	6	-138	40	68	14	148	6
79	145	64	149	-6	138	-40	-68	-14	-148	-6
80	-68	144	137	-5	-138	40	68	10	136	5
80	68	144	137	5	138	-40	-68	-10	-136	-5

Node	Axial Force N.	Shear Force N.	Bending Moment N.m.	Torsion Moment N.m.	FX N.	FY N.	FZ N.	MX N.m.	MY N.m.	MZ N.m.
88	-68	144	34	-5	-138	40	68	-22	26	5
88	68	144	34	5	138	-40	-68	22	-26	-5
89	-53	150	31	2	-138	40	68	-24	20	4
89	53	150	31	-2	138	-40	-68	24	-20	-4
90	-34	155	30	7	-138	40	68	-27	14	1
90	83	6	30	-7	5	48	-68	27	-14	-1
98	-83	6	22	7	-5	-48	68	-16	-9	-14
98	83	6	22	-7	5	48	-68	16	9	14
99	-78	27	20	11	-5	-48	68	-15	-9	-14
99	78	27	20	-11	5	48	-68	15	9	14
100	-68	48	17	15	-5	-48	68	-13	-10	-15
100	68	48	17	-15	5	48	-68	13	10	15
110	-68	48	82	15	-5	-48	68	80	-20	-15
110	68	62	82	-15	-58	-21	-68	-80	20	15
120	-68	62	213	15	58	21	68	-4	213	-15
120	68	451	213	-15	451	3	-68	4	-213	15
128	-68	451	170	15	-451	-3	68	-1	-170	-15
128	68	451	170	-15	451	3	-68	1	170	15
129	-367	271	216	10	-451	-3	68	-1	-215	-14
129	367	271	216	-10	451	3	-68	1	215	14
130	-451	68	229	-0	-451	-3	68	-0	-228	-14
130	451	68	229	0	451	3	-68	0	228	14
140	-451	68	167	-0	-451	-3	68	-0	167	5
140	451	58	167	0	451	-0	58	0	-167	-5
150	-451	58	184	-0	-451	0	-58	-0	-184	2
150	451	126	184	0	451	-3	-126	0	184	-2
160	-451	126	571	-0	-451	3	126	-0	571	-15
160	451	803	571	0	451	16	803	0	-571	15
168	-451	803	913	-0	-451	-16	-803	-0	-913	14
168	451	803	913	0	451	16	803	0	913	-14

Node	Axial Force N.	Shear Force N.	Bending Moment N.m.	Torsion Moment N.m.	FX N.	FY N.	FZ N.	MX N.m.	MY N.m.	MZ N.m.
169	-887	249	979	10	-451	-16	-803	-1	-979	16
169	887	249	979	-10	451	16	803	1	979	-16
170	-803	451	966	16	-451	-16	-803	-3	-966	16
170	803	451	966	-16	451	16	803	3	966	-16
180	-803	451	772	16	-451	-16	-803	-63	769	16
180	803	241	772	-16	-234	-59	803	63	-769	-16
188	-803	241	208	16	234	59	-803	163	-130	16
188	803	241	208	-16	-234	-59	803	-163	130	-16
189	-609	576	170	114	234	59	-803	133	-156	6
189	609	576	170	-114	-234	-59	803	-133	156	-6
190	-59	836	53	166	234	59	-803	49	-166	-19
190	59	836	53	-166	-234	-59	803	-49	166	19
200	-59	836	668	166	234	59	-803	-631	-166	-217

Stresses:

Table 3.2-4: *Discharge line stresses due to thermal expansion*

Node	Axial Stress KPa	Bending Stress KPa	Torsion Stress KPa	Hoop Stress KPa	Max Stress Intensity KPa	SIF/Index In Plane	SIF/Index Out Plane	Code Stress KPa	Allowable Stress KPa	Ratio %	Piping Code
10	0.0	0.0	-0.0	0.0	0.0	1.000	1.000	0.0	333872.8	0.0	B31.3
20	0.0	14752.6	0.0	0.0	14752.6	3.169	3.892	14752.6	319002.5	4.6	B31.3
20	67.4	9880.0	-1734.1	0.0	10534.6	3.169	3.892	10718.9	319154.4	3.4	B31.3
30	67.4	226.7	1734.1	0.0	3480.6	1.000	1.000	3480.6	328842.5	1.1	B31.3
20	-74.6	26968.5	1003.1	0.0	27117.4	3.169	3.892	27332.6	323069.1	8.5	B31.3
38	-74.6	4001.5	-1003.1	0.0	4543.1	1.000	1.000	4543.1	322424.8	1.4	B31.3
38	-74.6	7093.8	1003.1	0.0	7443.9	1.912	1.594	7443.9	312168.8	2.4	B31.3
39	-83.0	5852.5	-1727.5	0.0	6867.9	1.912	1.594	6867.9	313036.4	2.2	B31.3
39	-83.0	5852.5	1727.5	0.0	6867.9	1.912	1.594	6867.9	313036.4	2.2	B31.3
40	-42.8	5852.3	-1556.9	0.0	6667.0	1.912	1.594	6667.0	314701.9	2.1	B31.3
40	-42.8	3186.6	1556.9	0.0	4486.1	1.000	1.000	4486.1	323590.1	1.4	B31.3
48	-42.8	3566.8	-1556.9	0.0	4767.1	1.000	1.000	4767.1	327354.0	1.5	B31.3
48	-42.8	6816.1	1556.9	0.0	7532.7	1.912	1.594	7532.7	321936.5	2.3	B31.3
49	-100.9	8329.4	-1027.0	0.0	8676.9	1.912	1.594	8676.9	320686.3	2.7	B31.3
49	-100.9	8329.4	1027.0	0.0	8676.9	1.912	1.594	8676.9	320686.3	2.7	B31.3

Node	Axial Stress KPa	Bending Stress KPa	Torsion Stress KPa	Hoop Stress KPa	Max Stress Intensity KPa	SIF/Index In Plane	SIF/Index Out Plane	Code Stress KPa	Allowable Stress KPa	Ratio %	Piping Code
50	-99.9	8891.5	84.1	0.0	8992.9	1.912	1.594	8992.9	321385.6	2.8	B31.3
50	-99.9	4944.7	-84.1	0.0	5047.4	1.000	1.000	5047.4	326936.4	1.5	B31.3
58	-99.9	1933.4	84.1	0.0	2040.2	1.000	1.000	2040.2	330872.3	0.6	B31.3
58	-99.9	3692.4	-84.1	0.0	3795.9	1.912	1.594	3795.9	328724.3	1.2	B31.3
59	-89.3	3576.1	118.5	0.0	3673.1	1.912	1.594	3673.1	329190.2	1.1	B31.3
59	-89.3	3576.1	-118.5	0.0	3673.1	1.912	1.594	3673.1	329190.2	1.1	B31.3
60	-67.4	3327.6	154.0	0.0	3409.0	1.912	1.594	3409.0	328899.9	1.0	B31.3
60	-67.4	1743.3	-154.0	0.0	1836.8	1.000	1.000	1836.8	330856.2	0.6	B31.3
70	-67.4	5193.4	154.0	0.0	5269.8	1.000	1.000	5269.8	313221.0	1.7	B31.3
70	-67.4	5193.4	-154.0	0.0	5269.8	1.000	1.000	5269.8	313221.0	1.7	B31.3
78	-67.4	2797.8	154.0	0.0	2881.8	1.000	1.000	2881.8	332626.5	0.9	B31.3
78	-67.4	5346.0	-154.0	0.0	5422.2	1.912	1.594	5422.2	331862.1	1.6	B31.3
79	-71.0	5395.2	53.6	0.0	5467.3	1.912	1.594	5467.3	328911.3	1.7	B31.3
79	-71.0	5395.2	-53.6	0.0	5467.3	1.912	1.594	5467.3	328911.3	1.7	B31.3
80	-33.0	4955.7	-44.2	0.0	4989.5	1.912	1.594	4989.5	327463.8	1.5	B31.3
80	-33.0	2593.6	44.2	0.0	2628.1	1.000	1.000	2628.1	329851.8	0.8	B31.3
88	-33.0	642.4	-44.2	0.0	681.1	1.000	1.000	681.1	322418.6	0.2	B31.3
88	-33.0	1115.5	44.2	0.0	1151.9	1.912	1.594	1151.9	311993.8	0.4	B31.3
89	-25.9	1066.3	19.6	0.0	1092.9	1.912	1.594	1092.9	310941.5	0.4	B31.3
89	-25.9	1066.3	-19.6	0.0	1092.9	1.912	1.594	1092.9	310941.5	0.4	B31.3
90	-16.6	1055.2	64.7	0.0	1079.5	1.912	1.594	1079.5	309924.0	0.3	B31.3
90	-40.4	566.5	-64.7	0.0	620.5	1.000	1.000	620.5	321662.4	0.2	B31.3
98	-40.4	422.8	64.7	0.0	480.8	1.000	1.000	480.8	326053.3	0.1	B31.3
98	-40.4	744.5	-64.7	0.0	795.5	1.912	1.594	795.5	319027.9	0.2	B31.3
99	-38.3	681.4	105.4	0.0	750.0	1.912	1.594	750.0	319621.3	0.2	B31.3
99	-38.3	681.4	-105.4	0.0	750.0	1.912	1.594	750.0	319621.3	0.2	B31.3
100	-33.0	571.5	137.7	0.0	664.4	1.912	1.594	664.4	320239.2	0.2	B31.3
100	-33.0	315.8	-137.7	0.0	444.5	1.000	1.000	444.5	326731.7	0.1	B31.3
110	-33.0	1557.5	137.7	0.0	1614.1	1.000	1.000	1614.1	319711.5	0.5	B31.3
110	-33.0	1557.5	-137.7	0.0	1614.1	1.000	1.000	1614.1	319711.5	0.5	B31.3
120	-33.0	4036.1	137.7	0.0	4078.4	1.000	1.000	4078.4	321883.8	1.3	B31.3
120	-33.0	4036.1	-137.7	0.0	4078.4	1.000	1.000	4078.4	321883.8	1.3	B31.3
128	-33.0	3222.5	137.7	0.0	3267.2	1.000	1.000	3267.2	330757.2	1.0	B31.3
128	-33.0	6162.5	-137.7	0.0	6201.6	1.912	1.594	6201.6	328049.0	1.9	B31.3
129	-179.1	7824.1	92.9	0.0	8005.3	1.912	1.594	8005.3	328287.8	2.4	B31.3
129	-179.1	7824.1	-92.9	0.0	8005.3	1.912	1.594	8005.3	328287.8	2.4	B31.3
130	-220.3	8295.0	-3.5	0.0	8515.3	1.912	1.594	8515.3	328492.7	2.6	B31.3
130	-220.3	4340.2	3.5	0.0	4560.5	1.000	1.000	4560.5	331052.8	1.4	B31.3
140	-220.3	3170.2	-3.5	0.0	3390.5	1.000	1.000	3390.5	316180.4	1.1	B31.3
140	-220.3	3170.2	3.5	0.0	3390.5	1.000	1.000	3390.5	316180.4	1.1	B31.3

Node	Axial Stress KPa	Bending Stress KPa	Torsion Stress KPa	Hoop Stress KPa	Max Stress Intensity KPa	SIF/Index In Plane	SIF/Index Out Plane	Code Stress KPa	Allowable Stress KPa	Ratio %	Piping Code
150	-220.3	3493.9	-3.5	0.0	3714.2	1.000	1.000	3714.2	323122.6	1.1	B31.3
150	-220.3	3493.9	3.5	0.0	3714.2	1.000	1.000	3714.2	323122.6	1.1	B31.3
160	-220.3	10835.8	-3.5	0.0	11056.1	1.000	1.000	11056.1	315693.6	3.5	B31.3
160	-220.3	10835.8	3.5	0.0	11056.1	1.000	1.000	11056.1	315693.6	3.5	B31.3
168	-220.3	17330.4	-3.5	0.0	17550.7	1.000	1.000	17550.7	332740.0	5.3	B31.3
168	-220.3	33140.0	3.5	0.0	33360.3	1.912	1.594	33360.3	331931.0	10.1	B31.3
169	-433.0	35549.2	97.9	0.0	35982.7	1.912	1.594	35982.7	331802.4	10.8	B31.3
169	-433.0	35549.2	-97.9	0.0	35982.7	1.912	1.594	35982.7	331802.4	10.8	B31.3
170	-392.1	35083.9	155.1	0.0	35477.3	1.912	1.594	35477.3	332277.0	10.7	B31.3
170	-392.1	18346.3	-155.1	0.0	18741.0	1.000	1.000	18741.0	332955.4	5.6	B31.3
180	-392.1	14649.2	155.1	0.0	15044.5	1.000	1.000	15044.5	322211.8	4.7	B31.3
180	-392.1	14649.2	-155.1	0.0	15044.5	1.000	1.000	15044.5	322211.8	4.7	B31.3
188	-392.1	3957.7	155.1	0.0	4360.8	1.000	1.000	4360.8	333097.5	1.3	B31.3
188	-392.1	7102.0	-155.1	0.0	7500.5	1.912	1.594	7500.5	332576.3	2.3	B31.3
189	-297.5	5798.3	1083.5	0.0	6469.5	1.912	1.594	6469.5	331267.3	2.0	B31.3
189	-297.5	5798.3	-1083.5	0.0	6469.5	1.912	1.594	6469.5	331267.3	2.0	B31.3
190	-28.6	1881.5	1575.3	0.0	3684.4	1.912	1.594	3684.4	330267.1	1.1	B31.3
190	-28.6	1004.5	-1575.3	0.0	3315.7	1.000	1.000	3315.7	331836.6	1.0	B31.3
200	-28.6	12674.5	1575.3	0.0	13087.9	1.000	1.000	13087.9	332470.9	3.9	B31.3

The results of the analysis are within the allowable stress range therefore ASME code compliance is met. The highest stresses experienced by the Discharge Line due to thermal expansion is as follows:

Highest Stresses:	(KPa)		
Ratio (%):	10.8	@Node 169	
Code Stress:	35982.7	Allowable Stress:	331802.4
Axial Stress:	433.0	@Node 169	
Bending Stress:	35549.2	@Node 169	
Torsion Stress:	1734.1	@Node 30	
Hoop Stress:	0.0	@Node 20	
Max Stress Intensity:	35982.7	@Node 169	

CHAPTER 4

4.0 Effect of Multiple Loads

4.1 The Influence of Multiple Loads Experienced Simultaneously

The analysis of multiple loadings experienced on the piping system is analysed in this subsection. This will be done using the models created on CAESAR II software for the Discharge Line. The previous subsections focused on specific load cases due to Pressure, Deadweight, and Thermal expansion. An analysis will be performed on the system with all three load cases acting on the system simultaneously. To demonstrate the effects of simultaneously loading, the stress analysis was performed on the discharge pipe route.

Discharge Line:

Displacements:

Table 4.1-1: *Discharge line displacements due to combined loading*

Node	DX cm.	DY cm.	DZ cm.	RX deg.	RY deg.	RZ deg.
10	0.0488	0.0000	0.0000	0.0124	-0.0007	0.0022
20	0.0244	0.0005	0.0002	0.0124	0.0011	-0.0038
30	0.0000	-0.0000	-0.0000	0.0000	0.0000	0.0000
38	0.4081	-0.2341	0.2025	0.0194	0.0699	-0.0656
39	0.4250	-0.2415	0.2023	0.0066	0.0701	-0.0570
40	0.4428	-0.2442	0.1959	-0.0058	0.0734	-0.0538
48	0.6627	-0.2075	0.0925	-0.0092	0.0663	-0.0068
49	0.6721	-0.2084	0.0824	-0.0016	0.0516	-0.0014
50	0.6702	-0.2122	0.0738	0.0069	0.0367	0.0101
58	0.4661	-0.2056	0.0671	0.0248	0.0107	0.0520
59	0.4606	-0.2029	0.0675	0.0245	0.0109	0.0557
60	0.4564	-0.1981	0.0668	0.0243	0.0113	0.0592
70	0.3379	-0.0000	-0.0000	0.0190	0.0355	0.0447
78	0.0423	0.0004	-0.4929	0.0057	0.0462	-0.0239
79	0.0328	-0.0038	-0.4978	0.0050	0.0341	-0.0248
80	0.0248	-0.0049	-0.4936	0.0041	0.0225	-0.0253

Node	DX cm.	DY cm.	DZ cm.	RX deg.	RY deg.	RZ deg.
88	0.0008	0.0008	-0.4447	0.0047	0.0140	-0.0259
89	0.0000	0.0008	-0.4419	0.0054	0.0134	-0.0260
90	-0.0000	0.0000	-0.4393	0.0062	0.0129	-0.0262
98	0.0446	-0.0693	-0.0958	0.0211	0.0105	-0.0204
99	0.0445	-0.0690	-0.0926	0.0216	0.0109	-0.0202
100	0.0439	-0.0677	-0.0897	0.0220	0.0112	-0.0200
110	-0.0000	-0.0000	0.0295	0.0136	0.0150	-0.0152
120	0.0000	0.0000	0.2735	-0.0063	-0.0354	-0.0054
128	0.0601	-0.0091	0.3252	-0.0060	-0.0378	-0.0033
129	0.0632	-0.0104	0.3340	-0.0057	-0.0220	-0.0028
130	0.0579	-0.0113	0.3391	-0.0054	-0.0038	-0.0018
140	-0.2981	-0.0000	0.0000	-0.0051	0.0197	0.0016
150	-0.6633	-0.0000	-0.0000	-0.0047	0.0264	-0.0013
160	-1.0286	0.0000	0.0000	-0.0043	-0.1255	0.0035
168	-1.1410	0.0135	0.4368	-0.0042	-0.0841	0.0036
169	-1.1502	0.0144	0.4432	-0.0039	-0.0069	0.0026
170	-1.1463	0.0153	0.4351	-0.0034	0.0725	0.0021
180	-0.0000	-0.0000	0.2014	0.0130	0.1222	-0.0086
188	0.0255	-0.0667	-0.0324	-0.0122	-0.0387	-0.0192
189	0.0176	-0.0605	-0.0373	-0.0247	-0.0289	-0.0167
190	0.0128	-0.0517	-0.0344	-0.0323	-0.0238	-0.0131
200	0.0000	0.0000	-0.0000	-0.0000	-0.0000	-0.0000

Restraints:

Table 4.1-2: *Discharge line restraints due to combined loading*

Node	FX N.	FY N.	FZ N.	Resultant Force N.	MX N.m.	MY N.m.	MZ N.m.	Resultant Moment N.m.	
10	0	806	0	806	0	0	0	0	Rigid Y
10	0	0	240	240	0	0	0	0	Rigid Z
30	193	-592	-117	633	256	5	16	256	Rigid ANC

Node	FX N.	FY N.	FZ N.	Resultant Force N.	MX N.m.	MY N.m.	MZ N.m.	Resultant Moment N.m.	
70	0	0	-217	217	0	0	0	0	Rigid Z
70	0	-270	0	270	0	0	0	0	Rigid Y
90	-186	0	0	186	0	0	0	0	Rigid X
90	0	123	0	123	0	0	0	0	Rigid Y
110	-89	0	0	89	0	0	0	0	Rigid X
110	0	-96	0	96	0	0	0	0	Rigid Y
120	713	0	0	713	0	0	0	0	Rigid X
120	0	34	0	34	0	0	0	0	Rigid Y
140	0	-5	0	5	0	0	0	0	Rigid Y
140	0	0	176	176	0	0	0	0	Rigid Z
150	0	-3	0	3	0	0	0	0	Rigid Y
150	0	0	-258	258	0	0	0	0	Rigid Z
160	0	26	0	26	0	0	0	0	Rigid Y
160	0	0	1299	1299	0	0	0	0	Rigid Z
180	-958	0	0	958	0	0	0	0	Rigid X
180	0	-104	0	104	0	0	0	0	Rigid Y
200	327	82	-1123	1173	-883	-232	-304	963	Rigid ANC

Global Element Forces:

Table 4.1-3: *Discharge line global element forces due to combined loading*

Node	Axial Force N.	Shear Force N.	Bending Moment N.m.	Torsion Moment N.m.	FX N.	FY N.	FZ N.	MX N.m.	MY N.m.	MZ N.m.
10	0	841	0	0	0	-806	-240	0	0	-0
20	-0	841	336	0	-0	806	240	0	96	-322
20	193	603	227	256	193	-592	-117	256	52	-221
30	-193	603	17	-256	-193	592	117	-256	-5	-16
20	-214	229	600	-148	-193	-214	-123	-256	-148	543
38	214	229	295	148	193	214	123	-217	148	200
38	-214	229	295	-148	-193	-214	-123	217	-148	-200
39	238	204	228	255	193	214	123	-220	139	221
39	-238	204	228	-255	-193	-214	-123	220	-139	-221
40	123	288	235	230	193	214	123	-203	118	230
40	-123	288	235	-230	-193	-214	-123	203	-118	-230
48	123	288	263	230	193	214	123	160	-209	230
48	-123	288	263	-230	-193	-214	-123	-160	209	-230
49	289	120	335	151	193	214	123	179	-226	228

Node	Axial Force N.	Shear Force N.	Bending Moment N.m.	Torsion Moment N.m.	FX N.	FY N.	FZ N.	MX N.m.	MY N.m.	MZ N.m.
49	-289	120	335	-151	-193	-214	-123	-179	226	-228
50	286	127	364	-12	193	214	123	180	-224	224
50	-286	127	364	12	-193	-214	-123	-180	224	-224
58	286	127	143	-12	193	214	123	-18	2	142
58	-286	127	143	12	-193	-214	-123	18	-2	-142
59	256	180	138	-17	193	214	123	-22	8	137
59	-256	180	138	17	-193	-214	-123	22	-8	-137
60	193	247	129	-23	193	214	123	-23	14	128
60	-193	247	129	23	-193	-214	-123	23	-14	-128
70	193	247	383	-23	193	214	123	-23	253	-288
70	-193	110	383	23	-193	56	95	23	-253	288
78	193	110	206	-23	193	-56	-95	-23	-206	-15
78	-193	110	206	23	-193	56	95	23	206	15
79	203	90	208	-8	193	-56	-95	-20	-207	-9
79	-203	90	208	8	-193	56	95	20	207	9
80	95	201	191	7	193	-56	-95	-14	-191	-7
80	-95	201	191	-7	-193	56	95	14	191	7
88	95	201	47	7	193	-56	-95	31	-36	-7
88	-95	201	47	-7	-193	56	95	-31	36	7
89	74	210	44	-3	193	-56	-95	34	-27	-5
89	-74	210	44	3	-193	56	95	-34	27	5
90	47	217	42	-10	193	-56	-95	38	-20	-2
90	-116	8	42	10	-7	-67	95	-38	20	2
98	116	8	31	-10	7	67	-95	22	13	20
98	-116	8	31	10	-7	-67	95	-22	-13	-20
99	110	37	28	-16	7	67	-95	21	13	20
99	-110	37	28	16	-7	-67	95	-21	-13	-20
100	95	67	23	-20	7	67	-95	19	14	20
100	-95	67	23	20	-7	-67	95	-19	-14	-20
110	95	67	115	-20	7	67	-95	-111	28	20

Node	Axial Force N.	Shear Force N.	Bending Moment N.m.	Torsion Moment N.m.	FX N.	FY N.	FZ N.	MX N.m.	MY N.m.	MZ N.m.
110	-95	86	115	20	81	29	95	111	-28	-20
120	95	86	298	-20	-81	-29	-95	5	-297	20
120	-95	631	298	20	-631	-5	95	-5	297	-20
128	95	631	238	-20	631	5	-95	1	238	20
128	-95	631	238	20	-631	-5	95	-1	-238	-20
129	513	379	302	-14	631	5	-95	1	301	20
129	-513	379	302	14	-631	-5	95	-1	-301	-20
130	631	95	320	1	631	5	-95	1	319	20
130	-631	95	320	-1	-631	-5	95	-1	-319	-20
140	631	95	234	1	631	5	-95	1	-234	-7
140	-631	82	234	-1	-631	1	-82	-1	234	7
150	631	82	258	1	631	-1	82	1	258	-3
150	-631	176	258	-1	-631	4	176	-1	-258	3
160	631	176	799	1	631	-4	-176	1	-798	21
160	-631	1124	799	-1	-631	-22	-1123	-1	798	-21
168	631	1124	1277	1	631	22	1123	1	1277	-20
168	-631	1124	1277	-1	-631	-22	-1123	-1	-1277	20
169	1241	349	1370	-14	631	22	1123	1	1370	-22
169	-1241	349	1370	14	-631	-22	-1123	-1	-1370	22
170	1123	632	1352	-23	631	22	1123	4	1352	-23
170	-1123	632	1352	23	-631	-22	-1123	-4	-1352	23
180	1123	632	1080	-23	631	22	1123	88	-1076	-23
180	-1123	337	1080	23	327	82	-1123	-88	1076	23
188	1123	337	292	-23	-327	-82	1123	-228	182	-23
188	-1123	337	292	23	327	82	-1123	228	-182	23
189	852	806	238	-160	-327	-82	1123	-186	218	-8
189	-852	806	238	160	327	82	-1123	186	-218	8

Node	Axial Force N.	Shear Force N.	Bending Moment N.m.	Torsion Moment N.m.	FX N.	FY N.	FZ N.	MX N.m.	MY N.m.	MZ N.m.
190	82	1170	74	-232	-327	-82	1123	-69	232	27
190	-82	1170	74	232	327	82	-1123	69	-232	-27
200	82	1170	934	-232	-327	-82	1123	883	232	304

Stresses:

Table 4.1-4: *Discharge line stresses due to combined loading*

Node	Axial Stress KPa	Bending Stress KPa	Torsion Stress KPa	Hoop Stress KPa	Max Stress Intensity KPa	SIF/Index In Plane	SIF/Index Out Plane	Code Stress KPa	Allowable Stress KPa	Ratio %	Piping Code
10	10865.1	0.0	0.0	23009.4	0.0	1.000	1.000	0.0	333872.8	0.0	B31.3
20	10865.1	20643.4	0.0	23009.4	20643.4	3.169	3.892	20643.4	319002.5	6.5	B31.3
20	10917.6	13825.2	2426.5	23009.4	14741.2	3.169	3.892	14999.0	319154.4	4.7	B31.3
30	10917.6	317.3	-2426.5	23009.4	4870.4	1.000	1.000	4870.4	328842.5	1.5	B31.3
20	10004.4	37737.2	-1403.6	23009.4	37945.6	3.169	3.892	38246.7	323069.1	11.8	B31.3
38	10434.7	5599.4	1403.6	23009.4	6357.2	1.000	1.000	6357.2	322424.8	2.0	B31.3
38	10434.7	9926.4	-1403.6	23009.4	10416.2	1.912	1.594	10416.2	312168.8	3.3	B31.3
39	10500.5	8189.5	2417.3	23009.4	9610.3	1.912	1.594	9610.3	313036.4	3.1	B31.3
39	10500.5	8189.5	-2417.3	23009.4	9610.3	1.912	1.594	9610.3	313036.4	3.1	B31.3
40	10766.4	8189.2	2178.6	23009.4	9329.2	1.912	1.594	9329.2	314701.9	3.0	B31.3
40	10766.4	4459.1	-2178.6	23009.4	6277.5	1.000	1.000	6277.5	323590.1	1.9	B31.3
48	10766.4	4991.0	2178.6	23009.4	6670.6	1.000	1.000	6670.6	327354.0	2.0	B31.3
48	10766.4	9537.8	-2178.6	23009.4	10540.5	1.912	1.594	10540.5	321936.5	3.3	B31.3
49	10674.0	11655.3	1437.1	23009.4	12141.7	1.912	1.594	12141.7	320686.3	3.8	B31.3
49	10674.0	11655.3	-1437.1	23009.4	12141.6	1.912	1.594	12141.6	320686.3	3.8	B31.3
50	10702.3	12441.9	-117.6	23009.4	12583.8	1.912	1.594	12583.8	321385.6	3.9	B31.3
50	10702.3	6919.2	117.6	23009.4	7062.8	1.000	1.000	7062.8	326936.4	2.2	B31.3
58	10882.5	2705.4	-117.6	23009.4	2854.9	1.000	1.000	2854.9	330872.3	0.9	B31.3
58	10882.5	5166.7	117.6	23009.4	5311.7	1.912	1.594	5311.7	328724.3	1.6	B31.3
59	10848.5	5004.0	-165.8	23009.4	5139.8	1.912	1.594	5139.8	329190.2	1.6	B31.3
59	10848.5	5004.0	165.8	23009.4	5139.8	1.912	1.594	5139.8	329190.2	1.6	B31.3
60	10812.6	4656.4	-215.5	23009.4	4770.2	1.912	1.594	4770.2	328899.9	1.5	B31.3
60	10812.6	2439.5	215.5	23009.4	2570.2	1.000	1.000	2570.2	330856.2	0.8	B31.3
70	10812.6	7267.2	-215.5	23009.4	7374.1	1.000	1.000	7374.1	313221.0	2.4	B31.3
70	10812.6	7267.2	215.5	23009.4	7374.1	1.000	1.000	7374.1	313221.0	2.4	B31.3
78	10812.6	3915.0	-215.5	23009.4	4032.5	1.000	1.000	4032.5	332626.5	1.2	B31.3
78	10812.6	7480.7	215.5	23009.4	7587.3	1.912	1.594	7587.3	331862.1	2.3	B31.3

Node	Axial Stress KPa	Bending Stress KPa	Torsion Stress KPa	Hoop Stress KPa	Max Stress Intensity KPa	SIF/Index In Plane	SIF/Index Out Plane	Code Stress KPa	Allowable Stress KPa	Ratio %	Piping Code
79	10784.3	7549.6	-75.0	23009.4	7650.4	1.912	1.594	7650.4	328911.3	2.3	B31.3
79	10784.3	7549.6	75.0	23009.4	7650.4	1.912	1.594	7650.4	328911.3	2.3	B31.3
80	10803.3	6934.5	61.8	23009.4	6981.8	1.912	1.594	6981.8	327463.8	2.1	B31.3
80	10803.3	3629.3	-61.8	23009.4	3677.5	1.000	1.000	3677.5	329851.8	1.1	B31.3
88	10803.3	898.9	61.8	23009.4	953.1	1.000	1.000	953.1	322418.6	0.3	B31.3
88	10803.3	1561.0	-61.8	23009.4	1611.9	1.912	1.594	1611.9	311993.8	0.5	B31.3
89	10895.8	1492.0	-27.5	23009.4	1529.3	1.912	1.594	1529.3	310941.5	0.5	B31.3
89	10895.8	1492.0	27.5	23009.4	1529.3	1.912	1.594	1529.3	310941.5	0.5	B31.3
90	10988.4	1476.5	-90.5	23009.4	1510.6	1.912	1.594	1510.6	309924.0	0.5	B31.3
90	10560.3	792.7	90.5	23009.4	868.3	1.000	1.000	868.3	321662.4	0.3	B31.3
98	10890.1	591.6	-90.5	23009.4	672.8	1.000	1.000	672.8	326053.3	0.2	B31.3
98	10890.1	1041.8	90.5	23009.4	1113.1	1.912	1.594	1113.1	319027.9	0.3	B31.3
99	10847.3	953.5	-147.5	23009.4	1049.4	1.912	1.594	1049.4	319621.3	0.3	B31.3
99	10847.3	953.5	147.5	23009.4	1049.4	1.912	1.594	1049.4	319621.3	0.3	B31.3
100	10803.3	799.8	-192.7	23009.4	929.6	1.912	1.594	929.6	320239.2	0.3	B31.3
100	10803.3	442.0	192.7	23009.4	622.0	1.000	1.000	622.0	326731.7	0.2	B31.3
110	10803.3	2179.4	-192.7	23009.4	2258.7	1.000	1.000	2258.7	319711.5	0.7	B31.3
110	10803.3	2179.4	192.7	23009.4	2258.7	1.000	1.000	2258.7	319711.5	0.7	B31.3
120	10803.3	5647.8	-192.7	23009.4	5707.0	1.000	1.000	5707.0	321883.8	1.8	B31.3
120	10803.3	5647.8	192.7	23009.4	5707.0	1.000	1.000	5707.0	321883.8	1.8	B31.3
128	10803.3	4509.3	-192.7	23009.4	4571.8	1.000	1.000	4571.8	330757.2	1.4	B31.3
128	10803.3	8623.2	192.7	23009.4	8677.9	1.912	1.594	8677.9	328049.0	2.6	B31.3
129	10658.2	10948.2	-130.1	23009.4	11201.9	1.912	1.594	11201.9	328287.8	3.4	B31.3
129	10658.2	10948.2	130.1	23009.4	11201.9	1.912	1.594	11201.9	328287.8	3.4	B31.3
130	10634.4	11607.3	5.0	23009.4	11915.5	1.912	1.594	11915.5	328492.7	3.6	B31.3
130	10634.4	6073.2	-5.0	23009.4	6381.5	1.000	1.000	6381.5	331052.8	1.9	B31.3
140	10634.4	4436.1	5.0	23009.4	4744.4	1.000	1.000	4744.4	316180.4	1.5	B31.3
140	10634.4	4436.1	-5.0	23009.4	4744.4	1.000	1.000	4744.4	316180.4	1.5	B31.3
150	10634.4	4889.1	5.0	23009.4	5197.3	1.000	1.000	5197.3	323122.6	1.6	B31.3
150	10634.4	4889.1	-5.0	23009.4	5197.3	1.000	1.000	5197.3	323122.6	1.6	B31.3
160	10634.4	15162.7	5.0	23009.4	15470.9	1.000	1.000	15470.9	315693.6	4.9	B31.3
160	10634.4	15162.7	-5.0	23009.4	15470.9	1.000	1.000	15470.9	315693.6	4.9	B31.3
168	10634.4	24250.6	5.0	23009.4	24558.8	1.000	1.000	24558.8	332740.0	7.4	B31.3
168	10634.4	46373.1	-5.0	23009.4	46681.3	1.912	1.594	46681.3	331931.0	14.1	B31.3
169	10412.0	49744.2	-137.0	23009.4	50350.9	1.912	1.594	50350.9	331802.4	15.2	B31.3
169	10412.0	49744.2	137.0	23009.4	50350.9	1.912	1.594	50350.9	331802.4	15.2	B31.3

Node	Axial Stress KPa	Bending Stress KPa	Torsion Stress KPa	Hoop Stress KPa	Max Stress Intensity KPa	SIF/Index In Plane	SIF/Index Out Plane	Code Stress KPa	Allowable Stress KPa	Ratio %	Piping Code
170	10455.0	49093.1	-217.1	23009.4	49643.6	1.912	1.594	49643.6	332277.0	14.9	B31.3
170	10455.0	25672.1	217.1	23009.4	26224.3	1.000	1.000	26224.3	332955.4	7.9	B31.3
180	10455.0	20498.7	-217.1	23009.4	21051.8	1.000	1.000	21051.8	322211.8	6.5	B31.3
180	10455.0	20498.7	217.1	23009.4	21051.8	1.000	1.000	21051.8	322211.8	6.5	B31.3
188	10455.0	5538.0	-217.1	23009.4	6102.1	1.000	1.000	6102.1	333097.5	1.8	B31.3
188	10455.0	9937.8	217.1	23009.4	10495.5	1.912	1.594	10495.5	332576.3	3.2	B31.3
189	10445.5	8113.6	-1516.2	23009.4	9052.8	1.912	1.594	9052.8	331267.3	2.7	B31.3
189	10445.5	8113.6	1516.2	23009.4	9052.8	1.912	1.594	9052.8	331267.3	2.7	B31.3
190	10668.5	2632.8	-2204.3	23009.4	5155.6	1.912	1.594	5155.6	330267.1	1.6	B31.3
190	10668.5	1405.6	2204.3	23009.4	4639.6	1.000	1.000	4639.6	331836.6	1.4	B31.3
200	10573.7	17735.4	-2204.3	23009.4	18314.0	1.000	1.000	18314.0	332470.9	5.5	B31.3

The results of the analysis are within the allowable stress range therefore ASME code compliance is met. The highest stresses experienced by the Discharge Line due to combined loadings are as follows:

Highest Stresses:	(KPa)		
Ratio (%):	15.2	@Node 169	
Code Stress:	50350.9	Allowable Stress:	331802.4
Axial Stress:	10988.4	@Node 169	
Bending Stress:	49744.2	@Node 169	
Torsion Stress:	2426.5	@Node 30	
Hoop Stress:	23009.4	@Node 20	
Max Stress Intensity:	50350.9	@Node 169	

CHAPTER 5

5.0 Conclusion and Recommendation

5.1 Summary of Study

This study has investigated all aspects of a piping system design and performed a detailed analysis of the various loading types. Solutions were determined using theoretical analyses and pipe stress analysis software. The analysis of independent load cases, as well as, simultaneous load cases were performed using CAESAR II software. As minimum compliance to the SANS and ASME statutory piping standards were met.

Three different types of analysis were performed namely Primary stress analysis, Secondary stress analysis, and Simultaneous stress analysis. The system was designed within the allowable stress limits of 138 000 kPa. In the comparison of the results obtained, Primary stress analysis and Secondary stress analysis produced results of similar magnitude. Where Primary stress max stress intensity was 35029.6 kPa; and Secondary stress analysis resulted in a max stress intensity of 35 982.7 kPa. Of particular attention is the result of simultaneous loading resulting in a max stress intensity of 50 350.9 kPa. Based on these results, it can be concluded that a system experiences approximately 40% higher stresses during simultaneous loading. Each stress contributor resulted in similar magnitude stresses therefore neglecting a load contributor could result in a failure of the system.

The results of the analysis were used to determine the following theories:

- Internal pressure in piping can rise exponentially in two situations. The first is based on the incorrect dimensional selection of the system, and the second relating to fluid entrapment within a closed loop. It can be noticed in tables 3.1-2 and 3.1-3 that pressure increases or decreases exponentially at every dimeter size change. Pressure increase due to fluid entrapment results from thermal expansion or fluid being pumped against a closed valve. The prevention of occurrence is done by installing pressure relief mechanisms at every isolation loop in a piping system.
- The rapid expansion of pressure can be caused by water hammer. The average maximum pressure of industry-standard petroleum pumps is 16 bar. The water hammer that can be experienced by the discharge line is almost double this value at 27.9 bar. Although pressure relief mechanisms can account for water hammer, the systems working design pressure should account for this phenomenon. The reason being, pressure build-up due to water hammer occurs quicker than the reaction of pressure relief mechanisms. This could result in crack propagations.
- Due to the geometry of a pipe, circumferential stresses are greater than longitudinal stresses. The variance could be almost twice the value of longitudinal stresses. An important observation made throughout this study, that should be followed here as well,

simultaneous loading is the cause of most piping failures therefore all stresses should be accounted for.

- The minimum thickness of piping components shall account for manufacturing quality and corrosion rates of the piping material. All stress analyses must account for the corrosion of the material throughout the life of the system. Piping systems are typically designed for a life of 50 years from the date of installation. Approximately 90% of all piping systems are fabricated out of steel which is prone to natural oxidation. Mild steel corrodes at a rate of 4 – 170 microns per year depending on the environment that the system is installed in. Based on these corrosion rates and the practical analysis done using CAESAR II software, a piping component can reach its maximum allowable stress within the first 20 years of serviceable life if corrosion and quality factors are not accounted for. Stress calculations must be done on piping components thickness less than the sum of corrosion over the expected life of the system. The maximum allowable stress of the system shall be reduced by a manufacturing quality factor depending on the type of manufacture and fabrication of the components (see Appendices A and B).
- The primary stress analysis performed using CAESAR II software calculated stress caused by dead weight (a combination of piping components and process fluids) and dynamic loadings. The calculation of dead weight is a fairly simple exercise to perform. Where this is not true for dynamic loadings. The principle of uniformly distributed loading for the design of supports cannot be used for systems that experience dynamic loadings. Two scenarios were done on CAESAR II – the first with anchor support throughout the piping run; and the second with applying anchors before process equipment and all other supports as guide supports. By constraining the piping throughout the length, an overall increase in stress was experienced, with some nodes increasing above the maximum allowable stress limits. The overstress of piping components and translation to pipe supports leads to failure. The guide supports to allow for minor free movement (displacements) in the piping. The free movement reduces the overall stress experienced by the system. Table 3.1-7 details the stresses experienced at supporting positions of the piping. This method removes any high stresses and displacements at the anchor supports near the connections of process equipment. The resultant force at the anchor support near process equipment was 234 N and 0 mm displacements compared to an average of 1300 N at all other guide supports. The solution presented is only applicable to primary stresses and not secondary stresses.
- Higher grade materials have higher maximum allowable stress ranges. This allows the thickness of components to be reduced which results in less dead weight of the system.
- Similar to the observation made on the primary stress analysis, allowing free movement of the system reduces the overall stresses experienced. However, based on the analysis done, secondary stresses due to thermal expansion results in much greater displacements (see Table 3.2-1). To account for high displacements in piping, added flexibility shall be design into the system. Piping must be sufficiently flexible to accommodate any movements caused by thermal expansion. This can be achieved by the introduction of expansion loops. As previously discussed piping components have

inherent flexibility, where, pipe bends have the greatest flexibility compared to all other piping components. Expansion loops provide the lengths of piping perpendicular to the piping's main axis to absorb thermal expansion. This results in lower axial resultant stress and bending moments.

All of the investigations pointed back to the shortfalls of the original design of Indy Oils piping systems. The design steps required for the installation of a safe piping system that is detailed throughout this thesis was not followed. For this reason, the entire process plants piping was reviewed to highlight any non-conformances. A project was initiated to address these non-conformances by replacing the piping systems with installations that followed all the design steps required for a safe system. This is a lesson learned as to why statutory design codes are developed to ensure minimum safety requirements are met.

Based on the theories generated from this study, the followings conclusions were made on the failures that have occurred at Indy Oil:

- Failures at process equipment connections were a result of high reaction and displacement forces transferred from piping systems. Inadequate stress distribution can cause piping anchor supports near process connections to fail. This will result in a direct transfer of forces and displacements from the piping system to the process connection. Vertical connections on process connections, such as pumps, are to be supported by spring hanger supports. These types of supports limit vertical reaction forces and at the same time allow for free movement along the horizontal axis.
- Piping weld cracks are caused by high internal pressures, crack propagation from thermal expansion, and/or the effects of dynamics loadings. This study has shown if any load category does not account for, failure is possible.
- Gasket blowouts are a high risk in petroleum plants. This could result in the harming of life. Blowouts are caused by displacements at flange connections that exceed the bolt and nuts torque specification. Flanged connections are to be avoided in areas of high thermal expansion.

5.2 Recommendations

Recommendations proposed for future study:

- Study of the influence of non-linear piping supports.
- The application of composite materials for piping systems in the Petroleum industry
- Comparison of results obtained using the classical beam theories method of analysis and FEA analysis.

Bibliography

(2019). Retrieved from Inge Expert: https://ingeoexpert.com/en/courses-online/introduction-to-pipe-stress-analysis-and-the-use-of-caesar-ii/

(2019). Retrieved from ENG-TIPS.com: https://www.eng-tips.com/viewthread.cfm?qid=246231

(2019). Retrieved from Coade Forums: http://forums.coade.com/ubbthreads/ubbthreads.php?ubb=showflat&Number=28454

A.Crowl, D. (2011). *informIT*. Retrieved June 06, 2017, from http://www.informit.com/articles/article.aspx?p=1717264&seqNum=8

Ababneh, D. A. (n.d.). *Flow in Conduits.*

About beam modeling. (2018). Retrieved from Abaqus : https://abaqus-docs.mit.edu/2017/English/SIMACAEELMRefMap/simaelm-c-beamoverview.htm

Antaki, G. A. (2003). *Piping and Pipeline Engineering: Design, Construction, Maintenance, Integrity, and Repair.* CRC Press.

ASME. (2017). *ASME Boiler and Pressure Vessel Code, Sec III, Div 1.* New York: Two Park Avenue.

Bagley, M. (2014, July 24). *Properties of Matter: Liquids*. Retrieved from Live Science: https://www.livescience.com/46972-liquids.html

base, P. E.–K. (2018). *Classification of Pipe Supports*. Retrieved October 2018, from http://www.piping-engineering.com/pipe-supports-classification-based-on-details-constructions-functions.html

Beale, R., & Bowers, P. (2018). *The Planning Guide to Piping Design.* Gulf Professional Publishing.

Beam Elements. (2018). Retrieved from Autodesk: http://download.autodesk.com/us/algor/userguides/mergedProjects/setting_up_the_analysis/linear/Elements/Beam_Elements.htm

Bhende, G. (2013). Stress Intensification & Flexibility in Pipe Stress Analysis. 1324 - 1329.

Bijlaard, P. (1955). *Stresses from Local Loadings in Cylindrical Pressure Vessels.* ASME Transactions.

Botermans, R. (2008). *Process Piping Design Handbook* (2nd ed.). Texas: Gulf Publishing Company.

Breen, J. (2000). *Modeling "U"-bolt guide and fix type*. Retrieved from Forums Coade: http://forums.coade.com/ubbthreads/ubbthreads.php?ubb=showflat&Number=6332

Breen, J. (2009). *B31.3 Thermal stresses*. Retrieved from ENG-TIPS: https://www.eng-tips.com/viewthread.cfm?qid=246231

C. Basavaraju, P. (2004). *Stress Analysis Of Piping SystemS.* New York: McGraw-Hill.

CAESAR II Users Guide. (2018). Retrieved from Hexagon PPM: https://docs.hexagonppm.com/reader/O04dxcwMfibZIK1cyksZvQ/vARM1FsBfEownXcNDtSgRA

Carrera, E. (2011). *Beam Structures.* New Jersey: Wiley.

Carter, R. (2005). *Background of SIFs and Stress Indices for Moment Loadings of Piping Components.* Electric Power Research Institute.

Churchill, S. (1987). *Viscous Flows: The Practical use of Theory.* Boston: Butterworths.

Cimbala, C. (2004). Flow in pipes. In C. Cimbala, *Fluid Mechanics* (pp. 321 - 398).

Coade. (1985). *Pipe Stress Analysis Seminar notes.* Texas.

Consultants, B. M. (2018). *Vibration, dynamics and noise*. Retrieved from Wood: http://www.betamachinery.com/services/pipe-stress-analysis

Dey, A. K. (2015). *Piping Elbow or Bend SIF (Stress Intensification Factor)*. Retrieved from What is Piping: https://whatispiping.com/bend-sif

Don Mckeehan, E. B. (1941). *Design of Piping Systems* (1st ed.). New York: The MW Kellogg company.

Don Mckeehan, E. B. (1956). *Design of Piping Systems* (2nd ed.). New York: The MW Kellogg company.

EC Rodabaugh, G. W. (1989). WFI/PVRC Moment Fatigue Tests on 4x3 ANSI B16.9 Tees. 1-8.

Ed Bausbacher, R. W. (1993). *Process Plant Layout and Piping Design.* PTR Prentice Hall.

Engineers, A. S. (2014). *ASME B31.3 code for Pressure Piping.* New York: Two Park Avenue.

ETIM, M.-A. P. (2015). *Laminar Flow And Turbulent Flow In Simple Pipe System.* Kwara State, Nigeria: Landmark University.

Fullwood, R. (1989). *Review of Pipe-break Probablity Assessment* (1st ed.). Martin Marietta.

Gaurav Bhende, G. T. (2013). Stress Intensification & Flexibility in Pipe Stress Analysis. *International Journal of Modern Engineering Research (IJMER)*, 1 - 6.

Hannah, J., & Stephens, R. (1972). *Mechanics of Machines.* Butler & Tanner Ltd.

Hashem, D. A.-A. (n.d.). *Oil and Gas Pipeline Design, Maintenance and Repair.* Giza, Egypt: Faculty of Engineering - Cairo University .

Hibbeler, R. (2014). *Mechanics of Materials.* Singapore: Pearson Education.

Introduction to Piping System. (2018). Retrieved from The Process Piping: https://www.theprocesspiping.com/introduction-to-piping-system/

J.E Meyer, J. F. (2014). *B31.3 Process Piping* . New York: The American Society of Mechanical Engineers.

Jr, J. J. (1992). *Piping Design Handbook.* CRC Press.

K.R., W. (1965). *Local Stresses in Spherical and Cylindrical Shells Due to External Loadings.*

Kannappan, S. (1986). *Introduction to Pipe Stress Analysis* (1986 ed.). New York: John Wiley & Sons Inc.

Kassimali, A. (1999). *Matrix Analysis of Structures.* Pacific Grove: Brooks / Coles Publishing company.

Khattak, M. (2016). Root cause analysis (RCA) of fractured ASTM A53 carbon steel pipe. 1 - 8.

Mahasuverachai, M. (1982). *Inelastic analysis of piping and Tubular structures.* California: University of California.

Markl, A. (1955). *Piping-FLexibility Analysis* (1st ed.). Transactions of ASME.

Materials, U. D. (2017, April 18). *Pipeline 101*. (Association of Oil Pipe Lines) Retrieved April 18, 2017, from www.pipeline101.org/The-History-of-Pipelines

Meyer, C. (1995). *Applications of Fluid Mechanics Part I.* Monumentpark: CFM Publications.

Meyer, C. (1995). *Applications of Fluid Mechanics Part II.* CFM Publications.

Monte Engelkemier, P. P. (2017). *How to perform a pipe stress analysis*. Retrieved from Consulting Specifying Engineer : https://www.csemag.com/articles/how-to-perform-a-pipe-stress-analysis/

Munson, B. (1998). *Fundamentals of Fluid Mechanics.* John Wiley and Sons.

Nakayama, Y. (1998). *Introduction to fluid Mechanics.* Tokyo: Yokendo CO. LTD.

Nayyar, M. L. (2000). *Piping Handbook* (7th ed.). Washingtn DC: Mcgraw-Hil.

Nielsen, L. A. (2008). *Elastic Beams in Three Dimensions.* Denmark: Aalborg University.

Parisher, R. A., & Rhea, R. A. (2012). *Pipe Drafting and Design* . Amsterdam: Elsevier.

Peng, L.-C. (. (2009). *Pipe Stress Engineering* (1st Edition ed.). Texas: ASME .

Peng, T.-L., & Peng, L.-C. (2009). *Pipe Stress Engineering.* American Society of Mechanical Engineers.

Practical 3: Friction and Minor Losses in Pipes. (2020). Retrieved from UNISA - Learn Online: https://lo.unisa.edu.au/mod/book/tool/print/index.php?id=466227

Rodabaugh, E. (1994). Developing Stress intensification factors. *Welding research council bulletin, II*(392), 16.

Rodgers, T. (2013). *Fluid Flow.*

Sam, K. (1986). *Introduction to Pipe Stress Analysis.* Wiley.

Sanders, R. E. (2005). *Chemical Process Safety Learning from case studies* (3rd ed.). Amsterdam: Elsevier Butterworth Heinemann.

Shieh, J. (2009, December 21). *Fundamentals of Fluid mechanics.* Retrieved from http://cau.ac.kr/~jjang14/FME/Chap8.pdf

Smith, P. (2007). *The Fundamentals of Piping Design.* Gulf Publishing Company.

Sondalini, M. (2018). *How Fluid Flows in Pipes*. Retrieved from Accendore Liability : https://accendoreliability.com/fluid-flows-pipes/

Spielvogel, S. (1955). *Piping Stress Calculations simplified.* New York: Lake Success.

Stewart, M. (2016). *Bulk Modulus*. Retrieved from Science Direct: https://www.sciencedirect.com/topics/engineering/bulk-modulus

Subramanian, R. S. (2011). *Pipe Flow Calculations.* New York: Clarkson University.

Supermarkets, M. (2015). *What Do Pipe Schedules Mean?* Retrieved 2018, from https://www.metalsupermarkets.com/what-do-pipe-schedules-mean/

Veritas, D. N. (2008). *Structural Analysis Of Piping Systems.* Norway.

Warhaft, Z. (1997). *Transition and Turbulence*. Retrieved from Princeton: https://www.princeton.edu/~asmits/Bicycle_web/transition.html

Weaver, R. (1986). *Process Piping Drafting.* Gulf Publishing Company.

What is the Reynolds Number? (2020). Retrieved from Sim Scale: https://www.simscale.com/docs/simwiki/numerics-background/what-is-the-reynolds-number/

White, F. (2011). *Fluid Mechanics, 7th Edition.* New York: McGraw-Hill.

Woods, G. (1989). WFI/PVRC Moment fatigue tests on 4x3 ANSI B16.9 Tees. *Welding research council bulletin, 346*(I), 9.

Woods, G. (1994). Developing Stress Intensification Factors. 1-16.

Zahid, U. (2016). A Methodology for Flexibility Analysis of Process Piping. 1 - 10.

Appendices

Appendix A – Weld Joint Strength Reduction Factor (Engineers, 2014)

Table 302.3.5 Weld Joint Strength Reduction Factor, *W*

Steel Group	Component Temperature, T_i, °C (°F)														
	427 (800)	454 (850)	482 (900)	510 (950)	538 (1,000)	566 (1,050)	593 (1,100)	621 (1,150)	649 (1,200)	677 (1,250)	704 (1,300)	732 (1,350)	760 (1,400)	788 (1,450)	816 (1,500)
CrMo [Notes (1)–(3)]	1	0.95	0.91	0.86	0.82	0.77	0.73	0.68	0.64	...	...	...	...	...	...
CSEF (N + T) [Notes (3)–(5)]	...	...	...	1	0.95	0.91	0.86	0.82	0.77	...	...	...	...	...	...
CSEF [Notes (3) and (4)] (Subcritical PWHT)	...	...	1	0.5	0.5	0.5	0.5	0.5	0.5	...	...	...	...	...	...
Autogenous welds in austenitic stainless grade 3xx, and N088xx and N066xx nickel alloys [Note (6)]	...	...	...	1	1	1	1	1	1	1	1	1	1	1	1
Austenitic stainless grade 3xx and N088xx nickel alloys [Notes (7) and (8)]	...	...	...	1	0.95	0.91	0.86	0.82	0.77	0.73	0.68	0.64	0.59	0.55	0.5
Other materials [Note (9)]	...	...	...	...	...	...	...	...	...	...	...	...	...	...	...

GENERAL NOTES:

(a) Weld joint strength reduction factors at temperatures above the upper temperature limit listed in Appendix A for the base metal or outside of the applicable range in Table 302.3.5 are the responsibility of the designer. At temperatures below those where weld joint strength reduction factors are tabulated, a value of 1.0 shall be used for the factor *W* where required; however, the additional rules of this Table and Notes do not apply.

(b) T_{cr} = temperature 25°C (50°F) below the temperature identifying the start of time-dependent properties listed under "NOTES – TIME-DEPENDENT PROPERTIES" (Txx) in the Notes to Tables 1A and 1B of the BPV Code Section II, Part D for the base metals joined by welding. For materials not listed in the BPV Code Section II, Part D, T_{cr} shall be the temperature where the creep rate or stress rupture criteria in paras. 302.3.2(d)(4), (5), and (6) governs the basic allowable stress value of the metals joined by welding. When the base metals differ, the lower value of T_{cr} shall be used for the weld joint.

(c) T_i = temperature, °C (°F), of the component for the coincident operating pressure–temperature condition, *i*, under consideration.

(d) CAUTIONARY NOTE: There are many factors that may affect the life of a welded joint at elevated temperature and all of those factors cannot be addressed in a table of weld strength reduction factors. For example, fabrication issues such as the deviation from a true circular form in pipe (e.g., "peaking" at longitudinal weld seams) or offset at the weld joint can cause an increase in stress that may result in reduced service life and control of these deviations is recommended.

(e) The weld joint strength reduction factor, *W*, may be determined using linear interpolation for intermediate temperature values.

NOTES:

(1) The Cr–Mo Steels include: ½Cr–½Mo, 1Cr–½Mo, 1¼Cr–½Mo–Si, 2¼Cr–1Mo, 3Cr–1Mo, 5Cr–½Mo, 9Cr–1Mo. Longitudinal and spiral (helical seam) welds shall be normalized, normalized and tempered, or subjected to proper subcritical postweld heat treatment (PWHT) for the alloy. Required examination is in accordance with para. 341.4.4 or 305.2.4.

(2) Longitudinal and spiral (helical seam) seam fusion welded construction is not permitted for C–½Mo steel above 850°F.

(3) The required carbon content of the weld filler metal shall be ≥0.05 C wt. %. See para. 341.4.4(b) for examination requirements. Basicity index of SAW flux ≥1.0.

(4) The CSEF (Creep Strength Enhanced Ferritic) steels include grades 91, 92, 911, 122, and 23.

(5) N + T = Normalizing + Tempering PWHT.

(6) Autogenous welds without filler metal in austenitic stainless steel (grade 3xx) and austenitic nickel alloys UNS Nos. N066xx and N088xx. A solution anneal after welding is required for use of the factors in the Table. See para. 341.4.3(b) for examination requirements.

(7) Alternatively, the 100,000 hr Stress Rupture Factors listed in ASME Section III, Division 1, Subsection NH, Tables I-14.10 A-xx, B-xx, and C-xx may be used as the weld joint strength reduction factor for the materials and welding consumables specified.

(8) Certain heats of the austenitic stainless steels, particularly for those grades whose creep strength is enhanced by the precipitation of temper-resistant carbides and carbonitrides, can suffer from an embrittlement condition in the weld heat affected zone that can lead to premature failure of welded components operating at elevated temperatures. A solution annealing heat treatment of the weld area mitigates this susceptibility.

(9) For carbon steel, $W = 1.0$ for all temperatures. For materials other than carbon steel, CrMo, CSEF, and the austenitic alloys listed in Table 302.3.5, *W* shall be as follows: For $T_i \le T_{cr}$, $W = 1.0$. For $T_{cr} < T_i \le 1{,}500$°F, $W = 1 - 0.000909(T_i - T_{cr})$. If T_i exceeds the upper temperature for which an allowable stress value is listed in Appendix A for the base metal, the value for *W* is the responsibility of the designer.

Appendix B – Weld Joint Strength Reduction Factor (Engineers, 2014)

Table 302.3.4 Longitudinal Weld Joint Quality Factor, E_j

No.	Type of Joint		Type of Seam	Examination	Factor, E_j
1	Furnace butt weld, continuous weld		Straight	As required by listed specification	0.60 [Note (1)]
2	Electric resistance weld		Straight or spiral (helical seam)	As required by listed specification	0.85 [Note (1)]
3	Electric fusion weld				
	(a) Single butt weld		Straight or spiral (helical seam)	As required by listed specification or this Code	0.80
	(with or without filler metal)			Additionally spot radiographed in accordance with para. 341.5.1	0.90
				Additionally 100% radiographed in accordance with para. 344.5.1 and Table 341.3.2	1.00
	(b) Double butt weld		Straight or spiral (helical seam) [except as provided in 4 below]	As required by listed specification or this Code	0.85
	(with or without filler metal)			Additionally spot radiographed in accordance with para. 341.5.1	0.90
				Additionally 100% radiographed in accordance with para. 344.5.1 and Table 341.3.2	1.00
4	Specific specification				
	API 5L	Submerged arc weld (SAW) Gas metal arc weld (GMAW) Combined GMAW, SAW 	Straight with one or two seams Spiral (helical seam)	As required by specification	0.95
				Additionally 100% radiographed in accordance with para. 344.5.1 and Table 341.3.2	1.00

NOTE:
(1) It is not permitted to increase the joint quality factor by additional examination for joint 1 or 2.

Appendix C – Values for Coefficient Y, For T < D/6 (Engineers, 2014)

Table 304.1.1 Values of Coefficient *Y* for $t < D/6$

Material	Temperature, °C (°F)							
	482 (900) and Below	510 (950)	538 (1,000)	566 (1,050)	593 (1,100)	621 (1,150)	649 (1,200)	677 (1,250) and Above
Ferritic steels	0.4	0.5	0.7	0.7	0.7	0.7	0.7	0.7
Austenitic steels	0.4	0.4	0.4	0.4	0.5	0.7	0.7	0.7
Nickel alloys UNS Nos. N06617, N08800, N08810, and N08825	0.4	0.4	0.4	0.4	0.4	0.4	0.5	0.7
Gray iron	0.0	...	...	...	...	...	...	...
Other ductile metals	0.4	0.4	0.4	0.4	0.4	0.4	0.4	0.4

Appendix D – Modulus of Elasticity (Engineers, 2014)

Table C-6 Modulus of Elasticity, U.S. Units, for Metals

Material	E = Modulus of Elasticity, Msi (Millions of psi), at Temperature, °F									
	−425	−400	−350	−325	−200	−100	70	200	300	400
Ferrous Metals										
Gray iron	...	...	...	...	...	...	13.4	13.2	12.9	12.6
Carbon steels, C ≤ 0.3%	31.9	...	...	31.4	30.8	30.2	29.5	28.8	28.3	27.7
Carbon steels, C > 0.3%	31.7	...	...	31.2	30.6	30.0	29.3	28.6	28.1	27.5
Carbon–moly steels	31.7	...	...	31.1	30.5	29.9	29.2	28.5	28.0	27.4
Nickel steels, Ni 2%–9%	30.1	...	...	29.6	29.1	28.5	27.8	27.1	26.7	26.1
Cr–Mo steels, Cr ½%–2%	32.1	...	...	31.6	31.0	30.4	29.7	29.0	28.5	27.9
Cr–Mo steels, Cr 2¼%–3%	33.1	...	...	32.6	32.0	31.4	30.6	29.8	29.4	28.8
Cr–Mo steels, Cr 5%–9%	33.4	...	...	32.9	32.3	31.7	30.9	30.1	29.7	29.0
Chromium steels, Cr 12%, 17%, 27%	31.8	...	...	31.2	30.7	30.1	29.2	28.5	27.9	27.3
Austenitic steels (TP304, 310, 316, 321, 347)	30.8	...	...	30.3	29.7	29.0	28.3	27.6	27.0	26.5
Copper and Copper Alloys (UNS Nos.)										
Comp. and leaded Sn–bronze (C83600, C92200)	...	...	...	14.8	14.6	14.4	14.0	13.7	13.4	13.2
Naval and Si–brass, Si– & Al–bronze (C46400, C65500, C95200, C95400)	...	...	...	15.9	15.6	15.4	15.0	14.6	14.4	14.1
Copper (C11000)	...	...	...	16.9	16.6	16.5	16.0	15.6	15.4	15.0
Copper, red brass, Al–bronze (C10200, C12000, C12200, C12500, C14200, C23000, C61400)	...	...	...	18.0	17.7	17.5	17.0	16.6	16.3	16.0
90Cu–10Ni (C70600)	...	...	...	19.0	18.7	18.5	18.0	17.6	17.3	16.9
Leaded Ni–bronze	...	...	...	20.1	19.8	19.6	19.0	18.5	18.2	17.9
80Cu–20Ni (C71000)	...	...	...	21.2	20.8	20.6	20.0	19.5	19.2	18.8
70Cu–30Ni (C71500)	...	...	...	23.3	22.9	22.7	22.0	21.5	21.1	20.7
Nickel and Nickel Alloys (UNS Nos.)										
Alloy 400 N04400	28.3	...	...	27.8	27.3	26.8	26.0	25.4	25.0	24.7
Alloy N06035	29.2	...	...	29.1	29.0	28.8	28.5	28.1	27.8	27.5
Alloys N06007, N08320	30.3	...	...	29.5	29.2	28.6	27.8	27.1	26.7	26.4
Alloys N08800, N08810, N06002	31.1	...	...	30.5	29.9	29.4	28.5	27.8	27.4	27.1
Alloys N06455, N10276	32.5	...	...	31.6	31.3	30.6	29.8	29.1	28.6	28.3
Alloys N02200, N02201, N06625	32.7	...	...	32.1	31.5	30.9	30.0	29.3	28.8	28.5
Alloy N06600	33.8	...	...	33.2	32.6	31.9	31.0	30.2	29.9	29.5
Alloy N10001	33.9	...	...	33.3	32.7	32.0	31.1	30.3	29.9	29.5
Alloy N10665	34.2	...	...	33.3	33.0	32.3	31.4	30.6	30.1	29.8
Alloy N10675	...	...	...	33.7	32.9	32.3	31.4	30.7	30.2	29.8
Unalloyed Titanium										
Grades 1, 2, 3, and 7	...	...	...	...	...	...	15.5	15.0	14.6	14.0
Zirconium Alloys										
R60702	...	...	...	...	...	...	14.4	14.4	14.4	14.4
R60705	...	...	...	...	...	...	14.2	14.2	14.2	14.2

(14)

Table A-1M Basic Allowable Stresses in Tension for Metals (Metric) (Cont'd)

Numbers in Parentheses Refer to Notes for Appendix A Tables; Specifications Are ASTM Unless Otherwise Indicated

Line No.	Nominal Composition	Product Form	Spec. No.	Type/ Grade	UNS No.	Class/ Cond./ Temper	Size, mm	P-No. (5)	Notes	Min. Temp., °C (6)	Min. Tensile Str., MPa	Min. Yield Str., MPa	Max. Use Temp., °C
1	Carbon steel	Pipe & tube	A134	...	...	...	...	1	(2)(8b)(57)	B	310	165	482
2	Carbon steel	Pipe & tube	A672	A45	K01700	...	...	1	(2)(57)(59)(67)	B	310	165	593
3	Carbon steel	Pipe & tube	API 5L	A25	...	...	...	1	(2)(8a)(77)	−30	310	172	204
4	Carbon steel	Pipe & tube	API 5L	A25	...	...	...	1	(2)(57)(59)(77)	B	310	172	204
5	Carbon steel	Pipe & tube	A179	...	K01200	...	...	1	(2)(57)(59)	−30	324	179	593
6	Carbon steel	Pipe & tube	A53	A	K02504	...	...	1	(2)(8a)	−5	331	207	204
7	Carbon steel	Pipe & tube	A139	A	...	...	...	1	(2)(8b)	A	331	207	149
8	Carbon steel	Pipe & tube	A587	...	K11500	...	...	1	(2)(57)(59)	−30	331	207	454
9	Carbon steel	Pipe & tube	A53	A	K02504	...	...	1	(2)(57)(59)	B	331	207	593
10	Carbon steel	Pipe & tube	A106	A	K02501	...	...	1	(2)(57)	B	331	207	593
11	Carbon steel	Pipe & tube	A135	A	...	...	...	1	(2)(57)(59)	B	331	207	593
12	Carbon steel	Pipe & tube	A369	FPA	K02501	...	...	1	(2)(57)	B	331	207	593
13	Carbon steel	Pipe & tube	API 5L	A	...	...	...	1	(2)(57)(59)(77)	B	331	207	593
14	Carbon steel	Pipe & tube	A134	...	...	...	...	1	(2)(8b)(57)	B	345	186	482
15	Carbon steel	Pipe & tube	A672	A50	K02200	...	...	1	(2)(57)(59)(67)	B	345	186	593
16	Carbon steel	Pipe & tube	A134	...	...	...	...	1	(2)(8b)(57)	A	379	207	482
17	Carbon steel	Pipe & tube	A524	II	K02104	...	...	1	(2)(57)	−30	379	207	538
18	Carbon steel	Pipe & tube	A333	1	K03008	...	...	1	(2)(57)(59)	−45	379	207	593
19	Carbon steel	Pipe & tube	A334	1	K03008	...	...	1	(2)(57)(59)	−45	379	207	593
20	Carbon steel	Pipe & tube	A671	CA55	K02801	...	...	1	(2)(59)(67)	A	379	207	593
21	Carbon steel	Pipe & tube	A672	A55	K02801	...	...	1	(2)(57)(59)(67)	A	379	207	593
22	Carbon steel	Pipe & tube	A672	C55	K01800	...	...	1	(2)(57)(67)	C	379	207	593
23	Carbon steel	Pipe & tube	A671	CC60	K02100	...	...	1	(2)(57)(67)	C	414	221	538
24	Carbon steel	Pipe & tube	A671	CB60	K02401	...	...	1	(2)(57)(67)	B	414	221	593
25	Carbon steel	Pipe & tube	A672	B60	K02401	...	...	1	(2)(57)(67)	B	414	221	593
26	Carbon steel	Pipe & tube	A672	C60	K02100	...	...	1	(2)(57)(67)	C	414	221	593
27	Carbon steel	Pipe & tube	A139	B	K03003	...	...	1	(2)(8b)	A	414	241	149
28	Carbon steel	Pipe & tube	A135	B	K03018	...	...	1	(2)(57)(59)	B	414	241	538
29	Carbon steel	Pipe & tube	A524	I	K02104	...	...	1	(2)(57)	−30	414	241	538

Basic Allowable Stress, *S*, MPa, at Metal Temperature, °C [Notes (1) and (4b)]

Line No.	Min. Temp. to 40	65	100	150	200	250	300	325	350	375	400	425	450	475	500	525	550	575	600
1	*103*	*103*	101	97.5	94.6	90.8	86.1	83.6	81.1	78.6	**73.3**	**64.0**	**55.8**	**43.9**	**40.7**	...	...	...	...
2	*103*	*103*	101	97.5	94.6	90.8	86.1	83.6	81.1	78.6	**73.3**	**64.0**	**55.8**	**43.9**	**31.7**	**21.4**	**14.2**	**9.40**	**6.89**
3	*103*	*103*	*103*	102	98.5	...	...	...	...	...	...	...	...	...	...	...	...	...	...
4	*103*	*103*	*103*	102	98.5	...	...	...	...	...	...	...	...	...	...	...	...	...	...
5	*108*	*108*	*108*	106	102	98.3	93.3	90.6	87.8	**84.3**	**73.3**	**64.0**	**55.8**	**43.9**	**31.7**	**21.4**	**14.2**	**9.40**	**6.89**
6	*110*	*110*	*110*	*110*	*110*	...	...	...	...	...	...	...	...	...	...	...	...	...	...
7	*110*	*110*	*110*	*110*	...	...	...	...	...	...	...	...	...	...	...	...	...	...	...
8	*110*	*110*	*110*	*110*	*110*	*110*	108	105	**97.0**	**84.3**	**73.3**	**64.0**	**55.8**	**54.5**	...	...	...	...	...
9	*110*	*110*	*110*	*110*	*110*	*110*	108	105	**97.0**	**84.3**	**73.3**	**64.0**	**55.8**	**43.9**	**31.7**	**21.4**	**14.2**	**9.40**	**6.89**
10	*110*	*110*	*110*	*110*	*110*	*110*	108	105	**97.0**	**84.3**	**73.3**	**64.0**	**55.8**	**43.9**	**31.7**	**21.4**	**14.2**	**9.40**	**6.89**
11	*110*	*110*	*110*	*110*	*110*	*110*	108	105	**97.0**	**84.3**	**73.3**	**64.0**	**55.8**	**43.9**	**31.7**	**21.4**	**14.2**	**9.40**	**6.89**
12	*110*	*110*	*110*	*110*	*110*	*110*	108	105	**97.0**	**84.3**	**73.3**	**64.0**	**55.8**	**43.9**	**31.7**	**21.4**	**14.2**	**9.40**	**6.89**
13	*110*	*110*	*110*	*110*	*110*	*110*	108	105	**97.0**	**84.3**	**73.3**	**64.0**	**55.8**	**43.9**	**31.7**	**21.4**	**14.2**	**9.40**	**6.89**
14	*115*	*115*	113	110	106	102	96.9	94.1	91.2	**84.3**	**73.3**	**64.0**	**55.8**	**43.9**	**40.7**	...	...	...	...
15	*115*	*115*	113	110	106	102	96.9	94.1	91.2	**84.3**	**73.3**	**64.0**	**55.8**	**43.9**	**31.7**	**21.4**	**14.2**	**9.40**	**6.89**
16	*126*	*126*	126	122	118	113	108	105	101	98.3	**89.0**	**75.3**	**62.1**	**45.0**	**40.7**	...	...	...	...
17	*126*	*126*	126	122	118	113	108	105	101	98.3	**89.0**	**75.3**	**62.1**	**45.0**	**31.7**	**21.4**	**17.2**	...	...
18	*126*	*126*	126	122	118	113	108	105	101	98.3	**89.0**	**75.3**	**62.1**	**45.0**	**31.7**	**21.4**	**14.2**	**9.40**	**6.89**
19	*126*	*126*	126	122	118	113	108	105	101	98.3	**89.0**	**75.3**	**62.1**	**45.0**	**31.7**	**21.4**	**14.2**	**9.40**	**6.89**
20	*126*	*126*	126	122	118	113	108	105	101	98.3	**89.0**	**75.3**	**62.1**	**45.0**	**31.7**	**21.4**	**14.2**	**9.40**	**6.89**
21	*126*	*126*	126	122	118	113	108	105	101	98.3	**89.0**	**75.3**	**62.1**	**45.0**	**31.7**	**21.4**	**14.2**	**9.40**	**6.89**
22	*126*	*126*	126	122	118	113	108	105	101	98.3	**89.0**	**75.3**	**62.1**	**45.0**	**31.7**	**21.4**	**14.2**	**9.40**	**6.89**
23	*138*	*138*	134	130	126	121	115	111	108	105	**95.1**	**79.5**	**62.6**	**45.0**	**31.7**	**21.4**	**17.2**	...	...
24	*138*	*138*	134	130	126	121	115	111	108	105	**95.1**	**79.5**	**62.6**	**45.0**	**31.7**	**21.4**	**14.2**	**9.40**	**6.89**
25	*138*	*138*	134	130	126	121	115	111	108	105	**95.1**	**79.5**	**62.6**	**45.0**	**31.7**	**21.4**	**14.2**	**9.40**	**6.89**
26	*138*	*138*	134	130	126	121	115	111	108	105	**95.1**	**79.5**	**62.6**	**45.0**	**31.7**	**21.4**	**14.2**	**9.40**	**6.89**
27	*138*	*138*	*138*	*138*	...	...	...	...	...	...	...	...	...	...	...	...	...	...	...
28	*138*	*138*	*138*	*138*	*138*	132	126	122	118	**113**	**95.1**	**79.5**	**62.6**	**45.0**	**31.7**	**21.4**	**17.2**	...	...
29	*138*	*138*	*138*	*138*	*138*	132	126	122	118	**113**	**95.1**	**79.5**	**62.6**	**45.0**	**31.7**	**21.4**	**17.2**	...	...

Line No.	Nominal Composition	Product Form	Spec. No.	Type/ Grade	UNS No.	Class/ Cond./ Temper	Size, mm	P-No. (5)	Notes	Min. Temp., °C (6)	Min. Tensile Str., MPa	Min. Yield Str., MPa	Max. Use Temp., °C
30	Carbon steel	Pipe & tube	A53	B	K03005	...	...	1	(2)(57)(59)	B	414	241	593
31	Carbon steel	Pipe & tube	A106	B	K03006	...	...	1	(2)(57)	B	414	241	593
32	Carbon steel	Pipe & tube	A333	6	K03006	...	...	1	(2)(57)	−45	414	241	593
33	Carbon steel	Pipe & tube	A334	6	K03006	...	...	1	(2)(57)	−45	414	241	593
34	Carbon steel	Pipe & tube	A369	FPB	K03006	...	...	1	(2)(57)	−30	414	241	593
35	Carbon steel	Pipe & tube	A381	Y35	...	...	...	1	(2)	A	414	241	593
36	Carbon steel	Pipe & tube	API 5L	B	...	...	...	1	(2)(57)(59)(77)	B	414	241	593
37	Carbon steel	Pipe & tube	A139	C	K03004	...	...	1	(2)(8b)	A	414	290	149
38	Carbon steel	Pipe & tube	A139	D	K03010	...	...	1	(2)(8b)	A	414	317	149
39	Carbon steel	Pipe & tube	API 5L	X42	...	...	...	1	(2)(55)(77)	A	414	290	204
40	Carbon steel	Pipe & tube	A381	Y42	...	...	...	1	(2)	A	414	290	204
41	Carbon steel	Pipe & tube	A381	Y48	...	...	...	1	(2)	A	427	331	343
42	Carbon steel	Pipe & tube	API 5L	X46	...	...	...	1	(2)(55)(77)	A	434	317	204
43	Carbon steel	Pipe & tube	A381	Y46	...	...	...	1	(2)	A	434	317	204
44	Carbon steel	Pipe & tube	A381	Y50	...	...	...	1	(2)	A	441	345	343
45	Carbon steel	Pipe & tube	A671	CC65	K02403	...	...	1	(2)(57)(67)	B	448	241	538
46	Carbon steel	Pipe & tube	A671	CB65	K02800	...	...	1	(2)(57)(67)	A	448	241	593
47	Carbon steel	Pipe & tube	A672	B65	K02800	...	...	1	(2)(57)(67)	A	448	241	593
48	Carbon steel	Pipe & tube	A672	C65	K02403	...	...	1	(2)(57)(67)	B	448	241	593
49	Carbon steel	Pipe & tube	A139	E	K03012	...	...	1	(2)(8b)	A	455	359	149
50	Carbon steel	Pipe & tube	API 5L	X52	...	...	...	1	(2)(55)(77)	A	455	359	204
51	Carbon steel	Pipe & tube	A381	Y52	...	...	...	1	(2)	A	455	359	204
52	Carbon steel	Pipe & tube	A671	CC70	K02700	...	...	1	(2)(57)(67)	B	483	262	538
53	Carbon steel	Pipe & tube	A671	CB70	K03101	...	...	1	(2)(57)(67)	A	483	262	593
54	Carbon steel	Pipe & tube	A672	B70	K03101	...	...	1	(2)(57)(67)	A	483	262	593
55	Carbon steel	Pipe & tube	A672	C70	K02700	...	...	1	(2)(57)(67)	B	483	262	593
56	Carbon steel	Pipe & tube	A106	C	K03501	...	...	1	(2)(57)	B	483	276	427
57	Carbon steel	Pipe & tube	A671	CD70	K12437	...	≤64	1	(2)(67)	D	483	345	371
58	Carbon steel	Pipe & tube	A672	D70	K12437	...	≤64	1	(2)(67)	D	483	345	371
59	Carbon steel	Pipe & tube	A691	CMSH-70	K12437	...	≤64	1	(2)(67)	D	483	345	371

Line No.	Min. Temp. to 40	65	100	150	200	250	300	325	350	375	400	425	450	475	500	525	550	575	600
	Basic Allowable Stress, *S*, MPa, at Metal Temperature, °C [Notes (1) and (4b)]																		
30	*138*	*138*	*138*	*138*	*138*	132	126	122	118	**113**	**95.1**	**79.5**	**62.6**	**45.0**	**31.7**	**21.4**	**14.2**	**9.40**	**6.89**
31	*138*	*138*	*138*	*138*	*138*	132	126	122	118	**113**	**95.1**	**79.5**	**62.6**	**45.0**	**31.7**	**21.4**	**14.2**	**9.40**	**6.89**
32	*138*	*138*	*138*	*138*	*138*	132	126	122	118	**113**	**95.1**	**79.5**	**62.6**	**45.0**	**31.7**	**21.4**	**14.2**	**9.40**	**6.89**
33	*138*	*138*	*138*	*138*	*138*	132	126	122	118	**113**	**95.1**	**79.5**	**62.6**	**45.0**	**31.7**	**21.4**	**14.2**	**9.40**	**6.89**
34	*138*	*138*	*138*	*138*	*138*	132	126	122	118	**113**	**95.1**	**79.5**	**62.6**	**45.0**	**31.7**	**21.4**	**14.2**	**9.40**	**6.89**
35	*138*	*138*	*138*	*138*	*138*	132	126	122	118	**113**	**95.1**	**79.5**	**62.6**	**45.0**	**31.7**	**21.4**	**14.2**	**9.40**	**6.89**
36	*138*	*138*	*138*	*138*	*138*	132	126	122	118	**113**	**95.1**	**79.5**	**62.6**	**45.0**	**31.7**	**21.4**	**14.2**	**9.40**	**6.89**
37	*138*	*138*	*138*	*138*	...	...	...	...	...	...	...	...	...	...	...	...	...	...	...
38	*138*	*138*	*138*	*138*	...	...	...	...	...	...	...	...	...	...	...	...	...	...	...
39	*138*	*138*	*138*	*138*	*138*	...	...	...	...	...	...	...	...	...	...	...	...	...	...
40	*138*	*138*	*138*	*138*	*138*	...	...	...	...	...	...	...	...	...	...	...	...	...	...
41	*142*	*142*	*142*	*142*	*142*	*142*	*142*	*142*	*129*	...	...	...	...	...	...	...	...	...	...
42	*145*	*145*	*145*	*145*	*145*	...	...	...	...	...	...	...	...	...	...	...	...	...	...
43	*145*	*145*	*145*	*145*	*145*	...	...	...	...	...	...	...	...	...	...	...	...	...	...
44	*147*	*147*	*147*	*147*	*147*	*147*	*147*	*147*	*129*	...	...	...	...	...	...	...	...	...	...
45	*149*	*149*	147	142	138	132	126	122	118	**113**	**95.1**	**79.5**	**64.4**	**47.7**	**32.5**	**21.4**	**17.2**	...	...
46	*149*	*149*	147	142	138	132	126	122	118	**113**	**95.1**	**79.5**	**64.4**	**47.7**	**32.5**	**21.4**	**14.2**	**9.40**	**6.89**
47	*149*	*149*	147	142	138	132	126	122	118	**113**	**95.1**	**79.5**	**64.4**	**47.7**	**32.5**	**21.4**	**14.2**	**9.40**	**6.89**
48	*149*	*149*	147	142	138	132	126	122	118	**113**	**95.1**	**79.5**	**64.4**	**47.7**	**32.5**	**21.4**	**14.2**	**9.40**	**6.89**
49	*152*	*152*	*152*	*152*	...	...	...	...	...	...	...	...	...	...	...	...	...	...	...
50	*152*	*152*	*152*	*152*	*152*	...	...	...	...	...	...	...	...	...	...	...	...	...	...
51	*152*	*152*	*152*	*152*	*152*	...	...	...	...	...	...	...	...	...	...	...	...	...	...
52	*161*	*161*	159	154	150	144	136	132	128	**122**	**101**	**83.8**	**66.8**	**50.3**	**33.2**	**21.4**	**17.2**	...	...
53	*161*	*161*	159	154	150	144	136	132	128	**122**	**101**	**83.8**	**66.8**	**50.3**	**33.2**	**21.4**	**14.2**	**9.40**	**6.89**
54	*161*	*161*	159	154	150	144	136	132	128	**122**	**101**	**83.8**	**66.8**	**50.3**	**33.2**	**21.4**	**14.2**	**9.40**	**6.89**
55	*161*	*161*	159	154	150	144	136	132	128	**122**	**101**	**83.8**	**66.8**	**50.3**	**33.2**	**21.4**	**14.2**	**9.40**	**6.89**
56	*161*	*161*	*161*	*161*	158	151	144	139	135	**122**	**101**	**83.8**	**82.7**	...	...	...	...	...	...
57	*161*	*161*	*161*	*157*	*156*	*156*	156	154	**148**	**126**	...	...	...	...	...	...	...	...	...
58	*161*	*161*	*161*	*157*	*156*	*156*	156	154	**148**	**126**	...	...	...	...	...	...	...	...	...
59	*161*	*161*	*161*	*157*	*156*	*156*	156	154	**148**	**126**	...	...	...	...	...	...	...	...	...

(14) **Table D300 Flexibility Factor, k, and Stress Intensification Factor, i**

Description	Flexibility Factor, k	Stress Intensification Factor [Notes (1), (2)] Out-of-Plane, i_o	Stress Intensification Factor [Notes (1), (2)] In-Plane, i_i	Flexibility Characteristic, h	Sketch
Welding elbow or pipe bend [Notes (1), (3)–(6)]	$\frac{1.65}{h}$	$\frac{0.75}{h^{2/3}}$	$\frac{0.9}{h^{2/3}}$	$\frac{\overline{T}R_1}{r_2^2}$	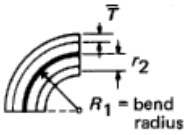
Closely spaced miter bend $s < r_2(1 + \tan\theta)$ [Notes (1), (3), (4), (6)]	$\frac{1.52}{h^{5/6}}$	$\frac{0.9}{h^{2/3}}$	$\frac{0.9}{h^{2/3}}$	$\frac{\cot\theta}{2}\left(\frac{s\overline{T}}{r_2^2}\right)$	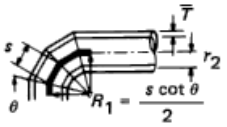
Single miter bend or widely spaced miter bend $s \geq r_2(1 + \tan\theta)$ [Notes (1), (3), (6)]	$\frac{1.52}{h^{5/6}}$	$\frac{0.9}{h^{2/3}}$	$\frac{0.9}{h^{2/3}}$	$\frac{1 + \cot\theta}{2}\left(\frac{\overline{T}}{r_2}\right)$	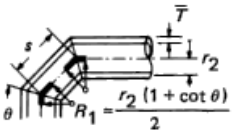
Welding tee in accordance with ASME B16.9 [Notes (1), (3), (5), (7), (8)]	1	$\frac{0.9}{h^{2/3}}$	$\frac{3}{4}i_o + \frac{1}{4}$	$3.1\frac{\overline{T}}{r_2}$	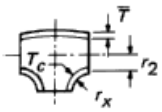
Reinforced fabricated tee with pad or saddle [Notes (1), (3), (8), (9), (10)]	1	$\frac{0.9}{h^{2/3}}$	$\frac{3}{4}i_o + \frac{1}{4}$	$\frac{(\overline{T} + \frac{1}{2}\overline{T}_r)^{2.5}}{\overline{T}^{1.5}r_2}$	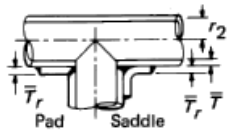

Table D300 Flexibility Factor, k, and Stress Intensification Factor, i (Cont'd) (14)

Description	Flexibility Factor, k	Stress Intensification Factor [Notes (1), (2)] Out-of-Plane, i_o	Stress Intensification Factor [Notes (1), (2)] In-Plane, i_i	Flexibility Characteristic, h	Sketch
Unreinforced fabricated tee [Notes (1), (3), (8), (10)]	1	$\frac{0.9}{h^{2/3}}$	$\frac{3}{4}i_o + \frac{1}{4}$	$\frac{T}{r_2}$	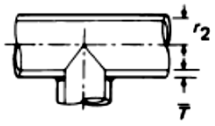
Extruded welding tee with $r_x \geq 0.05\ D_b$ $T_c < 1.5\ T$ [Notes (1), (3), (8)]	1	$\frac{0.9}{h^{2/3}}$	$\frac{3}{4}i_o + \frac{1}{4}$	$\left(1 + \frac{r_x}{r_2}\right)\frac{T}{r_2}$	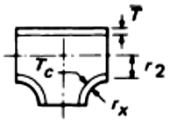
Welded-in contour insert [Notes (1), (3), (7), (8)]	1	$\frac{0.9}{h^{2/3}}$	$\frac{3}{4}i_o + \frac{1}{4}$	$3.1\frac{T}{r_2}$	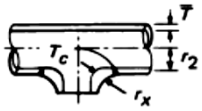
Branch welded-on fitting (integrally reinforced) [Notes (1), (3), (10), (11)]	1	$\frac{0.9}{h^{2/3}}$	$\frac{0.9}{h^{2/3}}$	$3.3\frac{T}{r_2}$	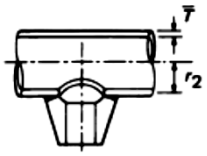

Description	Flexibility Factor, k	Stress Intensification Factor, i
Butt welded joint, reducer, or weld neck flange	1	1.0
Double-welded slip-on flange	1	1.2
Fillet or socket weld	1	1.3 [Note (12)]
Lap joint flange (with ASME B16.9 lap joint stub)	1	1.6
Threaded pipe joint or threaded flange	1	2.3
Corrugated straight pipe, or corrugated or creased bend [Note (13)]	5	2.5

Table D300 Flexibility Factor, k, and Stress Intensification Factor, i (Cont'd)

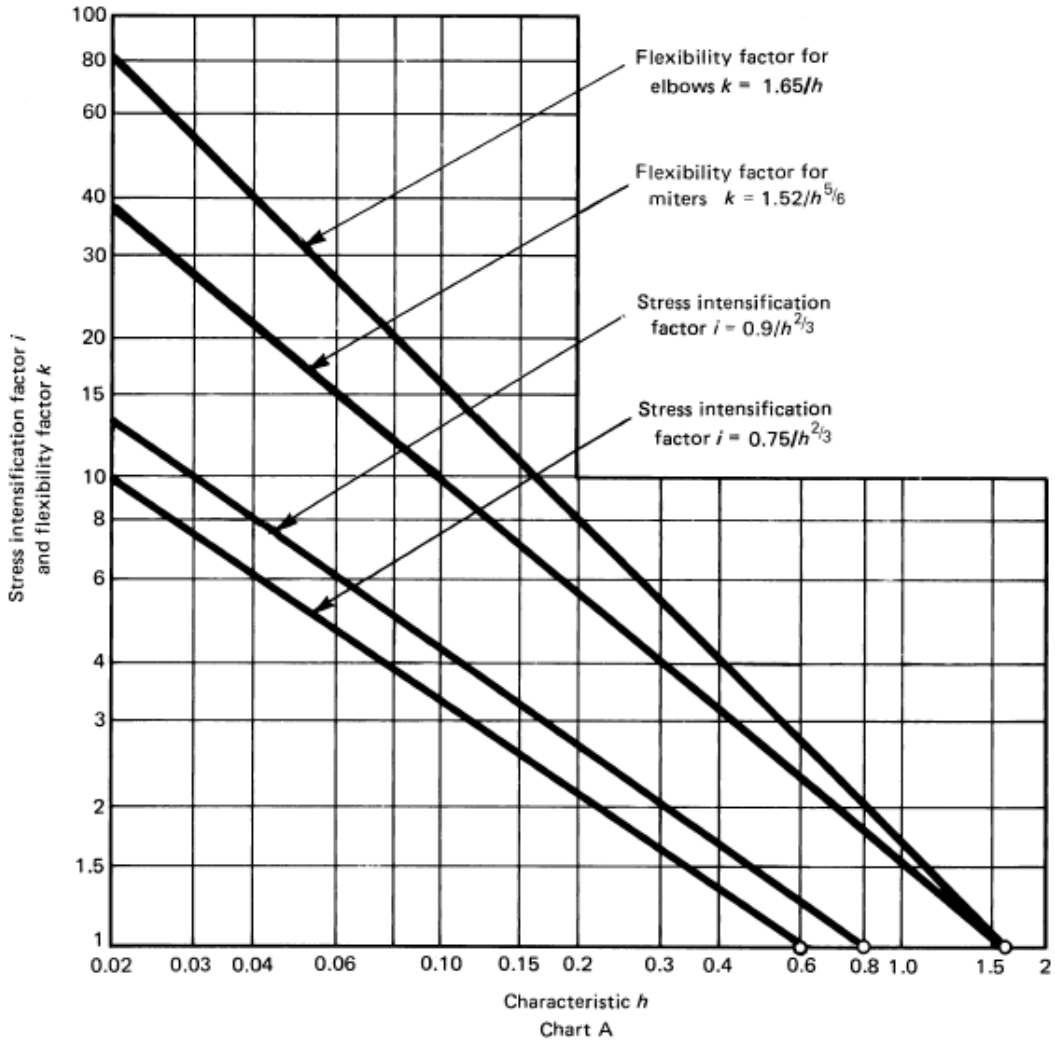

Chart A

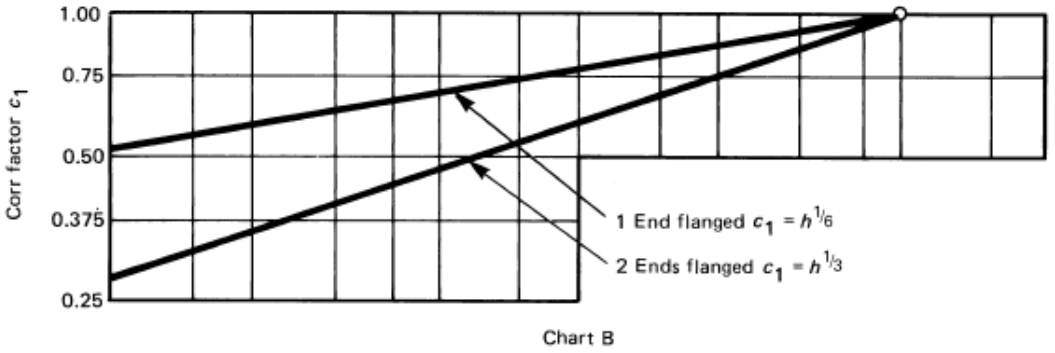

Chart B

Table C-1 Thermal Expansion Data

A = Mean Coefficient of Thermal Expansion, 10^{-6} in./in./°F
B = Linear Thermal Expansion, in./100 ft
} in Going From 70°F to Indicated Temperature [Note (1)]

Material	Coef-ficient	Temperature Range 70°F to																
		−325	−150	−50	70	200	300	400	500	600	700	800	900	1,000	1,100	1,200	1,300	1,400
Group 1 carbon and low alloy steels [Note (2)]	*A*	5.5	5.9	6.2	6.4	6.7	6.9	7.1	7.3	7.4	7.6	7.8	7.9	8.1	8.2	8.3	8.4	8.4
	B	−2.6	−1.6	−0.9	0	1.0	1.9	2.8	3.7	4.7	5.7	6.8	7.9	9.0	10.1	11.3	12.4	14.7
Group 2 low alloy steels [Note (3)]	*A*	6.0	6.5	6.7	7.0	7.3	7.4	7.6	7.7	7.8	7.9	8.0	8.1	8.2	8.3	8.4	8.4	8.5
	B	−2.9	−1.7	−1.0	0	1.1	2.0	3.0	4.0	5.0	6.0	7.0	8.1	9.2	10.3	11.4	12.5	13.5
5Cr–1Mo steels	*A*	5.6	6.0	6.2	6.4	6.7	6.9	7.0	7.1	7.2	7.2	7.3	7.4	7.5	7.6	7.6	7.7	7.8
	B	−2.7	−1.6	−0.9	0	1.0	1.9	2.8	3.7	4.6	5.5	6.4	7.4	8.4	9.3	10.3	11.4	12.4
9Cr–1Mo steels	*A*	5.0	5.4	5.6	5.8	6.0	6.2	6.3	6.4	6.5	6.6	6.7	6.8	6.9	7.0	7.1	7.2	7.2
	B	−2.4	−1.4	−0.8	0	0.9	1.7	2.5	3.3	4.1	5.0	5.9	6.8	7.7	8.7	9.7	10.6	11.6
Straight chromium stainless steels																		
12Cr to 13Cr steels	*A*	5.1	5.5	5.7	5.9	6.2	6.3	6.4	6.5	6.5	6.6	6.7	6.7	6.8	6.8	6.9	6.9	7.0
	B	−2.4	−1.5	−0.8	0	1.0	1.7	2.5	3.3	4.2	5.0	5.8	6.7	7.6	8.5	9.4	10.2	11.1
15Cr to 17Cr steels	*A*	4.5	4.9	5.1	5.3	5.5	5.7	5.8	5.9	6.0	6.1	6.2	6.2	6.3	6.4	6.4	6.5	6.5
	B	−2.1	−1.3	−0.7	0	0.9	1.6	2.3	3.0	3.8	4.6	5.4	6.2	7.0	7.9	8.7	9.5	10.4
27Cr steels	*A*	4.3	4.7	4.9	5.0	5.2	5.2	5.3	5.4	5.4	5.5	5.6	5.7	5.7	5.8	5.9	5.9	6.0
	B	−2.0	−1.2	−0.7	0	0.8	1.4	2.1	2.8	3.5	4.2	4.9	5.6	6.4	7.2	8.0	8.7	9.6
Austenitic stainless steels (304, 305, 316, 317, 321, 347, 348 19-9DL, XM-15, etc.)	*A*	7.5	8.0	8.2	8.5	8.9	9.2	9.5	9.7	9.9	10.0	10.1	10.2	10.3	10.4	10.6	10.7	10.8
	B	−3.6	−2.1	−1.2	0	1.4	2.5	3.8	5.0	6.3	7.5	8.8	10.2	11.5	12.9	14.3	15.8	17.2
Other austenitic stainless steels (309, 310, 315, XM-19, etc.)	*A*	7.1	7.6	7.8	8.2	8.5	8.7	8.9	9.1	9.2	9.3	9.4	9.5	9.6	9.7	9.8	9.9	10.1
	B	−3.4	−2.0	−1.1	0	1.3	2.4	3.5	4.7	5.8	7.0	8.2	9.5	10.7	12.0	13.3	14.7	16.1
Gray iron	*A*	...	...	...	...	5.8	5.9	6.1	6.3	6.5	6.7	6.8	7.0	7.2	...	...	...	...
	B	...	...	...	0	0.9	1.6	2.4	3.2	4.1	5.0	6.0	7.0	8.0	...	...	...	...
Ductile cast iron	*A*	...	4.9	5.3	5.7	6.0	6.3	6.6	6.8	7.0	7.1	7.3	7.4	7.5	...	...	...	...
	B	...	−1.3	−0.8	0	0.9	1.7	2.6	3.5	4.5	5.4	6.4	7.3	8.4	...	...	...	...

Table C-1 Thermal Expansion Data (Cont'd)

A = Mean Coefficient of Thermal Expansion, 10^{-6} in./in./°F

B = Linear Thermal Expansion, in./100 ft

in Going From 70°F to Indicated Temperature [Note (1)]

Material	Coef-ficient	Temperature Range 70°F to																
		−325	−150	−50	70	200	300	400	500	600	700	800	900	1,000	1,100	1,200	1,300	1,400
Monel (67Ni–30Cu) N04400	*A*	5.8	6.8	7.2	7.7	8.1	8.3	8.5	8.7	8.8	8.9	8.9	9.0	9.1	9.1	9.2	9.2	9.3
	B	−2.7	−1.8	−1.0	0	1.3	2.3	3.4	4.5	5.6	6.7	7.8	9.0	10.1	11.3	12.4	13.6	14.8
Nickel alloys N02200 and N02201	*A*	5.3	6.0	6.3	6.6	7.2	7.5	7.7	7.9	8.0	8.2	8.3	8.4	8.5	8.6	8.7	8.8	8.9
	B	−2.7	−1.7	−1.0	0	1.1	2.1	3.1	4.1	5.1	6.2	7.3	8.4	9.5	10.7	11.8	13.0	14.2
Nickel alloy N06022	*A*	...	...	...	6.9	6.9	6.9	6.9	7.0	7.0	7.2	7.3	7.5	7.7	7.9	8.1	8.3	8.5
	B	...	...	...	0	1.1	1.9	2.7	3.6	4.5	5.4	6.4	7.5	8.6	9.8	11.0	12.2	13.6
Nickel alloy N06600	*A*	5.5	6.1	6.4	6.8	7.1	7.3	7.5	7.6	7.8	7.9	8.0	8.2	8.3	8.4	8.6	8.7	8.9
	B	−2.6	−1.6	−0.9	0	1.1	2.0	3.0	3.9	5.0	6.0	7.0	8.1	9.3	10.4	11.6	12.9	14.2
Nickel alloy N06625	*A*	...	...	...	6.7	7.1	7.2	7.3	7.4	7.4	7.5	7.6	7.7	7.9	8.0	8.2	8.4	8.5
	B	...	...	...	0	1.1	2.0	2.9	3.8	4.7	5.6	6.6	7.7	8.8	9.9	11.1	12.3	13.6
Nickel alloys N08800 and N08810	*A*	5.9	6.9	7.4	7.9	8.4	8.6	8.8	8.9	9.0	9.1	9.2	9.3	9.4	9.5	9.6	9.7	9.8
	B	−2.8	−1.7	−1.1	0	1.3	2.4	3.5	4.6	5.7	6.9	8.1	9.3	10.5	11.8	13.0	14.4	15.7
Nickel alloy N08825	*A*	...	...	7.2	7.5	7.7	7.9	8.0	8.1	8.2	8.3	8.4	8.5	8.6	...	...	...	...
	B	...	...	−1.0	0	1.2	2.2	3.2	4.2	5.2	6.3	7.4	8.5	9.6	...	...	...	...
Nickel alloy N10276	*A*	...	...	...	6.0	6.3	6.5	6.7	6.9	7.1	7.2	7.4	7.5	7.6	7.7	7.8	7.9	8.0
	B	...	...	...	0	1.0	1.8	2.7	3.6	4.5	5.5	6.4	7.5	8.5	9.5	10.6	11.7	12.8
Copper alloys C1XXXX series	*A*	7.7	8.7	9.0	9.3	9.6	9.7	9.8	9.9	10.0	...	...	...	...	...	...	...	...
	B	−3.7	−2.3	−1.3	0	1.5	2.7	3.9	5.1	6.4	...	...	...	...	...	...	...	...
Bronze alloys	*A*	8.4	8.8	9.2	9.6	10.0	10.1	10.2	10.3	10.4	10.5	10.6	10.7	10.8	10.9	11.0	...	...
	B	−4.0	−2.3	−1.3	0	1.6	2.8	4.0	5.3	6.6	8.0	9.3	10.7	12.1	13.5	14.9	...	...
Brass alloys	*A*	8.2	8.5	9.0	9.3	9.8	10.0	10.2	10.5	10.7	10.9	11.2	11.4	11.6	11.9	12.1	...	...
	B	−3.9	−2.2	−1.3	0	1.5	2.8	4.1	5.4	6.8	8.2	9.8	11.4	13.0	14.7	16.4	...	...
Copper–nickel (70Cu–30Ni)	*A*	6.7	7.4	7.8	8.1	8.5	8.7	8.9	9.1	9.2	9.2	...	...	...	...	...	...	...
	B	−3.2	−2.0	−1.1	0	1.3	2.4	3.5	4.7	5.8	7.0	...	...	...	...	...	...	...
Aluminum alloys	*A*	9.9	10.9	11.6	12.1	13.0	13.3	13.6	13.9	14.2	...	...	...	...	...	...	...	...
	B	−4.7	−2.9	−1.7	0	2.0	3.7	5.4	7.2	9.0	...	...	...	...	...	...	...	...
Titanium alloys (Grades 1, 2, 3, 7, and 12)	*A*	...	...	4.5	4.6	4.7	4.8	4.8	4.9	4.9	5.0	5.1	...	...	...	...	...	...
	B	...	...	−0.6	0	0.7	1.3	1.9	2.5	3.1	3.8	4.5	...	...	...	...	...	...

Appendix H – Pipe Schedules and Weights (Supermarkets, 2015)

PIPE SCHEDULES & WEIGHTS					
		SCHEDULE 40		SCHEDULE 80	
NOMINAL PIPE SIZE	OUTSIDE DIAMETER	Wall Thick.	Wt. Per Ft.	Wall Thick.	Weight Per Ft.
1/8	0.405	0.068	0.245	0.095	0.315
1/4	0.540	0.088	0.425	0.119	0.535
3/8	0.675	0.091	0.568	0.126	0.739
1/2	0.840	0.109	0.851	0.147	1.088
3/4	1.050	0.113	1.131	0.154	1.474
1	1.315	0.133	1.679	0.179	2.172
1-1/4	1.660	0.140	2.273	0.191	2.997
1-1/2	1.900	0.145	2.718	0.200	3.631
2	2.375	0.154	3.653	0.218	5.022
2-1/2	2.875	0.203	5.793	0.275	7.661
3	3.500	0.216	7.576	0.300	10.250
3-1/2	4.000	0.226	9.109	0.318	12.510
4	4.500	0.237	10.790	0.337	14.980
5	5.563	0.258	14.620	0.375	20.780
6	6.625	0.280	18.970	0.432	28.570
8	8.625	0.322	28.550	0.500	43.390
10	10.750	0.365	40.480	0.500	54.740
12	12.750	0.375	49.560	0.500	65.420